Second-Life Batteries for Ancillary Services

Year 1
Task 1: Literature Review
Task 2: Technical Assessment

April 23, 2025

Work conducted for Dr. Cyrille Decès-Petit at National Research Council (Contract #1021365)

Work conducted by Chris White (PhD), Ryan Ning (MASc), Mitchell Gregory (MASc), Bryan Ellis (MASc), and Lukas Swan (PhD) at Dalhousie University

Principal Investigator: Lukas Swan, PhD, PEng
Professor, Department of Mechanical Engineering
Director, Renewable Energy Storage Laboratory
Dalhousie University
Sexton Campus, 5269 Morris St, Halifax, Nova Scotia, B3J 0H6, Canada
T: 902-830-0349, E: Lukas.Swan@Dal.Ca, W: http://resl.me.dal.ca

Abstract

The demand for electricity grid energy storage is growing rapidly in response to the ongoing shift towards variable wind- and solar-based electricity generation. To help meet this demand, used batteries from electric vehicles can be repurposed for a 'second-life' as stationary energy storage providing electricity grid services. A subset, ancillary services, such as frequency regulation, contingency reserves, and voltage support are critical for ensuring grid reliability. This report draws on published literature as well as the engineering experience of the Renewable Energy Storage Laboratory at Dalhousie University to evaluate second-life batteries providing ancillary services in terms of suitability, challenges, and performance. Second-life batteries are found to be suitable due to their original design specifications, power and energy capabilities, and degradation patterns. Key challenges include battery design diversity, battery state-of-health uncertainties, and performance disadvantages compared to new batteries. Performance evaluations of second-life batteries show technical suitability for ancillary services, however, the only dedicated studies were for the specific ancillary service of frequency regulation. Recommendations are made regarding test methods, performance metrics, and standardization opportunities that will facilitate the repurposing of used electric vehicle batteries into ancillary service applications.

Table of Contents

List of Abbreviations

AC	Alternating current
ACE	Area control error
AGC	Automatic generation control
BMS	Battery management system
BOL	Beginning of life
CAN	Controller area network
DC	Direct current
DV	Differential voltage
EIS	Electrochemical impedance spectroscopy
EOL	End of life
EOVL	End of vehicular life
EV	Electric vehicle
IC	Incremental capacity
ISO	Independent system operator
LAM	Loss of active material
LFP	Lithium iron phosphate
LLI	Loss of lithium inventory
LMO	Lithium manganese oxide
NMC	Lithium nickel manganese cobalt oxide
NCA	Lithium nickel cobalt aluminum oxide
PNNL	Pacific Northwest National Laboratories
RUL	Remaining useful life
SEI	Solid electrolyte interphase
SOC	State of charge
SOH	State of health
SNL	Sandia National Laboratory
TMS	Thermal management system

1 Introduction

The Nissan Leaf electric vehicle (EV) was introduced in the year 2010, and with it, brought about a step change to large format, high voltage, high energy capacity lithium-ion batteries. Over the last decade and half, the EV market has matured considerably in a multitude of ways. First, battery packs have become larger and higher energy capacity. Second, technology has improved and battery life is greatly extended. While vehicle life is restricted due to mileage and vehicle wear, the combination of these two battery improvements has led to the batteries outlasting their 'first life' in the EV. The batteries then potentially become available for a 'second-life' by being repurposed, typically into a stationary electricity grid energy storage application. This supports general product ethos where repurposing/reuse is a better alternative than immediate recycling, to extract additional value from items before they are finally recycled.

This is further underpinned by the dramatic growth in sales, with many millions of EVs now on the road. Only now, as the original EVs are reaching end of life, is this second-life opportunity presenting itself with quantities and qualities of batteries that give repurposing the potential to be techno-economically viable. Because EV batteries are designed to be reliable in the complex application of motive transport (e.g. washboard roads, deserts, freezing, etc.) repurposing them into stationary applications such as electricity grid energy storage would likely lie within the original technical specification.

1.1 Our experience

The Dalhousie University Renewable Energy Storage Laboratory was founded in 2010, the year the Nissan Leaf EV was introduced. In 2011, prototype EV battery packs were obtained and tested as an initial means to gain access to the state-of-the art lithium-ion battery technology. The results were used as the foundation for assessments of batteries in electricity grid services that were published in 2012[1]. Over the next few years, many EV batteries were obtained and used for a wide variety of investigations.

In 2015-2021, a major Natural Sciences and Engineering Research Council of Canada Strategic research grant[2] was obtained for research of second-life EV batteries. During this time, several major equipment grants[3] were obtained from Canada Foundation for Innovation, fully outfitting the laboratory with thermal chambers, battery cyclers, and test equipment necessary for full characterization of second-life EV batteries in grid services. Continued funding from 2021-2027 was obtained through a Discovery and a CREATE grant[4] from Natural Sciences and Engineering Research Council of Canada. In the last 10 years, approximately 12 journal publications[5] have been produced that test or model second-life batteries, several of which are reviewed in this report.

As such, this report is based upon our testing/operating/reviewing experience and engineering judgment in handling dozens of unique second-life EV battery packs, in all aspects, including removal

[1] http://dx.doi.org/10.1016/j.jpowsour.2012.05.081
[2] https://www.torontomu.ca/cue/research/nestnet/
[3] https://springboardatlantic.ca/researcher-highlights-dr-lukas-swan/
[4] https://energy.dal.ca/
[5] https://resl.me.dal.ca/publications/

from the vehicle, assessment, modification, rearrangement, addition of componentry, implementation into systems, testing, data analysis, and finally recycling.

1.2 Motivation

The concept of second-life for EV batteries has been considered, evaluated, and researched for approximately 15 years. These studies are often in the general sense and focused on remaining usable life and based on broad economic assumptions. Laboratory prototypes and pilot facilities of second-life EV batteries for grid energy storage have been constructed and evaluated. These are often focused on bulk energy transfers, with simple control.

With the advent of higher power EV battery packs designed for ultra-fast charging, a new opportunity presents itself: the repurposing of EV batteries into a second-life electricity grid energy storage application that is of high power and lower energy needs. These applications are typically termed 'ancillary services' and cover a range of applications that are either highly power dynamic, or intermittently invoked. This is a new topic area and as such is not presently well understood in terms of technology complementarity, technoeconomic potential, market size opportunity, integration methods, or expected lifetime performance.

1.3 Objectives

It is the objective of this report to evaluate the repurposing of EV batteries into a second-life of electricity grid ancillary services applications. The report examines the present literature and gives commentary/perspective based on engineering judgement and experience with numerous second-life batteries. In one sense, it is an evaluation of the state-of-art, and in another sense a projection of future roles that used second-life EV batteries can play in delivering ancillary services.

1.4 Overview of the report

The remainder of this report is divided into the following sections:

- Section 2 provides background information to contextualize second-life batteries and ancillary service energy storage applications. The reviewed second-life battery concepts include the EV market size and evolution; when/how vehicles are retired; the remaining useful life of the batteries; and the basics of battery repurposing and recycling. The functions of various electricity grid ancillary services are described in detail, with specific ancillary services being designated as in/out of scope for this report.
- Section 3 reviews the existing literature on EV battery design features and battery repurposing processes. The reviewed design features including pack, module, and cell configurations; battery management systems; and thermal management systems. The reviewed repurposing processes include the removal, inspection, and reconfiguration of the batteries to suit second-life; screening techniques for technical validity; testing/certification techniques necessary for second-life systems; and key integration and operating characteristics.
- Section 4 reviews the existing literature on second-life battery performance in ancillary services to examine their general suitability for these applications. Several key publications have developed performance test protocols for evaluating energy storage performance in

different ancillary services. A number of experimental studies have published results demonstrating the electrical, thermal, and degradation performance characteristics of second-life batteries in frequency regulation service, but such studies are lacking for other ancillary services. Generalized discussions are instead provided regarding second-life battery performance in these other ancillary services.

- Section 5 presents our experience and engineering judgement in a technical assessment of second-life batteries providing ancillary services. We first discuss the suitability of second-life batteries for ancillary services in terms of energy capacity, energy efficiency, power rate, heat generation, and cycle life based on the range of batteries we have directly encountered. We then discuss major implementation challenges due to packs design, battery/thermal management systems, and safety, based on our experience in designing, implementing, and operating second-life battery systems.
- Section 6 presents our main conclusions and recommendations. We describe a set of recommended technical criteria for testing second-life batteries in ancillary services, as well as a set of potential opportunities for standardization in research and industry.

2 Background

This section provides essential background information on the subject of second-life batteries for ancillary services. Context is provided regarding the general concept of second-life batteries as well as the nature of specific electricity grid ancillary services. A more detailed review of lithium-ion battery technology and stationary energy storage applications can be found in [1].

2.1 Overview of second-life batteries

Lithium-ion batteries are a key technology for the global transition toward renewable energy. These high-performance energy storage devices make it possible to manufacture EVs that can meet the mobility demands of the modern world, thereby enabling the ongoing electrification of the transportation sector and reduced reliance on fossil fuels. At the same time, lithium-ion batteries have also become the technology of choice for constructing new stationary energy storage systems that provide services for electricity grid operators as well as electricity consumers. These stationary batteries are especially critical for ensuring electricity grid reliability as traditional fossil fuel power plants are displaced by variable-output wind turbines and photovoltaic solar panels. This in turn allows for EVs to be charged with more renewably sourced electricity, further reducing greenhouse gas emissions. Lithium-ion batteries are therefore enabling global decarbonization on two connected fronts: transportation and electricity supply.

The urgency of the climate crisis has compelled many governments to set ambitious targets for the rapid adoption of both EVs and renewable energy. In Canada, the European Union, the United Kingdom, and many other regions around the world, all new vehicle sales will be required to be zero-emission by 2035 [2]. Based on currently stated energy policies, the International Energy Agency projects that wind and solar resources will provide 35 % of global electricity supply by 2035 and 60 % by 2050 [3]. As illustrated in Figure 2.1, both these trends call for major upscaling in lithium-ion battery production, with EV batteries accounting for about 90 % of the combined annual demand [4].

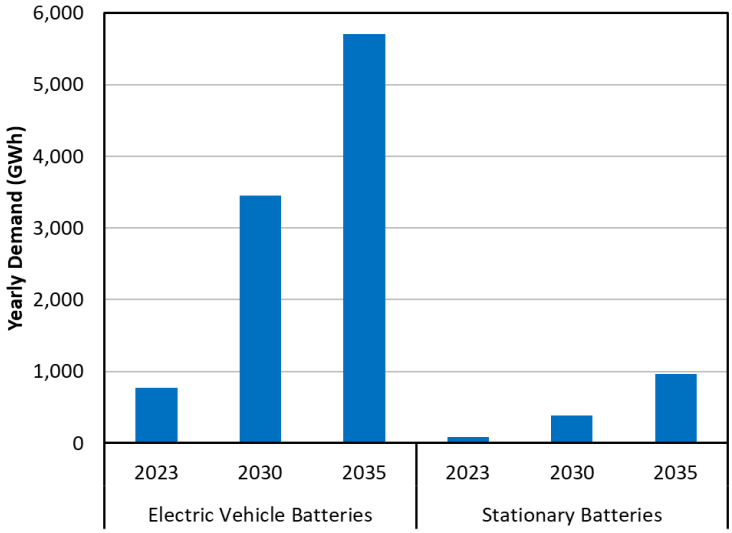

Figure 2.1 Projected growth in annual battery demand for transportation and electricity sectors. Based on data from [4] and [5].

Due to the anticipated increase in EV battery production in particular, there are growing concerns surrounding the environmental consequences of increased mining, processing, manufacturing, and inevitable battery disposal. This sustainability problem has spurred significant research and investment focused on improving the circularity of the EV battery supply chain, with the goal of maximizing the reuse, repurposing, and recycling of EV batteries.

2.1.1 End of vehicular life

Every EV battery will eventually reach the end of its useful life for the vehicle. This can occur in one of two ways: either the vehicle itself reaches the end of its life (due to collision or natural aging of the vehicle); or the battery degrades to the point that it no longer meets the minimum requirements for EV applications [6]. In either case, this point in the battery life cycle is often called the 'end of vehicle life' (EOVL). When the battery is fully degraded to the point of having no practical use other than the recycling of its constituent components, the battery is considered to have reached 'end of life' (EOL).

The specific threshold that triggers EOVL is an interesting subject discussed widely in the literature. Many early EVs (approximately year 2010 to 2015) featured relatively small battery capacities ranging from 20 to 25 kWh (e.g. first generation Nissan Leaf and BMW i3), corresponding to driving ranges of 100 to 150 km. Due to this low driving range, it was commonly expected that EOVL would be reached due to reduced range when these relatively small batteries degraded to approximately 80 % state of health (SOH) [7], at which point the battery could be replaced and the vehicle continue in service. Newer EVs usually feature battery capacities ranging from 40 to 80 kWh (e.g. Chevrolet Bolt and Tesla Model 3), with some exceeding 100 kWh (e.g. BMW i7), corresponding to driving ranges of 250 to 700 km. This means that lower SOH levels can still provide functional EV driving ranges (for resale if not for the original driver). Another important point is that larger EV batteries will tend to degrade at slower rates in EV service (per year and per km travelled) compared to smaller EV batteries [7]. For example, if a 30 kWh battery and a 60 kWh battery are subjected to the same EV drive cycle and power magnitude (neglecting differences in cell, module, and pack design as well as

vehicle mass), the 30 kWh battery will experience double the depth of discharge, double the energy throughput, double the power density, and therefore significantly higher temperatures, all of which tend to accelerate lithium-ion battery degradation mechanisms [8-12]. The combination of higher battery capacity, lower battery degradation rates, and technology evolution/maturation/quality in newer EVs increases the likelihood that the vehicle will trigger EOVL before the battery does. A 2020 analysis of global EV battery data concluded that the average EV battery installed in a 2020 private passenger vehicle will be able to last 15 years or more before SOH declines to 80 % [13].

To better quantify EOVL expectations in the coming years, Casals et al. [7] conducted a 2022 statistical analysis for the United Kingdom market based on publicly available EV battery degradation data. The authors assumed that publicly available age and mileage data for retired diesel vehicles (which generally last longer than gasoline vehicles) give reasonable expectations for the retirement age and mileage of EVs independent of battery degradation (distributions of 2 to 20 years and up to 500,000 km). Some of the key results of the study are summarized in Figure 2.2. The left chart shows that retired EV batteries at present day are a mix of small (e.g. 24 kWh), medium (e.g. 40 kWh), and large (e.g. 70 kWh) batteries, with smaller batteries most often retired below 75 % SOH (indicating retirement due to unacceptable driving range) and larger batteries most often retired above 85 % SOH (indicating early vehicle retirement, perhaps due to collision). However, Figure 2.2 also shows that the overall quantities of retired EV batteries are currently very small compared to what is expected in the coming years. The right chart shows that small batteries will soon make up an insignificant portion of retired EV batteries, while quantities of retired medium and large EV batteries will increase dramatically and frequently reach EOVL at SOH levels of 85 % or higher (indicating batteries outlasting the vehicles). The study concluded that by 2035, 55 % of all retired EV batteries in the UK will have reached EOVL above 85 % SOH; and 89 % of all retired EV batteries above 75 % SOH. Only 1 % were projected to reach EOVL below 60 % SOH. The authors also noted that the UK only represents about 5 % of the global EV market, so the 500,000 scale in the right chart of Figure 2.2 could be scaled up to 10 million to get a global sense.

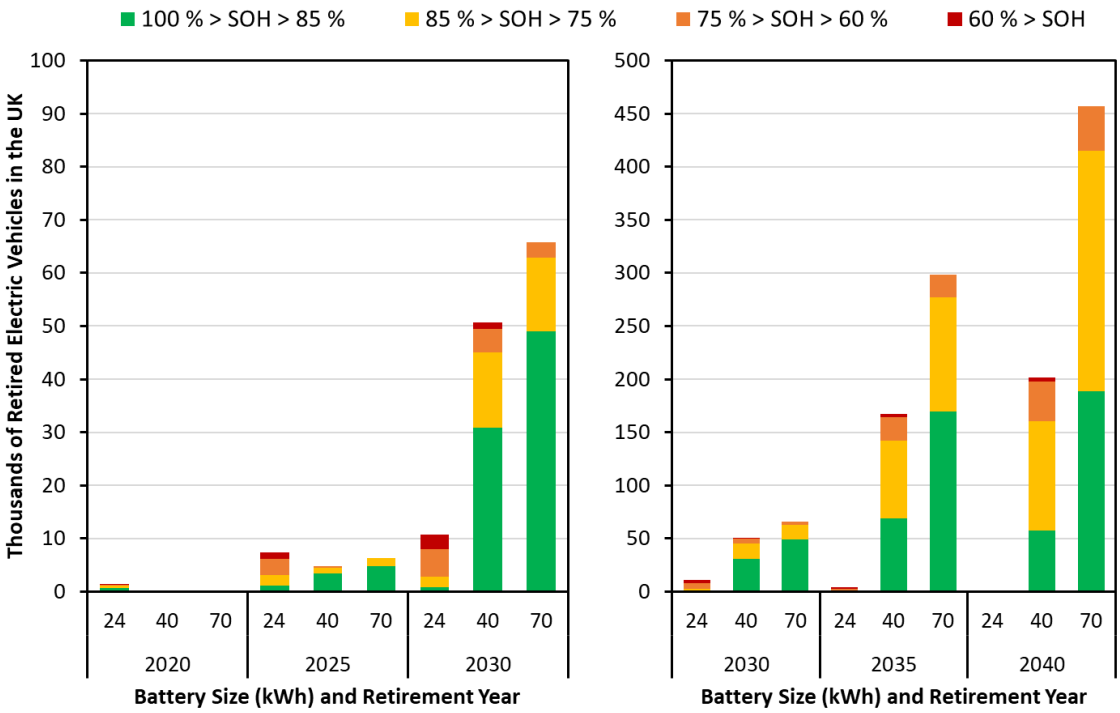

Figure 2.2 Expected quantities of retired EV batteries by size and SOH in the United Kingdom. Based on data from [7].

It is important to note that battery SOH levels at EOVL may be influenced by emerging technologies and markets that allow EVs to exercise their batteries for non-motive purposes such as vehicle-to-grid, vehicle-to-home, etc. [14]. This would cause the EV battery to degrade faster over time, since the battery would be cycling even when the vehicle is parked for long periods. These technologies are still in development, so they are not factored into the results shown in Figure 2.2.

2.1.2 Battery recycling and repurposing

With many millions of retired EV batteries entering waste management streams, effective recycling processes are essential for sustainability. Battery recycling can also provide a domestic supply of essential base materials that might otherwise need to be imported from foreign mining industries [15]. When EV batteries enter the recycling stream, they must first be discharged, disassembled, and sorted before being treated with one of the two established lithium-ion battery recycling technologies: pyrometallurgy and hydrometallurgy. Pyrometallurgical methods use a high-temperature furnace to smelt full cells or modules such that valuable metals can be separated out and recovered [15]. This approach is relatively efficient in terms of time, equipment, and labour requirements, but it requires large amounts of energy and releases significant environmental pollutants [16]. Hydrometallurgical methods use an acid or other leaching fluid to dissolve and extract key metals from the battery components. This is the preferred approach for newer recycling facilities since it consumes less energy, generates less pollution, and produces purer end products [17]. However, hydrometallurgy requires additional pre-processing steps to disassemble the cells and separate the various cell components, which results in additional time and labour [18]. Alternative recycling technologies are being researched extensively, but are not yet commercialized.

One example is 'direct recycling', which physically separates electrode materials from the cell so they can be restored to commercial-grade quality without breaking them down into base elements [19].

The EV battery recycling industry still faces substantial challenges. For one, the wide diversity in EV battery designs makes it difficult to automate the various recycling processes. It is commonly stated in the literature that the battery manufacturers should 'design for recycling' to make recycling easier and more economical [16]. It is also widely acknowledged that material recovery rates still need to be significantly improved as the battery recycling industry scales up to meet the rapidly growing demand [18].

Another important consideration arises when referring back to Figure 2.2. If the vast majority of EV batteries will be reaching EOVL at 75 % SOH or higher in the coming years, then significant value will be wasted if these batteries are sent directly to recycling after EOVL. To make better use of the manufacturing value embedded in retired EV batteries, these batteries should be reused as much as possible before they are sent to a recycling facility. While some used EV batteries may be suitable for reuse in another EV with lower driving demands [20], many will be better suited for repurposing into 'second-life' stationary energy storage applications where lithium-ion batteries are already being deployed. This additional utilization step within the EV battery life cycle is illustrated in Figure 2.3.

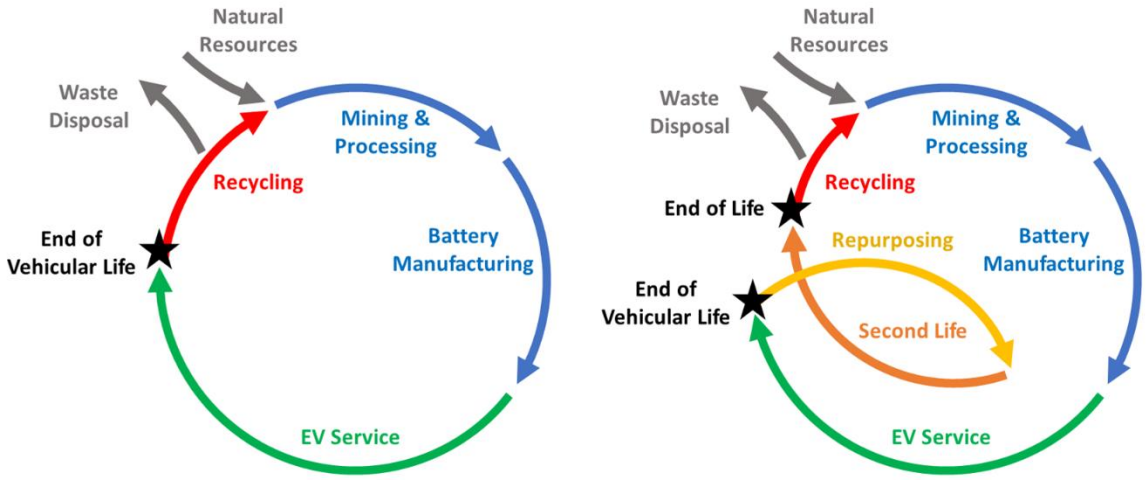

Figure 2.3 Illustration of EV battery life cycle without repurposing (left) and with repurposing (right). Partially based on figure from [21].

Stationary energy storage applications are typically less demanding than EV applications as they are not subject to vibration, outdoor climatic conditions, and sporadic drive cycles [20], [22]. This makes stationary applications a viable option for used EV batteries at EOVL. There are a variety of stationary energy storage applications that benefit electricity grid operators as well as electricity consumers. These stationary applications are summarized graphically in Figure 2.4, with the four main categories being grid capacity, grid energy management, grid ancillary service, and consumer services. The command signal update rates and/or durations associated with each service can range from seconds to minutes to hours, so Figure 2.4 indicates the typical discharge period of each application by colour. Note that while there is considerable overlap among some of these applications, Figure 2.4 separates them based on how the direct benefits of energy storage are realized. For example, 'peak shaving' and 'demand charge reduction' are very similar, but peak shaving directly benefits the electricity grid

operator while demand charge reduction directly benefits the consumer. Ultimately, all stationary energy storage applications provide the same basic function: to store electricity when demand is relatively low and dispatch it later when demand is relatively high. This report is focused exclusively on grid ancillary services, which will be explained in greater detail in Section 2.2. Other stationary energy storage applications are reviewed in [23-32].

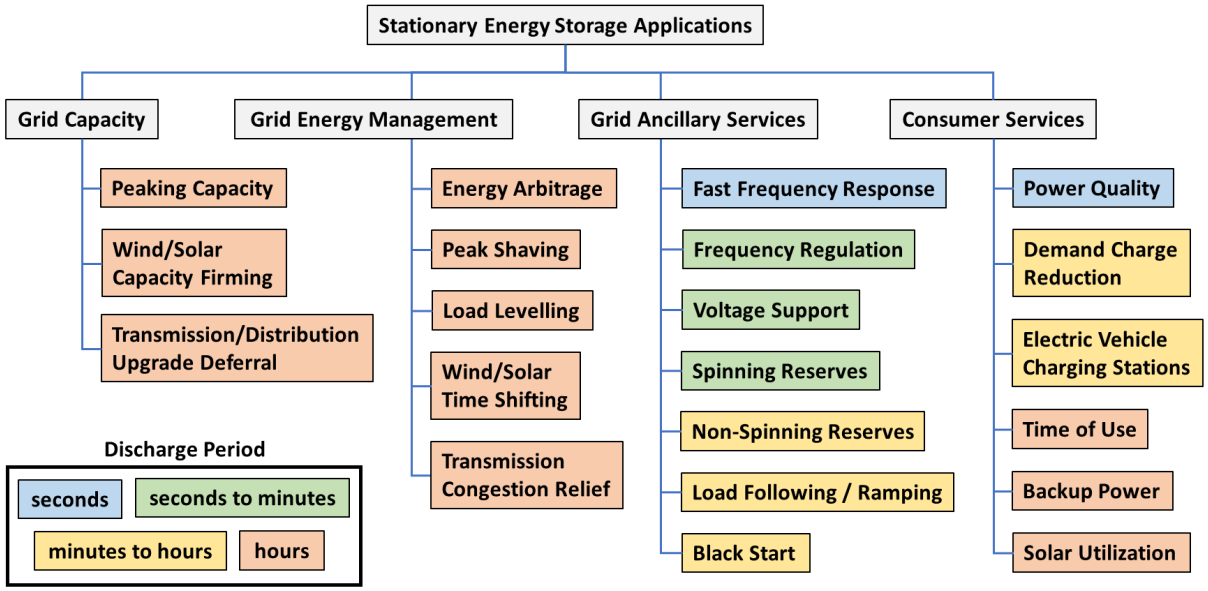

Figure 2.4 Graphical summary of stationary battery energy storage applications.

Compared to newly built batteries, second-life batteries can offer lower prices and reduced environmental impact as stationary energy storage systems, but there are still significant technoeconomic challenges for the second-life battery industry, such as: evaluating the remaining operational value in each used EV battery [9]; reducing the costs and complexity associated with the repurposing process [10]; and accounting for performance limitations compared to new stationary batteries (systems composed of fresh/new cells) [35]. Despite these challenges, many EV manufacturers and startup companies are already deploying second-life battery systems [36-39], and governments around the world are starting to develop new regulations [40] and funding programs [41], [42] to facilitate industry growth.

Not all second-life batteries will come from EV applications. Some stationary batteries will reach the end of useful life in the original stationary application/project and become available for repurposing in a different stationary application/project [43]. Such batteries will still need to be resized or modified to suit the intended second-life. However, Figure 2.1 has shown that the quantity of used EV batteries will far exceed used stationary batteries.

2.2 Overview of electricity grid ancillary services

Electricity grid operators must generate a reliable and versatile electricity supply in order to meet electricity demands, which can exhibit significant variability on different time scales ranging from seconds to seasons. Ancillary services help maintain grid reliability in real time by maintaining power, frequency, and voltage to counter the continual fluctuations of the supply-demand balance as

well as unexpected disruptions on the grid. Demand for these ancillary services is expected to increase as electricity grids become more reliant on variable and low-inertia renewable energy sources (i.e. onshore and offshore wind turbines as well as photovoltaic solar panels) in place of conventional high-inertia power plants (i.e. coal, oil, gas, nuclear, and hydroelectric) [44].

Electricity grids are operated at a nominal electrical frequency (60 Hz in the Americas and 50 Hz in most other countries). Conventional power plants generate electricity with a turbine (driven by water, steam, or combustion exhaust) coupled or geared to a generator which rotates at a nominal mechanical frequency to give the electricity grid its nominal electrical frequency (the ratio between the two frequencies being dependent on the number of magnetic pole pairs in the generator) [45]. Conventional power plants are considered 'synchronous' since the generators are synchronized to this common electrical frequency on a given electricity grid, even if individual power plants are separated by significant geographical distance. Variable renewable energy sources are not synchronized to the grid in this way. Photovoltaic solar panels generate direct current (DC) electricity, so power electronics are required to convert the generated DC electricity to match the alternating current (AC) frequency of the electricity grid. Wind farms are generally composed of variable-speed wind turbines, which require power electronics to convert the variable AC frequency to match the AC frequency of the grid [46]. Wind turbines and solar panels are therefore often referred to as 'asynchronous', 'nonsynchronous', and/or 'inverter-based' resources to distinguish them from synchronous generators.

2.2.1 Load following and frequency regulation

Electrical equipment is designed for the nominal frequency of a given electricity grid, so the frequency is typically held within a normal operating band of ± 0.2 Hz, and more typically ± 0.05 Hz, to ensure efficient operation of electrical equipment across the grid [47]. If electricity supply and demand remain in perfect balance, then the generators will remain at the nominal frequency. However, this balance is never perfectly maintained in practice since electrical loads are in continual flux due to human activity. When electricity demand exceeds supply, the increased torque on the generator decreases the rotational speed (thereby lowering the electrical frequency) until the power output is increased to match the demand [48]. Conversely, when electricity supply exceeds demand, frequency increases until the power output is decreased to match the demand. Maintaining an optimal frequency range is therefore an effective means of maintaining the balance of electricity supply and demand. Electricity system operators use 'automatic generation control' (AGC) to accomplish this. As the measured system frequency continually deviates from the nominal value under normal operating conditions, the AGC algorithm sends control signals to continually adjust the power output of designated power plants every few seconds of every day (e.g. every 2 s in PJM Interconnect, the independent system operator or ISO for the mid-Atlantic United States) so that the frequency converges back towards the nominal value [49]. This operation is called 'frequency regulation'. Note that AGC is actually determined by the 'area control error' (ACE), which accounts for both deviations from the nominal system frequency and deviations from scheduled power flows between defined jurisdictional areas within the system [50]. On longer time scales of minutes to hours (e.g. 5 minutes in the California ISO), the system operator will continually make larger adjustments to the total electricity supply by ramping capable power plants (e.g. hydroelectric or gas turbine) up or down to match the evolving trends of electricity demand throughout the day [51]. This operation is called 'load following', and the rate at which it occurs is often called 'ramping'. Figure 2.5

illustrates how the real-time electricity demand can be separated into load following and frequency regulation components based on the time scale of variability (3 h time period shown).

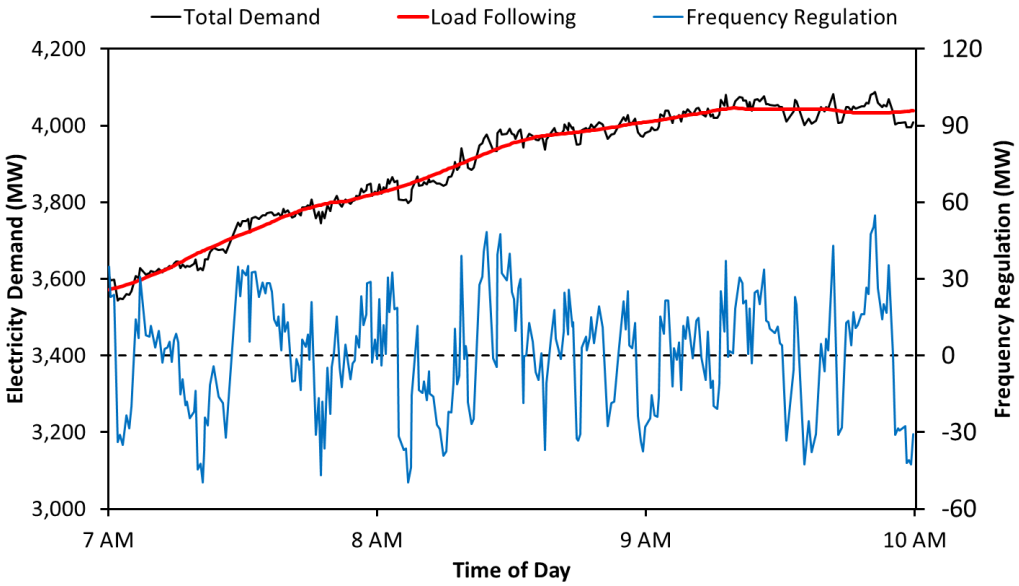

Figure 2.5 Example of load following and frequency regulation as components of total electricity demand. Based on data and figure from [51].

Since batteries can ramp quickly and charge or discharge for several hours, batteries can provide load following and ramping services by participating in energy markets and reserve markets, or by being dispatched accordingly by vertically integrated utilities [26]. Batteries can also be co-located with wind farms or solar farms to provide ramping compensation to smooth the generated power output when wind speed or cloud cover is in flux [52]. Note that load following is not considered in the remainder of this report since it is carried out through the normal real-time dispatch of generation assets, which is different from other ancillary services. Load following is described here mainly to clarify the role of frequency regulation service.

Batteries are particularly well-suited for frequency regulation, since this ancillary service requires continuous cycles of ramping up and down for seconds or minutes at a time (as shown previously in Figure 2.5). This type of operation tends to incur costs for power plants, such as reduced efficiency, mechanical wear and tear, as well as opportunity costs in the energy market [47], [51]. The opportunity costs arise because power plants must retain operational headroom in order to 'regulate up', which results in lost revenue in the energy market if energy prices are high (e.g. during peak load periods). Conversely, power plants must operate above a minimum load in order to 'regulate down', which can be uneconomical if energy prices are low (e.g. overnight). Batteries designated for frequency regulation service can simply fluctuate about a mid-level state of charge (SOC) and incur lower costs than conventional power plants.

The rapid response capabilities of batteries also enables more accurate tracking of volatile AGC signals compared to conventional power plants, thereby providing a more tightly regulated grid frequency. Recognizing that certain power sources offer superior frequency regulation performance, the Federal Energy Regulatory Commission (the government agency that regulates the various ISOs

and RTOs in the United States outside of Texas) issued Order 755 in 2011, which sets 'pay for performance' rules so that superior frequency regulation providers get paid at a higher price [53]. This enhances the economic opportunity for stationary battery systems to provide frequency regulation services. PJM Interconnect filters its frequency regulation signal into a '*Regulation A*' signal and a '*Regulation D*' signal, the latter of which is more volatile and is designated specifically for fast-response technologies like batteries [54]

2.2.2 Frequency response and contingency reserves

Unexpected events on the electricity grid can cause abrupt and significant deviations in frequency. A relatively common example is an unplanned generator outage, creating a sudden deficiency in electricity supply which causes the frequency to drop. Such significant deviations from the nominal frequency can cause damage to electrical equipment and cascading failures that can lead to a blackout [50]. Electricity grid operators must therefore ensure that the system can respond swiftly to unexpected disruptions in the supply-demand balance. In the case of an unplanned generator outage, electricity grid operators will implement 'under-frequency load shedding' if the frequency falls below a set threshold (e.g. 0.5 Hz below nominal), effectively cutting off power supply to certain loads as a means of restoring the supply-demand balance so the rest of the grid remains operational [48]. However, other mechanisms can help to slow and arrest the frequency decline so that load shedding does not become necessary.

The first measure to avoid load shedding is the 'inertial response' of conventional power plants. Large turbines and generators store significant rotational kinetic energy, and when a system disturbance causes the generator to slow down, some of that stored energy is discharged into the electricity grid. This inertial response is instantaneous, autonomous, and lasts for a few seconds [50]. The discharge of kinetic energy through the generator provides additional electricity supply to partially offset the supply-demand imbalance, which slows the rate of frequency decline following the disturbance [55]. Conventional power plants also feature a governor mechanism which provides 'primary frequency response' by rapidly converting a change in frequency to a counteracting change in power output [48]. For example, steam power plants feature a valve which throttles the steam flow into the turbine. As long as the steam is partially throttled, the power plant has some reserve capacity that can be used to provide primary frequency response. Historically, mechanical governors were used to directly convert a change in generator speed to a counteracting change in valve position. Electronic governors are more common today, relying on sensors and control signals to provide primary frequency response [48].

While the inertial response is instantaneous, primary frequency response engages within a few seconds and typically lasts for no more than a minute or so [50]. These two responses are often sufficient to slow and arrest the frequency decline. A 'secondary frequency response' is then required to bring the frequency back up to its optimal range. This secondary response is provided by the same AGC mechanism that carries out frequency regulation, engaging in less than a minute and typically running for no more than a few minutes [50]. If the generator outage has not yet been corrected during the secondary response, a 'tertiary frequency response' is manually initiated to maintain the necessary power supply and restore the optimal frequency range. The tertiary response is provided by 'spinning reserves', which are power plants that are synchronized to the electricity grid but do not operate at full power output unless called upon during a contingency event [55]. This reserve

capacity is left 'spinning' so that the power plant can respond to a contingency in less than a minute and ramp up to full power within 10 minutes. Spinning reserves typically operate for less than an hour. If the contingency is not corrected within this time frame, 'non-spinning reserves' must be provided by offline power plants that can be brought online in 10 to 30 minutes and operate for several hours [55]. If the contingency lasts for many hours, additional offline power plants may need to be brought online to provide 'replacement reserves'. Figure 2.6 shows an illustrative example of how the different system mechanisms respond on different time scales to an electricity grid disruption causing a sudden drop in frequency. Note that this refers to relatively infrequent contingency events rather than normal system operating conditions.

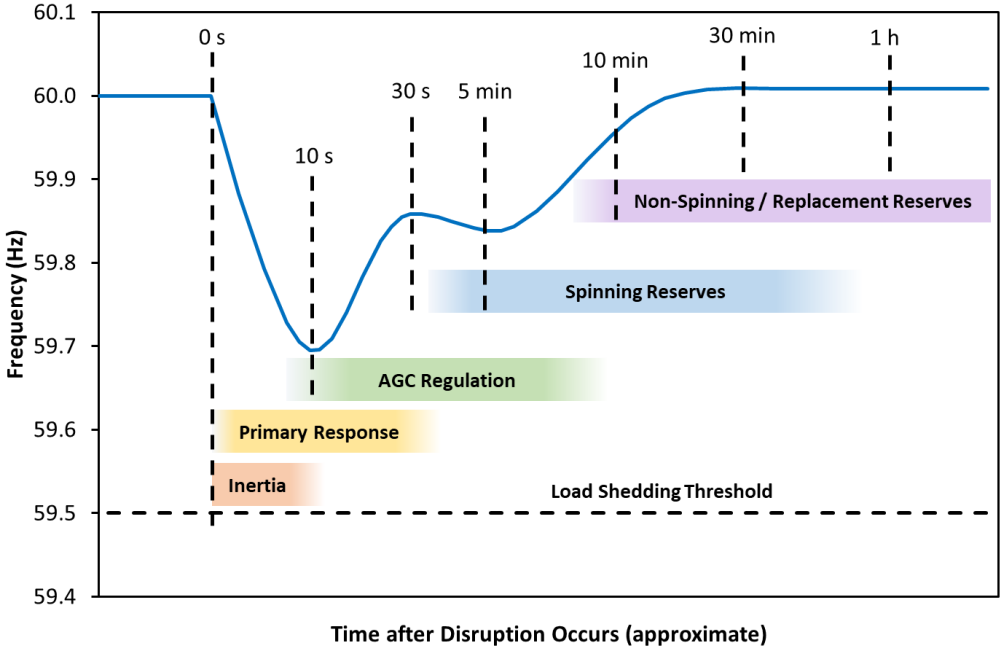

Figure 2.6 Illustrative example of an electricity grid disruption causing a sudden frequency drop and the time scales of the main system response mechanisms used to restore the frequency. Based on figure from [55].

Since wind turbines and solar panels are asynchronous, they do not inherently convert stored kinetic energy into additional electricity supply when the grid frequency drops. Wind turbines and solar panels also do not feature governors like those featured in conventional power plants, which means they do not feature a built-in primary frequency response mechanism. This suggests that significant levels of wind and solar power generation will leave electricity grids with a reduced ability to respond to sudden frequency disruptions during the critical first few seconds, leading to a greater number of load shedding events and blackouts. However, 'fast frequency response' technology can overcome this issue. This inverter-based solution uses sensors and control algorithms to rapidly sense a sudden drop in frequency and draw additional power from the wind turbines or solar panels, effectively mimicking the inertial response and primary frequency response of conventional generators [48].

Both wind turbines and solar panels can provide fast frequency response if they are pre-curtailed so that there is operational 'headroom' for a sudden power increase on command. This pre-curtailment also allows wind farms and solar farms to provide frequency regulation and spinning reserves [55]. Unlike solar panels, wind turbines can also provide fast frequency response from the kinetic energy

stored in the spinning rotor. While synchronous generators inherently provide an inertial response, wind turbines rely on sensors and controls to quickly detect a drop in grid frequency and then increase the torque in the system such that the rotor speed rapidly decreases, thereby discharging the stored kinetic energy through the generator and into the grid [56]. This produces a short burst of extra power supply to counteract a sudden supply deficiency on the grid, bridging the gap until other power reserves can engage [48].

In Quebec and Texas, wind turbines have been providing fast frequency response capabilities to the electricity grid for more than a decade [48]. These two jurisdictions feature the smallest of the four main North American electrical interconnections, which makes them more susceptible to frequency deviations. Smaller grid size combined with high levels of wind energy production makes fast frequency response capabilities especially important. Researchers are still investigating how the stability of electricity grid frequency will be impacted as more and more synchronous generators get replaced by inverter-based wind and solar farms in the future [48].

Fast frequency response typically requires a power response within 0.5 to 2.0 s of a frequency excursion [57]. Since batteries can ramp up to full power very quickly, fast frequency response capabilities are actually limited by the inverter rather than the battery [58]. Studies have shown that response times of 80 ms can be achieved for batteries connected to the grid through an inverter [58], making stationary battery systems well-suited for fast frequency response. Batteries can also discharge their stored energy over minutes or hours to provide spinning or non-spinning reserves in response to a contingency event, but batteries are not suitable for providing replacement reserves for many hours.

2.2.3 Voltage support and reactive power

Just as electricity grid frequency must be maintained within a set tolerance to ensure system reliability, so must electricity grid voltage. But while frequency is constant across the grid, voltage varies by location [55]. The system voltage is controlled by injecting or absorbing reactive power at appropriate locations. Since reactive power cannot be transmitted over long distances, voltage support services must be provided at various points throughout the grid, including the point of generation, the transmission system, and the distribution network [55]. Conventional power plants and inverter-based resources (including batteries) are capable of injecting and absorbing reactive power to provide voltage support services [59]. The modular nature of batteries is also well-suited for siting voltage support services at various locations in the electricity system. However, since voltage support requires very little energy throughput, it typically only makes sense to use a battery for this service if the battery is already performing other electricity grid energy storage services. Section 2.2.5 will cover the stacking of multiple energy storage services.

2.2.4 Black start

When a major contingency event results in a system blackout, relatively small black-start power plants must be used to provide the necessary startup power to bring larger power plants back online. Stationary batteries can be installed at power plants to provide these black-start services [60]. Black start is rarely called upon and is a relatively low value service. It is well provided by diesel generation because they are low capital cost and can be placed in standby with a full fuel tank for long periods of time without diminishment. Conversely, it would require batteries to typically be at 100% SOC

which causes significant degradation. As such, this service is not considered in the remainder of this report.

2.2.5 Stacked services

Stationary battery systems are not always capable of yielding a net economic benefit when serving a single energy storage service, but the economics can be improved by 'value stacking' so that a single battery system can perform multiple energy storage services and thereby access multiple revenue streams [26]. A stationary battery can participate in energy markets and ancillary service markets at the same time, or provide multiple ancillary services (e.g. frequency regulation and spinning reserves). Some regulatory barriers have limited the potential of value stacking [24], but regulations are trending towards opening up more opportunities for stationary energy storage. In 2018 for example, the Federal Energy Regulatory Commission issued Order 841 to guide ISOs and RTOs towards the removal of barriers for stationary energy storage systems to participate in all capacity, energy, and ancillary service markets [61].

3 Review of Second-life Battery Technology

This section provides a literature review on the current state of second-life battery technology, including EV battery design characteristics and battery repurposing processes. Practical experience with different EV battery pack designs at Dalhousie University will also be shared. Several important opportunities for standardization are identified.

3.1 Design of EV batteries

Two major EV manufacturers currently dominate the global market: China-based BYD and US-based Tesla together accounted for 35 % of all passenger car EV sales in 2023 [4]. Numerous unique EV models are also being produced by major vehicle brands across the United States, Europe, and Asia, including Chevrolet, Ford, BMW, Mercedez-Benz, Renault, Volkswagen, Volvo, Honda, Hyundai, Nissan, Toyota, and many others. The growing number of unique EV battery models tend to feature unique battery designs, which can vary significantly in terms of cell design, module design, and pack design. The numerous EV battery design parameters produce a wide range of EV battery energy ratings, typically ranging from 20 to 100 kWh in nominal energy capacity.

3.1.1 Packs, modules, and cells

A given EV battery pack generally comprises multiple battery modules connected in a series string, each of which comprises multiple cells connected in series and/or parallel strings. These three battery design levels are illustrated in Figure 3.2 for the example of a 2018 Chevrolet Bolt electric car. This particular battery pack features two different module sizes. Eight of the ten modules feature a '10S3P' configuration (i.e. ten series-connected cell groups and three parallel-connected cells within each cell group) while the other two modules feature an 8S3P configuration. The ten modules are connected in series to give an overall 96S3P configuration for the pack. Note that the bottom left image in Figure 3.2 shows the 'housing cover' removed from the 'housing base' to reveal the modules inside. The housing cover is sealed to the housing base in EV service, as pictured in the bottom right of Figure 3.2.

Most EV battery packs feature a 'module-to-pack' design such as the one shown in Figure 3.2. However, some manufacturers have begun adopting 'cell-to-pack' designs in recent years as a means of eliminating the inactive module components to increase EV driving range and reduce system complexity [62]. The latest evolution in EV battery design is the 'structural battery', which can further enhance driving range capabilities [63]. Structural batteries employ 'module-to-chassis' or 'cell-to-chassis' designs that eliminate the external housing from the battery pack in favour of integrating modules or cells directly into the vehicle chassis so that the battery acts as both an energy source and a structural component. The four pack design types are illustrated in Figure 3.1. Though development is ongoing, industry experts anticipate a shift towards cell-to-pack and cell-to-chassis batteries in the coming years [64], [65].

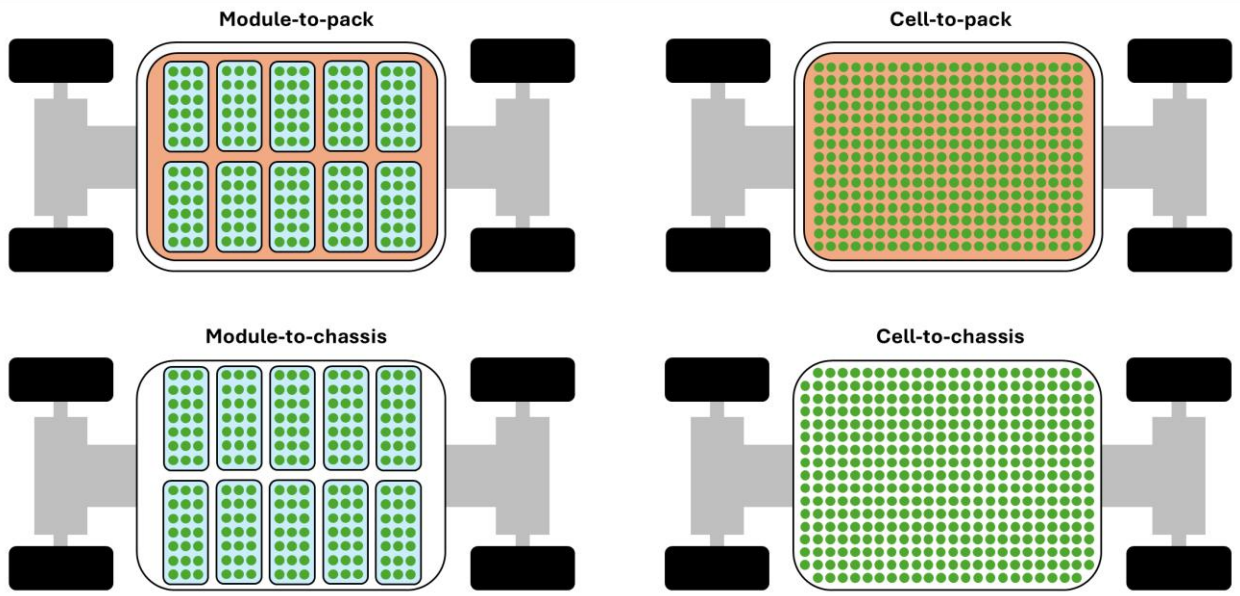

Figure 3.1 Illustrative comparison of four EV battery pack design types. Based on figure from [66].

All EV battery packs must of course be designed to fit within their intended vehicle. For passenger cars, the pack is generally situated at the base of the car, beneath the floor of the passenger cabin. A short and wide rectangular format is therefore commonly employed at the pack level, but some packs may feature irregular shapes that allow the pack to utilize more space within the vehicle. For example, the taller section of the EV battery pack shown in Figure 3.2 would sit beneath the rear passenger seats in the vehicle. Aside from size and shape, there are a number of pack-level design parameters which manufacturers can vary. These may include the quantity and layout of battery modules; the overall pack voltage (typically 400 V or 800 V nominal); the electrical circuitry (interconnects, contactors, fuses, etc.); the pack housing material; the method of fastening the housing cover to the housing base; the battery management system (BMS); and the thermal management system (TMS). Note that BMS and TMS designs will be elaborated on in Sections 3.1.2 and 3.1.4, respectively. Some EV battery packs also feature a mid-pack connector which allows for the high pack voltage to be manually halved for the sake of safety while technicians are handling the battery pack.

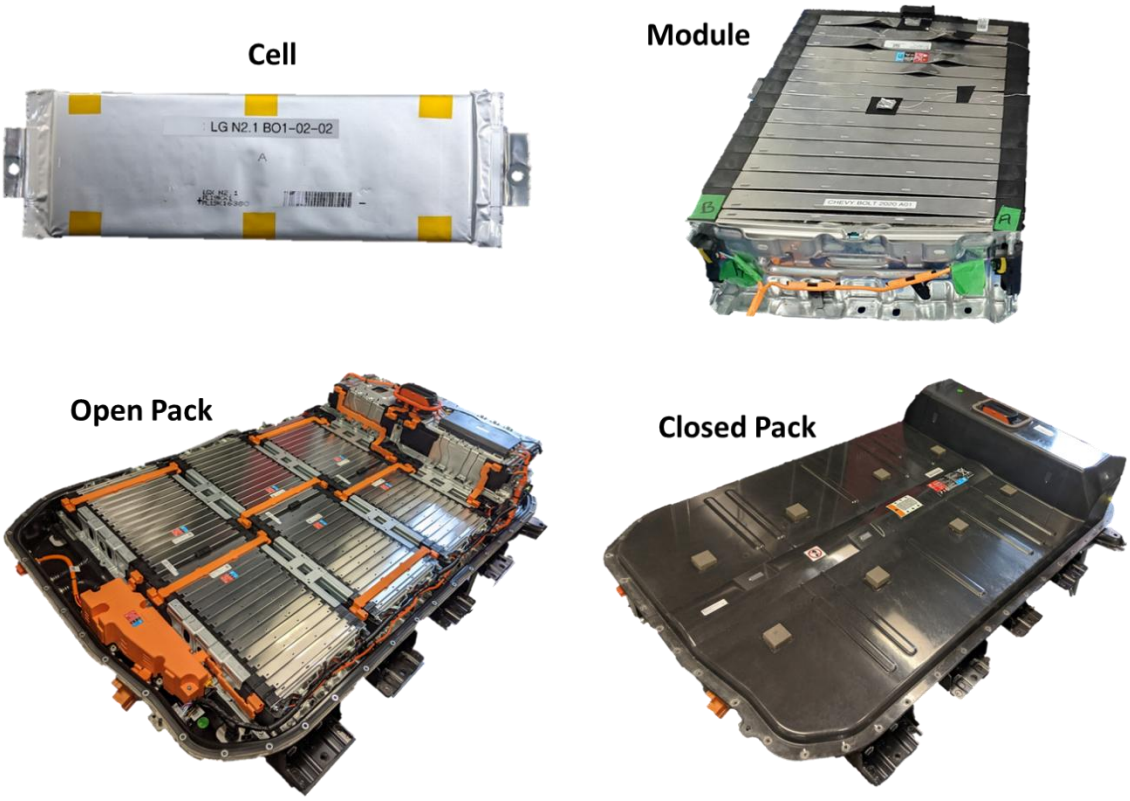

Figure 3.2 Example of a lithium-ion battery from a 2018 Chevrolet Bolt electric car, including single pouch cell (top left); single 10S3P module (top right); open pack comprising eight 10S3P modules and two 8S3P modules (bottom left); and closed pack with housing cover secured in place (bottom right).

The annotated photos in Figure 3.3 demonstrate the different shapes, sizes, housing materials, and module layouts among five battery unique EV battery packs tested at Dalhousie University. These include packs from a 2019 Tesla Model 3 SR+, a 2018 Chevrolet Bolt, a 2015 BMW i3, a 2012 Nissan Leaf, and a 2012 Lishen EV-LFP. Three of the packs feature a uniform module arrangement, with a consistent module height across the pack, while the Bolt and Leaf packs feature nonuniform module arrangements. The Bolt pack features eight uniform modules and two stacked modules at the rear, and the Leaf pack features three distinct module groupings. While the Lishen pack features a uniform module height, it includes three different module lengths with either five, six, or seven series-connected cell groups. Each of the five pictured battery packs features a unique quantity of modules: four for Model 3, ten for Bolt, eight for i3, 48 for Leaf, and 16 for EV-LFP. Note that the pictured i3 battery is missing two of its eight original modules.

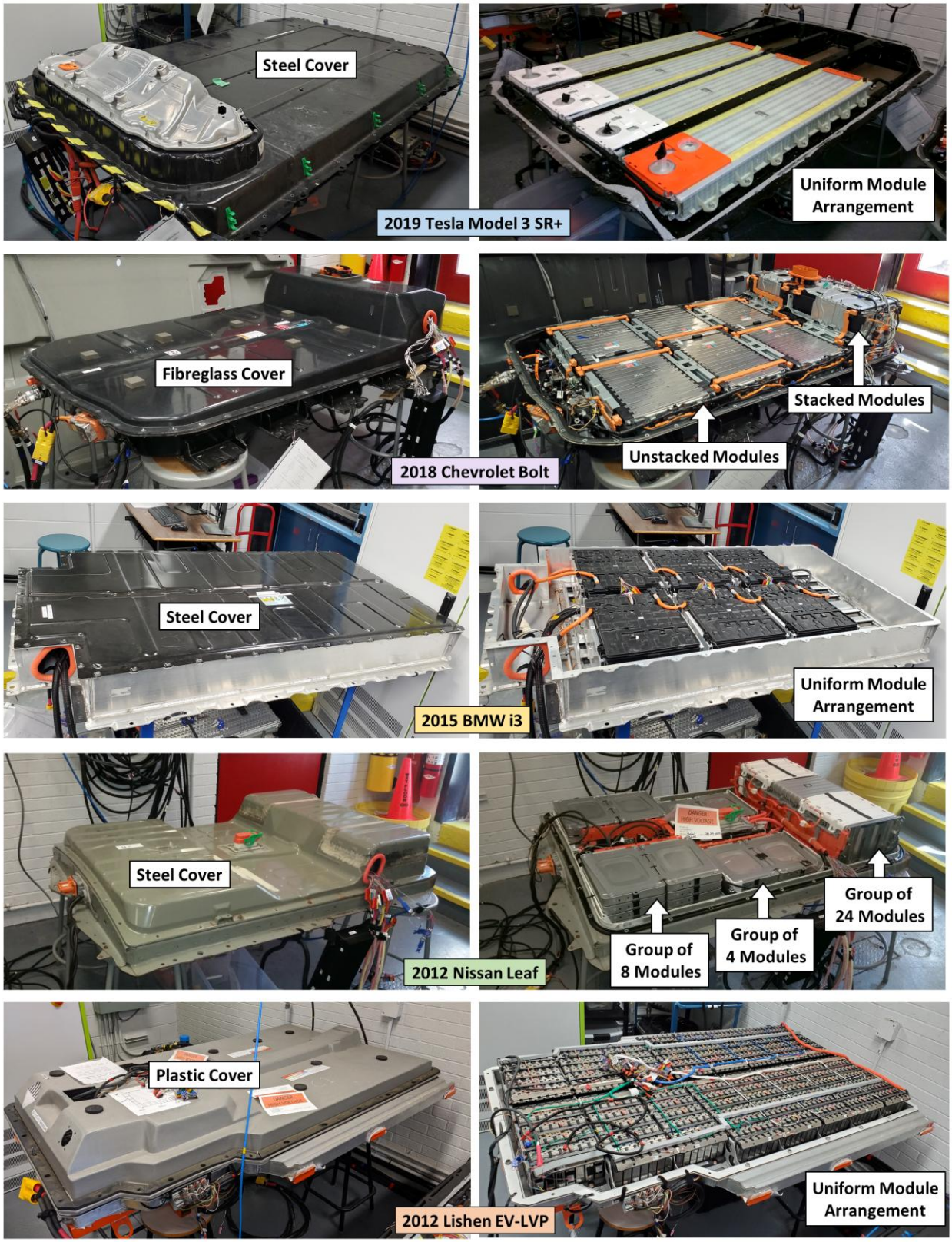

Figure 3.3 Examples of five unique EV battery pack designs shown in closed cover (left) and open cover (right) configurations.

Battery modules are generally constructed in a rectangular format, but there are many module-level design parameters which manufacturer can vary. These may include the number of cells connected in series and/or parallel strings; module housing materials; module dimensions; and the inclusion of other inactive materials which provide mechanical and/or thermal protection for the cells. For example, each of the four Tesla Model 3 modules pictured in Figure 3.3 features 24 series-connected cell groups each comprising 31 parallel-connected cells (2976 total cells in the pack), while each of the 48 Nissan Leaf modules features two series-connected cell groups each comprising two parallel-connected cells (192 total cells in the pack). The Tesla Model 3 battery also provides an example of other relatively complex module design features. Each of the four modules includes seven parallel liquid channels that pass between cylindrical cells as pictured in Figure 3.4, where the red circles are drawn at individual cell locations for illustrative purposes. The liquid channels make direct contact with one side of each cell as a means of heat rejection. Figure 3.4 also shows the light-green foam that fills all empty space within the Model 3 battery modules and separates each individual cylindrical cell from its neighbors. Specialized foams are sometimes featured in EV battery module designs to dampen mechanical vibrations, to absorb impact forces, and to thermally insulate neighbouring cells from each other to inhibit propagation in the event of thermal runaway [67]. Battery safety is discussed further in Section 3.1.2.

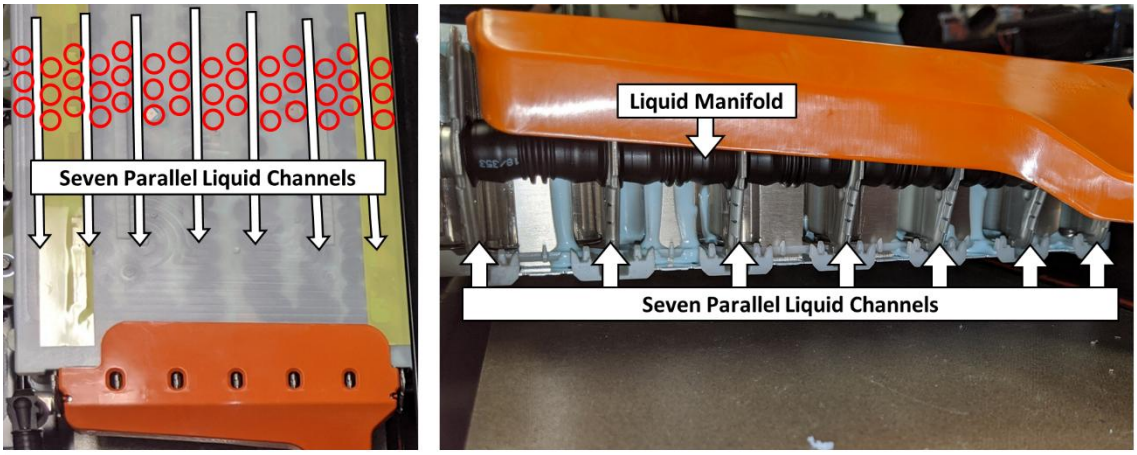

Figure 3.4 Construction of 2019 Tesla Model 3 SR+ battery module.

At the cell level, manufacturers can vary a wide range of cell component design parameters. One important consideration is the size and format of the cell housing. For EV applications, the 'cell stack' (a layered sequence of electrode, separator, electrode, separator, where each electrode layer consists of a metallic current collector with an active material coating) can be packaged into cylindrical, pouch, or prismatic cell formats [68], which are illustrated in Figure 3.5. In the cylindrical format, a single cell stack is constructed with a long length such that it can be wound into a 'jellyroll' and placed inside a cylindrical cell housing. Cylindrical cells are typically the smallest of the three formats and offer advantages for mechanical strength but disadvantages for packing density [69] as well as heat dissipation for larger diameters [70]. In the pouch format, the cell stack is cut to size such that it can be placed inside a flexible metal pouch without rolling or folding. Multiple cell stack units can be stacked on top of one another inside a single pouch. Pouch cells have advantages for weight and heat dissipation but disadvantages for mechanical durability due to the flexible pouch material [69], [70]. The prismatic format is essentially a thicker, hard-shell version of the pouch format, and can use

winding or stacking to fit the cell stack into the cell housing. Prismatic cells have advantages for packing density [69] and disadvantages for heat dissipation due to their relatively high volume-to-surface-area ratio [68]. For all three cell formats, the positive and negative current collectors respectively connect to the positive and negative terminals which protrude to the outside of the cell housing to connect with the external circuit.

Figure 3.5 The three main lithium-ion cell formats: cylindrical, pouch, and prismatic.

The wide range in EV battery cell sizes is illustrated in Figure 3.6, which shows a cylindrical Tesla Model 3 cell next to a large prismatic BYD Blade cell. The Model 3 cell is 21 mm in diameter and 70 mm in height, while the Blade cell is 960 mm in length (spanning the full width of the EV battery pack), 90 mm in height, and 13.5 mm in width. The Blade cell is used in a cell-to-pack battery design which eliminates the module level from the battery pack.

Figure 3.6 Comparison of Tesla Model 3 cell (cylindrical) and BYD Blade cell (large prismatic).

Cell chemistry can also vary significantly in terms of positive and negative active materials, dopants, binders, and conductive additives; electrode coating thickness, porosity, and particle size; electrolyte solvents, salt concentrations, and additives; separator material, thickness, and porosity; and current collector thickness. The selected materials must achieve an appropriate balance of energy capacity, power capability, safety (i.e. fire risk), cycle life, cost, and environmental impact to meet the requirements of the intended energy storage application. A number of lithium-ion intercalation materials have proven effective for EV applications, with the most common positive electrode materials being alloyed lithium nickel cobalt manages oxide ($LiNi_{1-y-z}Co_yMn_zO_2$ or NMC for short), alloyed lithium nickel cobalt aluminum oxide ($LiNi_{1-y-z}Co_yAl_zO_2$ or NCA for short), lithium manganese

oxide ($LiMn_2O_4$ or LMO for short) and lithium iron phosphate ($LiFePO_4$ or LFP for short) [71]. While the numerous other cell design parameters also influence battery characteristics, Table 3.1 draws on a number of publications [71-75] to give generalized qualifications demonstrating the main differences between these four positive electrode materials.

Table 3.1 Comparison of key characteristics for common positive electrode materials used in lithium-ion cells for EV applications.

Category	LMO	LFP	NMC [a]	NCA [b]
Energy	Poor	Poor	Good	Best
Power	Best	Good	Medium	Medium
Cycle life	Poor	Best	Good	Medium
Safety	Good	Best	Medium	Poor
Cost	Best	Good	Medium	Poor
Environment	Good	Best	Medium	Medium

[a] NMC considered to have 33 % ≤ Ni ≤ 60 %.
[b] NCA considered to have 80 % ≤ Ni ≤ 85 %.

Table 3.1 shows that while no single positive electrode material scores high in all categories, the weaknesses of some materials correspond to the strengths of others. Researchers have therefore developed 'blended' positive electrode materials which combine multiple distinct compounds to achieve synergistic benefits. Most studies in this area have experimented with the blending of NMC or NCA (high energy) with LMO or LFP (high-power, low-cost, good safety, low environmental impact) to achieve a more balanced electrode material [76-80]. A range of NMC-LMO blends have been deployed in commercial EVs such as the Nissan Leaf and BMW i3 [81].

Today, a large share of EV batteries feature a positive electrode composed of either NMC with Ni > 30 % or NCA with Ni ≥ 80 % [82]. The first commercial NMC batteries used a 1:1:1 ratio of Ni, Mn, and Co (termed NMC111), but continued research has progressively increased the nickel content to improve energy density and EV driving range, leading to a wide range of NMC variants such as NMC532, NMC622, and NMC811 [83]. Higher nickel content generally results in poorer safety and cycling stability [84], but a variety of techniques are being explored to improve these properties for EV applications, such as doping, particle coatings, and electrolyte additives [12], [85]. The latest advancements have sought to push this trend to Ni > 85 % by combining the benefits of NMC and NCA in new NMCA electrode variants such as $LiNi_{0.89}Co_{0.05}Mn_{0.05}Al_{0.01}O_2$ [86]. It was reported in 2022 that 65 to 70 % of EVs use NMC (some blended with LMO), 15 to 20 % use NCA (the preferred choice of Tesla), and 10 to 20 % use LFP (the dominant choice in China where urban driving allows for lower driving range and thus lower battery energy density) [71].

At the negative electrode, graphite has been the most common intercalation material for lithium-ion batteries since 1994 [87]. Hard carbon and lithium titanate ($Li_4Ti_5O_{12}$, or LTO for short) are also used as negative electrode materials, though far less commonly than graphite. It was reported in 2022 that > 99 % of EVs use graphite at the negative electrode [71]. However, there is still some variability in negative electrode material design among EV manufacturers. For example, lithium-ion batteries featuring graphite-silicon blended negative electrodes have been deployed in some modern EVs such as the Tesla Model 3 as a means of increasing battery energy density [88], [89].

3.1.2 Battery safety

One of the biggest safety concerns with lithium-ion batteries is that their components begin to react and decompose exothermically when the battery is at elevated temperatures (typically above 90 °C), which can lead to a dangerous self-heating chain reaction known as thermal runaway [193], [194]. This reaction can be highly exothermic, and the organic electrolyte components can auto-ignite at temperatures near 450 °C [90]. All the cell components eventually break down or melt as the temperature rises to 800 °C or more [91], resulting in catastrophic failure in the form of smoke, fire or explosion. A number of SOC-dependent positive electrode material properties influence the activation and severity of thermal runaway [92], but as shown in Table 3.1, it is generally accepted that LFP and LMO have the best safety properties among the main positive electrode types while nickel-rich materials like NCA have the poorest safety properties [72], [93].

The elevated temperatures which trigger thermal runaway may arise in a variety of ways. Continuous high-power cycling can generate enough heat to reach these temperatures if the heat cannot be effectively dissipated [94]. Temperature is typically monitored in commercial batteries so these elevated temperatures can be avoided, but large battery systems may feature localized hotspots due to poor thermal conductivity or nonuniform current distribution. A TMS is therefore commonly employed to maintain measured battery temperatures in a safe range; typically below 60 °C where solid electrolyte interface (SEI) decomposition can first be detected [91]. Thermal runaway incidents are usually triggered by unintentional overcharging or by a short circuit within an individual cell, which may be caused by external damage or by metallic dendrites penetrating the separator after extensive degradation by lithium plating [95]. Once an individual cell is in thermal runaway, the process can propagate via heat transfer or side rupture to neighboring cells in a battery pack.

In order to decrease the likelihood of thermal runaway, commercial lithium-ion cells include safety features designed to limit or interrupt the current when the voltage, temperature or pressure exceeds a set threshold. Some examples include pressure-sensitive current interrupt devices, vent ports, temperature-sensitive resistors, and specialized separators which shut down Li^+ transfer at a set temperature [95]. Note that pouch cells typically lack some of the safety features that cylindrical and prismatic cells feature (e.g. current interrupt devices, vent ports). When multiple cells are connected in series, a BMS is necessary to monitor and balance individual cell voltages to ensure that no cells become overcharged, or reversed on over-discharge [94]. The BMS can also monitor individual cell temperatures and report temperature alarms to the battery control system.

Safety can also be factored into module and pack designs. As shown previously in Figure 3.4, battery modules sometimes feature specialized foam materials to separate cells and inhibit propogation of thermal runaway. Modules can also be separated within a given pack for this same purpose. In the case of the Tesla Model 3 battery, the pack is designed such that the cylindrical cells would rupture downwards (i.e. away from the passengers) in the event of a major failure. All electrial connections are covered with insulating materials to prevent short circuits and human injury. Pack-level fuses, contactors, and manual disconnects provide additional mechanisms to interrupt current flow if necessary. The latest EV batteries employ active TMS designs (discussed further in Section 3.1.4) to mitigate temperature rise and reduce the likelihood of hot spots.

Additional safety considerations are applicable to second-life batteries. For one, the latest EV batteries are more likely to feature nickel-rich positive electrode materials (due to high energy density), which are inherently less safe than the LFP technology (lower energy density) commonly used in new batteries for stationary applications. Note however that LFP is becoming increasingly common in EVs with lower driving range requirements (particularly in urban China). Another consideration is that the series connection of EV battery modules or packs in second-life service should not exceed the rated voltage of electrical insulator materials. Furthermore, if an EV battery is designed with an active TMS, safety risks will likely increase if the active TMS is disabled in second-life service. All built-in battery safety features should be identified when repurposing a given EV battery so that informed decisions can be made regarding the design of the second-life system. This is especially true if the original battery pack is to be disassembled into modules and repackaged into a customized system for second-life service.

3.1.3 Battery management systems

The voltages of individual lithium-ion cells in a series string must be monitored and controlled to ensure that no cells become overcharged or enter into thermal runaway. This 'cell balancing' operation is performed by a BMS. A BMS may carry out a variety of important functions for a battery system, which are described in detail in [96]. This section will summarize the main functions of a BMS in a typical EV battery pack, which are illustrated in Figure 3.7.

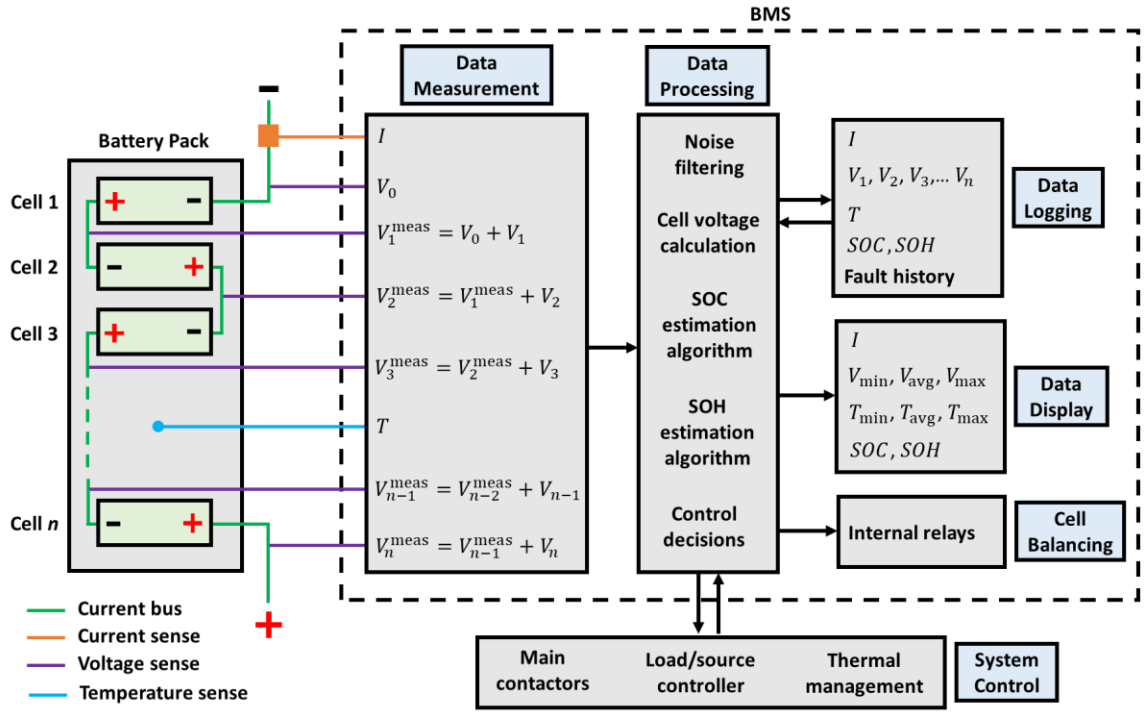

Figure 3.7 Basic schematic of the main functions of a battery management system.

The BMS monitors cell voltages using voltage sensors placed between each cell or cell group in the series string. The measured voltages (shown as V_i^{meas} in Figure 3.7) are referenced to a common voltage point (shown as V_0 in Figure 3.7) placed at the negative end of the string, allowing the BMS to calculate individual cell voltages (shown as V_i in Figure 3.7) using basic arithmetic. Typically, the

BMS also measures the battery current through a current transducer, as well as temperatures at various locations in the pack using thermistors. The measured data is processed, logged in internal recorders, and displayed on a user interface, often including statistical figures such as minimums, averages, and maximums.

Cell balancing is a key BMS function which prevents overcharge of individual cells while the battery is charging. There are passive and active cell balancing techniques, but passive balancing is most common due to its simplicity and affordability. To conduct passive balancing, the BMS features switches which can be closed to place a resistor across any individual cell. When a cell reaches a specified upper voltage limit during charge, the BMS closes the appropriate switch, causing a portion of the applied current to dissipate through the resistor as waste heat. This prevents the voltage of the cell in question from increasing further while the other cells continue to charge. The cell balancing process continues on subsequent cells until the whole battery reaches a specified charge termination threshold. Active balancing employs more advanced and expensive techniques to redirect current from a high-voltage cell to a low-voltage cell during charge or discharge. Passive balancing is typically only performed during charge or standby, and it results in some charge energy being curtailed as waste heat.

In addition to current, voltage, and temperature, modern BMS designs often feature specialized algorithms that can process present and historical measurements to estimate the SOC and SOH of the battery pack and/or individual cells [97]. For SOC estimation, algorithms often include a combination of 'coulomb counting' (i.e. integration of battery current over time) and a means of using voltage and temperature measurements to correct the coulomb counting error that inevitably accumulates over time due to imperfect current measurements and battery degradation. Correction techniques typically use a numerical battery model (e.g. equivalent circuit model) as the basis for Kalman filters, particle filters, fuzzy logic, or artificial neural networks, which vary in terms of complexity, reliability, and computational requirements [96], [98], [99]. For SOH estimation, algorithms often rely on historical measurements and complex predictive models to assess capacity fade and internal resistance growth. The same types of correction techniques that are applied to SOC estimation algorithms can also be applied to SOH algorithms.

The BMS also uses the processed data to detect faults and make decisions regarding battery control. For example, if the BMS detects that the battery is approaching a specified SOC limit, the BMS will communicate with the load/source controller to reduce the power envelope for discharge or charge. If the BMS detects that battery temperatures are outside the preferred range, the BMS will engage the TMS or adjust the power envelope. If the BMS detects that one or more cells have become disconnected or reached unsafe temperatures, the BMS will record a fault and open the main contactors to disconnect the battery from power flow. Communication between the BMS and external devices is typically done using a digital communication protocol such as CAN bus (vehicles) or Modbus (stationary).

BMS designs can vary considerably from one battery manufacturer to another, and can be generally categorized according to four main BMS topologies: centralized, modular, master-slave, and distributed [100]. These topologies are illustrated in Figure 3.8 and discussed below.

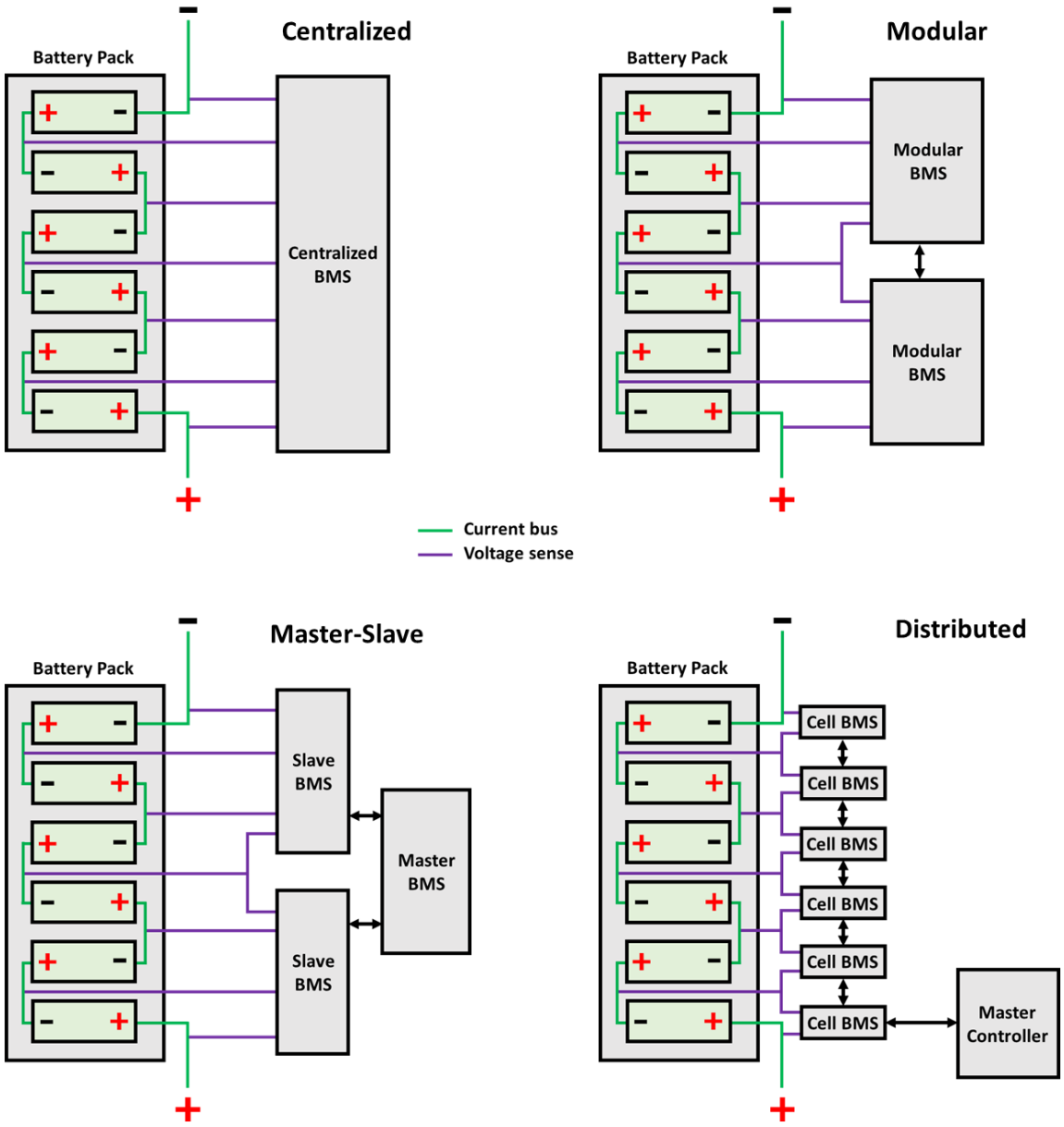

Figure 3.8 Illustrative comparison of four main BMS topologies. Partially based on figure from [100].

The centralized topology (used in Chevrolet Bolt, Nissan Leaf, and others) features a single hardware device connected to all cell groups, which is convenient if the BMS needs to be adapted or replaced during the battery repurposing process. However, the centralized topology presents the greatest safety risk, since all cell voltages (summing to the full pack voltage of 400 V or more) are wired into a single piece of hardware. The centralized topology also presents the greatest failure risk, since a centralized BMS represents a single-point failure for the battery pack (i.e. a BMS failure or single cell group failure makes the entire pack inoperable). Safety and failure risks are mitigated by modular, master-slave, and distributed BMS topologies, which divide the cell groups into multiple smaller BMS units. This means that safer voltage levels will be present at a given BMS unit, and that a single BMS failure or cell group failure will only impact a portion of the pack, making it easier to disconnect or

replace weak cells during the battery repurposing process. However, these topologies also introduce disadvantages for battery repurposing, such as increased wiring complexity and a greater number of hardware devices with specialized compatibility requirements.

The modular topology (used in Tesla Model 3) divides the BMS functions across multiple BMS units that share information with each other via communication lines. These modular BMS units are identical in terms of hardware, though one BMS unit may be designated as the primary decision maker for pack-level functions. The master-slave topology (less common in EV applications but common in stationary applications) uses a two-tier system, with multiple slave BMS units conducting cell monitoring and balancing while independently reporting information to a single master BMS unit that communicates with the main battery controller. Unlike the modular topology, the master BMS does not feature the same hardware as the slave BMS units. While the master unit represents a single-point failure, it is much easier to reprogram or replace than a centralized BMS. The distributed topology (used in Hyundai Genesis GV60) is similar to master-slave, but with a greater number of smaller BMS boards applied to smaller collections of cell groups. The individual cell boards have limited functionality compared to slave BMS units, primarily executing cell-level measurements and voltage balancing at the command of the master controller. The master controller handles the data and decision-making via communication lines with each individual cell board. This topology offers the greatest level of modularity and lowest failure risk. For example, the modular BMS of the Tesla Model 3 SR+ battery uses four BMS modules each responsible for 24 cell groups (25 % of the battery pack), while the Hyundai Genesis GV60 battery uses 32 distributed cell boards each responsible for 3 cell groups (3 % of the battery pack).

3.1.4 Thermal management systems

Lithium-ion batteries have an optimal operational temperature range of approximately 25 to 40 °C, and significant deviations outside this range can lead to accelerated degradation, reduced performance, and elevated safety risks [8], [9], [101]. Since EV battery packs feature many interconnected cells in a densely packed arrangement, it is also generally recommended that the temperature differential between the warmest and coolest cells in the pack be maintained below 5 °C to prevent cell SOH levels from diverging within the pack over time [101], [102]. The TMS of an EV battery pack is therefore essential to maintain battery temperatures and temperature gradients within the preferred range set by the manufacturer. Most studies on novel TMS designs for EV batteries use both the maximum temperature and the temperature differential as metrics to evaluate and optimize TMS performance [103].

Just as there is significant variability in battery design, there is also significant variability in TMS design. A wide variety of studies have investigated or reviewed various EV battery TMS technologies in recent years [103-110]. These TMS technologies are summarized graphically in Figure 3.9, where red bordering is used to designate the technologies that are presently deployed in commercial EV batteries. The various TMS technologies can generally be classified as either passive or active, which are respectively designated by blue and green shading in Figure 3.9. Passive TMS designs require no energy input during operation, while active TMS designs consume electrical energy to drive heat transfer. The main heat-transfer mediums discussed in the literature are air, liquid, phase change materials, the thermoelectric effect, as well as various hybrids of these unique technologies.

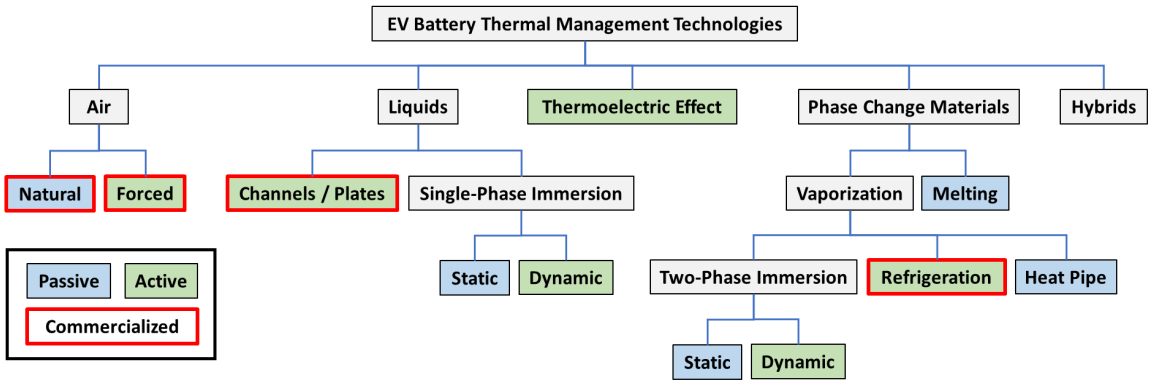

Figure 3.9 Summary of TMS technologies being researched for EV battery applications.

Passive-air TMS designs generally rely on natural convection (essentially the absence of a designated TMS), though some designs allow for air to flow through channels in the battery pack while the vehicle is in motion [109]. Active-air TMS designs include electric fans or blowers to force air through the battery (independent of vehicle speed), with a wide variety of air channel designs and flow patterns proposed in the literature. Both passive-air and active-air TMS designs have been deployed in commercial EV batteries. For example, the Nissan Leaf battery uses a passive-air TMS, while the Renault Zoe battery pack uses an active-air TMS [106].

For EV battery packs with greater thermal management loads, the relatively low thermal conductivity, heat capacity, and convection coefficients of air-based TMS designs can be improved upon with liquid-based TMS designs at the expense of system complexity and cost [105]. Many commercial EV batteries feature an active-liquid TMS using a glycol/water mixture as the liquid coolant. Since water-based coolants are electrically conductive, the coolant must not make direct contact with the cells or else an electrical short circuit could lead to a fire. Instead, an electric pump forces the liquid coolant through thermally conductive channels that exchange heat directly with cell or module surfaces. Many different liquid channel designs have been proposed in the literature, but commercial designs generally feature either 'side cooling' (i.e. channels passing between adjacent cells within a module) or 'bottom cooling' (i.e. channels within a large plate sitting directly above or below the module) [105]. Different liquid flow patterns have also been explored, such as multiple parallel channels with a common header vs a single serpentine channel [104]. For example, the active-liquid TMS designs of Tesla Model 3 and Chevrolet Bolt battery packs (pictured in Figure 3.3) respectively feature parallel side cooling and serpentine bottom cooling.

Active-liquid TMS designs featuring liquid channels or plates are sometimes referred to as 'indirect liquid' TMS designs. In contrast, 'direct liquid' TMS designs allow for the liquid to make direct contact with the cells or modules without the use of liquid channels. This TMS technology is also called 'immersion cooling'. The liquid used for immersion cooling is typically a dielectric fluid such as a silicone oil or specialized hydrocarbon so that electricity cannot be conducted through the liquid and short-circuit the battery. Immersion TMS designs can be passive or active depending on whether a pump is used to force the dielectric fluid through the battery for enhanced heat transfer. This TMS technology has not yet been widely commercialized in EV applications, but it has been introduced into high-end electric sports cars such as the McLaren Speedtail [105]. Wider commercial adoption is expected in the future.

Immersion TMS designs can be subdivided into 'single-phase' and 'two-phase' immersion. Single-phase immersion strictly uses a liquid to exchange sensible heat with the battery, while two-phase immersion uses a dielectric fluid with a boiling point below the specified upper temperature limit of the battery [105]. Figure 3.9 therefore classifies two-phase immersion with other phase change TMS technologies that can absorb latent heat to further mitigate battery temperature rise. Like two-phase immersion, refrigeration and heat pipe technologies also capitalize on the latent heat of vaporization, though in these cases the working fluid does not make direct contact with the battery. In contrast, solid-liquid phase change materials capitalize on the latent heat of melting, typically by encapsulating the cells in a specialized paraffin wax [103]. The BMW i3 is one commercial example of a refrigeration TMS in EV battery applications [111], but other phase change TMS technologies presently remain in the research stage due to performance limitations, cost, or technical immaturity [112]. For example, the poor thermal conductivity of suitable solid-liquid phase change materials makes it challenging to reject the heat that has been absorbed from the battery, so ongoing research seeks to embed thermally conductive materials such as metals or graphite within the phase change materials [110].

Research has also explored the possibility of actively exchanging heat with EV batteries using the thermoelectric effect. Though it has been generally concluded that the thermoelectric effect cannot efficiently meet TMS requirements for EV batteries [113], there is potential to combine thermoelectric technology with other TMS technologies for hybridized performance benefits. Combining various TMS technologies into hybrid TMS designs is the subject of much research [114], though no such systems have yet been commercialized in EV battery applications.

While all proposed TMS technologies can be used to prevent an EV battery from self-heating beyond a set upper temperature limit during operation, not all TMS technologies can be used to raise the temperature of an EV battery above a set lower temperature limit. To avoid the large overpotentials associated with low-temperature (e.g. < 0 °C) battery operation [104], an EV battery should be pre-heated before the vehicle is driven in cold environments. Battery pre-heating cannot be directly achieved by passive TMS technologies, so it is necessary to operate the battery in a specialized self-heating mode using resistive heaters applied directly to the battery instead of pre-heating the air or liquid in an active TMS [113]. It has also been proposed to apply an AC current to EV batteries while plugged in as a means of pre-heating in cold environments [104].

3.2 Repurposing processes for second-life batteries

The repurposing of a used EV battery entails a series of steps that may vary based on geography, EOVL circumstances, government regulations, and second-life business models. Figure 3.10. provides a generalized depiction of the main steps in the EV battery repurposing process, which include:

- Removing the battery from the vehicle
- Inspecting the battery for damage
- Transporting the battery to a specialized facility
- Evaluating the SOH of the battery to confirm its viability for second-life
- Modifying the battery for its intended second-life application (potentially including partial or complete disassembly of the original battery pack)

- Testing and certifying the repurposed battery
- Integrating the repurposed battery into a stationary energy storage system
- Operating, monitoring, and maintaining the second-life battery system until the battery reaches EOL and must be recycled

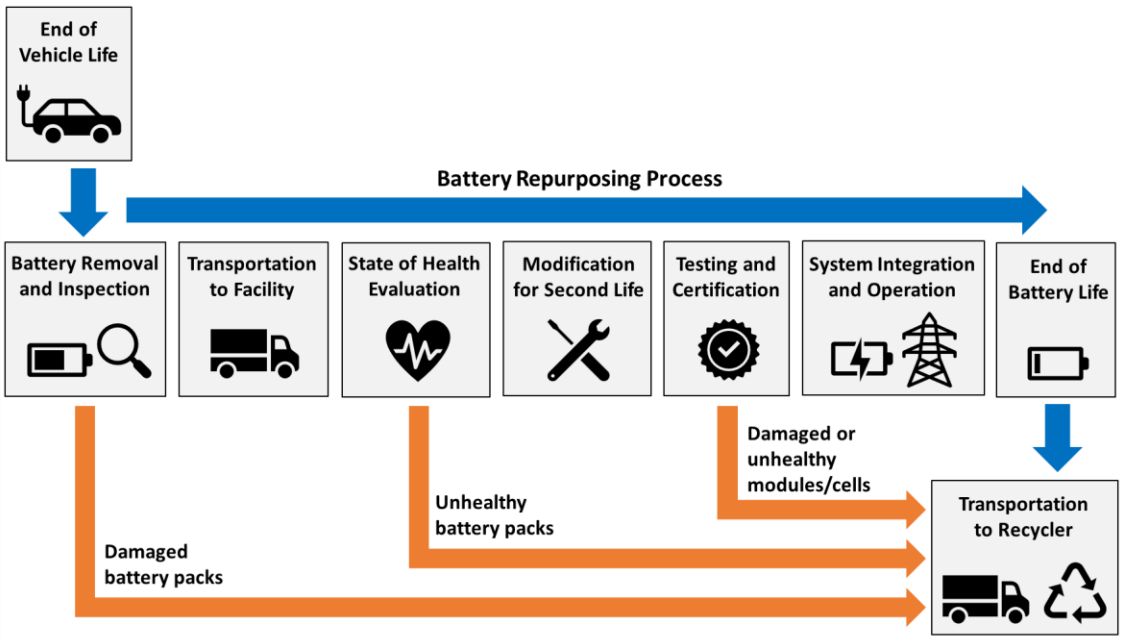

Figure 3.10 Graphical summary of the EV battery repurposing process.

There are different pathways that used EV batteries may follow before being repurposed in second-life applications, as illustrated in Figure 3.11. If an EV battery is being replaced under warranty, it will most likely be removed from the vehicle by dealerships and service centres that are owned or contracted by the original manufacturer [115]. The manufacturer will then determine whether the battery should be repaired or remanufactured for continued EV service, sold to a battery repurposing company, or sent to a battery recycler. In some cases, the original manufacturer will contract an independent battery remanufacturing facility (such as Cox Automotive in the United Sates [116]) to make this determination. If the battery is suitable for repurposing, the original manufacturer may elect to retain battery ownership for their own second-life battery projects instead of selling the battery to an independent battery repurposing company [22]. If the battery is initially removed from the vehicle after the warranty period (typically 8 to 10 years), then it may be an automotive recycler or repair garage that removes the battery and then sells it to a repurposing company, battery recycler, or a private buyer [115]. These different pathways mean that a battery repurposing company could acquire an EOVL battery that has already been identified and evaluated for SOH (e.g. from the original manufacturer or a remanufacturer), or acquire an EOVL battery with very little accompanying information (e.g. from an automotive recycler, repair shop, or private buyers). The second-life battery supply chain is nascent and still evolving.

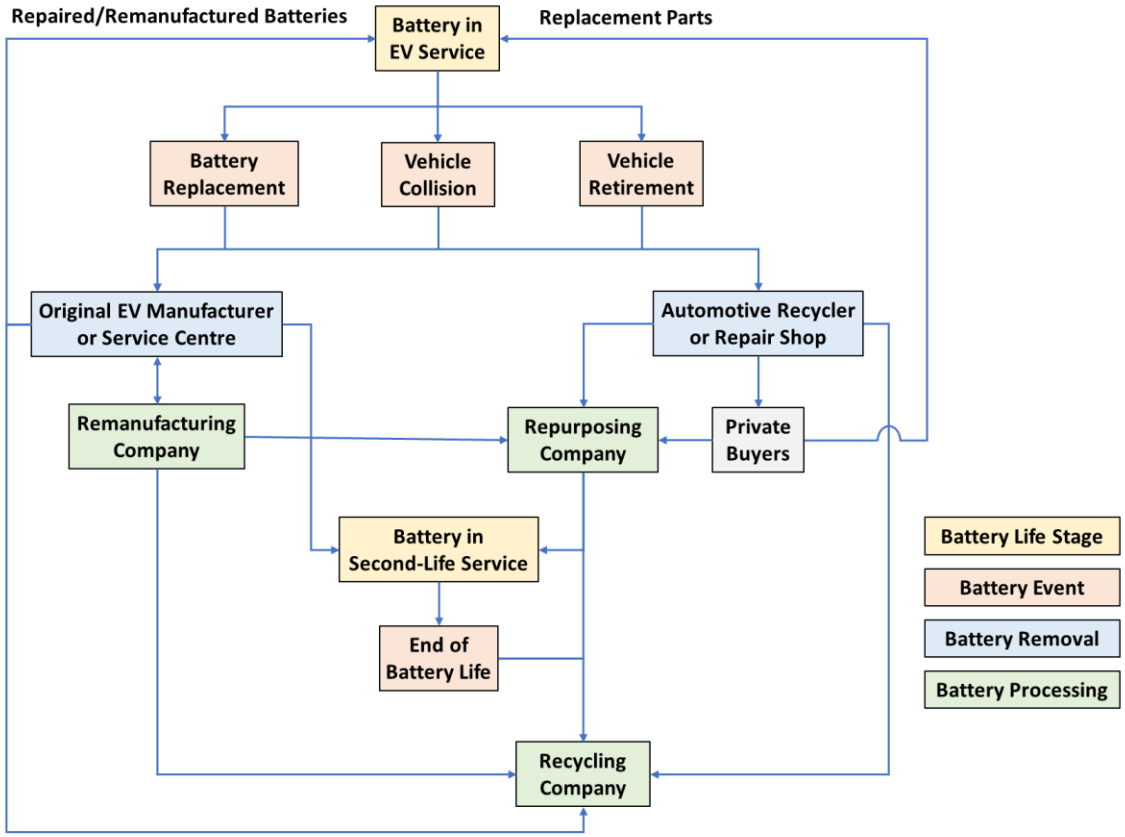

Figure 3.11 Possible repurposing pathways for EV batteries. Partially based on figure from [115].

3.2.1 Removing, inspecting, and transporting EV batteries

Removing an EV battery from the vehicle is not a straightforward task and should be carried out by qualified technicians [34]. Apart from the complexity of the procedure, the high voltage of EV batteries calls for appropriate training and safety equipment during handling. Transportation of the removed battery is also non-trivial, since used lithium-ion batteries are classified as dangerous goods and sometimes also as hazardous waste, and are therefore subject to transportation regulations that require the batteries to be handled by trained personnel and shipped in approved containers on approved vehicles [115]. It is also considered best practice that the batteries be discharged below 30 % SOC before being shipped. This figure comes from United Nations classification UN3480 for air shipment of lithium-ion batteries [117], though air shipment of used lithium-ion batteries is not permitted at all [20], [118]. If an immediate visual inspection reveals damage to the battery after removal from the vehicle, then it should be transported directly to a recycling facility [119]. Otherwise, the battery can proceed along the repurposing pipeline.

3.2.2 Identifying used EV batteries

Somewhere along the supply chain, used EV batteries must be identified and screened before they are repurposed. To ensure that a given EV battery can be repurposed safely and effectively, battery repurposing facilities must have as much identifying information about the battery as possible, such as make and model, manufacturing year, rated voltage and energy capacity, cell chemistry, module

design, TMS design, and pack disassembly steps. Table 3.2 provides examples of necessary identifying information for the five EV battery packs pictured previously in Figure 3.3. If the battery has been acquired directly from the original manufacturer, this information should be readily accessible. However, detailed identification may be challenging if the battery has been acquired from an automotive recycler or intermediate handler. Ensuring that necessary identifying information is available throughout the battery life cycle would facilitate both repurposing and recycling [120]. The concept of a 'battery passport' has been introduced in recent years to address this issue, which will be discussed further in Section 6.

Table 3.2 Specifications of sample EV battery packs.

Specification	Battery 1	Battery 2	Battery 3	Battery 4	Battery 5
EV manufacturer	Tesla	Chevrolet	BMW	Nissan	Lishen
EV model	Model 3 SR+	Bolt	i3	Leaf Gen 1	EV-LFP
EV build year	2019	2018	2015	2012	2012
Cell supplier	Panasonic	LG Chem	Samsung	AESC	Lishen
Positive electrode material	NCA	NMC622	NMC111 + LMO	LMO + LNO	LFP
Negative electrode material	Graphite + silicon	Graphite	Graphite	Graphite	Graphite
Cell format	Cylindrical	Pouch	Prismatic	Pouch	Prismatic
Cell housing	Steel	Pouch foil	Aluminum	Pouch foil	Aluminum
Cell grouping	96S 31P	96S 3P	96S	96S 2P	104S 7P
Module quantity	4	10	8	48	16
TMS type	Active liquid	Active liquid	Active refrigerant	Passive air	Passive air
Rated coulombic capacity (Ah)	144	170	60	65	115
Rated energy capacity (kWh)	50	60	22	24	38

3.2.3 Screening used EV batteries

Screening is the process of evaluating the SOH of the battery to determine its remaining value as an energy storage device. If the SOH is very high (e.g. > 95 %), then it may be most valuable in continued EV service. If the SOH is low (e.g. < 60 %) then it may be best to recycle the battery right away. Intermediate SOH levels are suitable for repurposing, and the specific SOH level of a given battery may help determine which stationary energy storage applications the battery is best suited for. Appropriate battery test equipment and expertise is of course required to determine the SOH of a given EV battery.

Battery SOH does not have a universal definition due to the many complex degradation pathways of lithium-ion batteries (discussed further in Section 4.3.1), which means there is no universal method for screening second-life batteries. The most basic SOH evaluations involve capacity tests (taking many hours) and/or pulse resistance tests (requiring very high current source/sink). Some of the more advanced methods include the equivalent circuit modelling, electrochemical impedance spectroscopy (EIS), differential voltage (DV) analysis, and incremental capacity (IC) analysis, each requiring highly specialized equipment or days of testing, while data-driven methods such as machine learning can be used to reduce test time when the usage history of the battery is available [33]. Detailed explanations of these complex methodologies are outside the scope of this report, but their advancement and standardization are of great importance for the second-life battery industry. One startup company claims they can perform a battery health assessment in less than 10 minutes [121].

The complexities of degradation also make it challenging to assess the long-term value of second-life batteries based on SOH alone. One consideration is that different lithium-ion cell designs can exhibit very different degradation characteristics, so two different EV batteries could degrade at very different rates in second-life service despite yielding the same SOH at EOVL. Even if two EV batteries are of identical design and SOH at EOVL, they might still degrade at different rates in second-life service if their usage histories are significantly different (e.g. city driving vs highway driving; slow charging vs fast charging). To address these challenges, 'remaining useful life' (RUL) is often used as an additional battery metric alongside SOH. However, RUL assessment typically requires complex data-driven methods fed with historical data for the battery in question, which may not be available to companies who acquire used EV batteries [122].

3.2.4 Modifying EV batteries for second-life service

Once a used EV battery has been deemed suitable for second-life service, it can be repurposed at either the pack level or the module level, as shown in Figure 3.12. Module level repurposing entails disassembling the original battery pack, removing the modules from the pack, and repackaging the modules into a new enclosure designed for the intended second-life application. Pack-level repurposing foregoes most or all of these steps so that the EV battery pack can be repurposed in its original battery housing. Cell-level repurposing is generally considered impractical due to the additional effort required to disassemble each module (often welded together) and repackage the cells [122].

Figure 3.12 Examples of pack-level (left) and module-level (right) repurposing of Nissan Leaf EV batteries in second-life energy storage applications.

There are advantages and disadvantages associated with both module-level and pack-level repurposing. Module-level repurposing provides more opportunity to customize the system for second-life service, as well as the opportunity to screen and sort individual modules to improve SOH homogeneity in the second-life system. However, the additional disassembly and repackaging steps associated with module-level repurposing can amount to significant time and labour costs, as the complexity and diversity of EV battery designs makes it difficult to automate these processes [122]. The time and labour requirements for complete pack disassembly depend on how difficult it is to remove the pack housing cover (typically bolted and sealed), disconnect the electrical circuitry and sensors (potentially hundreds of connections, with some at high voltage), disconnect and flush the TMS (where applicable), and remove the modules (typically fastened in place within the pack), all of which can vary substantially for different pack designs. Repackaging also comes with equipment costs, including a new BMS [123]. Repurposing the entire pack without modification would be the most economical approach, but there must be a reasonable level of SOH homogeneity among the cells since the useful energy capacity of the pack will be limited by the weakest cell group [124]. Partial pack disassembly can allow for weak cell groups to be removed from the pack, but this may render the original BMS inoperable unless it can be reprogrammed.

3.2.5 Testing and certifying second-life batteries

A variety of established safety standards are used to certify lithium-ion batteries both in EV and stationary applications [125], but very few standards give specific consideration to second-life batteries. Until very recently, the only notable standard for second-life batteries has been UL 1974, which was published in 2018 by Underwriters Laboratories [126]. The standard, titled *Standard for Evaluation for Repurposing Batteries*, outlines a procedure for testing, grading, and sorting used EV

batteries during repurposing, thereby offering certification for the second-life battery manufacturing process rather than the actual batteries. The cells are required to have been previously certified by the original manufacturer, otherwise the repurposing company must apply existing battery safety standards to ensure the cells are compliant. UL 1974 also recommends that repurposing companies adopt existing lithium-ion battery safety test methods (e.g. overcharge, thermal abuse, short circuit) and consider adjusting second-life battery operating limits based on how the test results compare to new batteries, but this is not officially standardized.

For the repurposing process, UL 1974 recommends a series of test protocols for evaluating the open-circuit voltage, high-voltage isolation, discharge capacity, internal resistance, BMS functionality, cycling performance, and self-discharge rate of acquired EV batteries so that underperforming batteries can be rejected. However, it is left up to the repurposing company to select appropriate pass/fail criteria for these tests, and the complexities of battery SOH are not directly considered. The main requirement of UL 1974 is that the repurposing company develop a grading system with which to rank battery test results, and that second-life energy storage systems be assembled using same-grade batteries to promote system homogeneity. Notably, UL 1974 does not allow for different EV battery designs to be assembled into the same second-life energy storage system.

In 2023, Canadian startup Moment Energy became the first North American company to achieve UL 1974 certification [127]. The only earlier UL 1974 certification was in 2019 by Japanese company 4R Energy, which is joint-owned by Nissan [128]. Representatives from Moment Energy have indicated that they have achieved UL 1974 certification for both pack-level and module-level repurposing. Note that commercial second-life battery systems must also achieve other certifications not specific to second-life batteries, such as UL 1973, titled *Standard for Batteries for Use in Stationary and Motive Auxiliary Power Applications*, and UL 9540, titled *Standard for Energy Storage Systems and Equipment* [129].

More recently, the International Electrotechnical Commission has also published standards focused on second-life batteries. These include IEC 63330, titled *Repurposing of Secondary Batteries*, and IEC 63338, titled *General Guidance on Reuse and Repurposing of Secondary Cells and Batteries*, both of which were published in 2024. These brand new standards have not yet been purchased for detailed review in this report, but other researchers have reported on some of the contents [125]. One noteworthy takeaway is that both IEC 63330 and IEC 63338 require repurposing companies to work directly with original manufacturers. This seems geared towards reducing uncertainty and risk in the second-life battery supply chain; however, such cooperation may present a significant hurdle and has the potential for conflict of interest between organizations.

3.2.6 Integrating second-life energy storage systems

The integration of second-life batteries into a complete energy storage system has its own unique technical considerations, primarily regarding power conversion. Relatively small-scale second-life battery systems (e.g. 50 kWh of repackaged modules in a behind-the-meter application) can be treated similarly to new stationary batteries, often requiring a single DC/AC power converter for the whole system. For larger systems (e.g. many units of repurposed packs), second-life batteries may require special power conversion considerations. This is especially true when different battery units

(e.g. unique pack designs) within the second-life energy storage system feature different voltage ratings, capacities, SOH levels, power limits, etc., since the power conversion system must be flexible to this heterogeneity [130]. In such cases it is necessary to install a power converter on each unique battery unit so that all battery units can connect to a common bus [131]. A number of different power converter architectures can be used to accomplish this, such as two examples illustrated in Figure 3.13. A detailed review of power conversion technology is outside the scope of this report, but these two simplified examples illustrate the kinds of considerations that second-life battery developers must address when integrating the energy storage system.

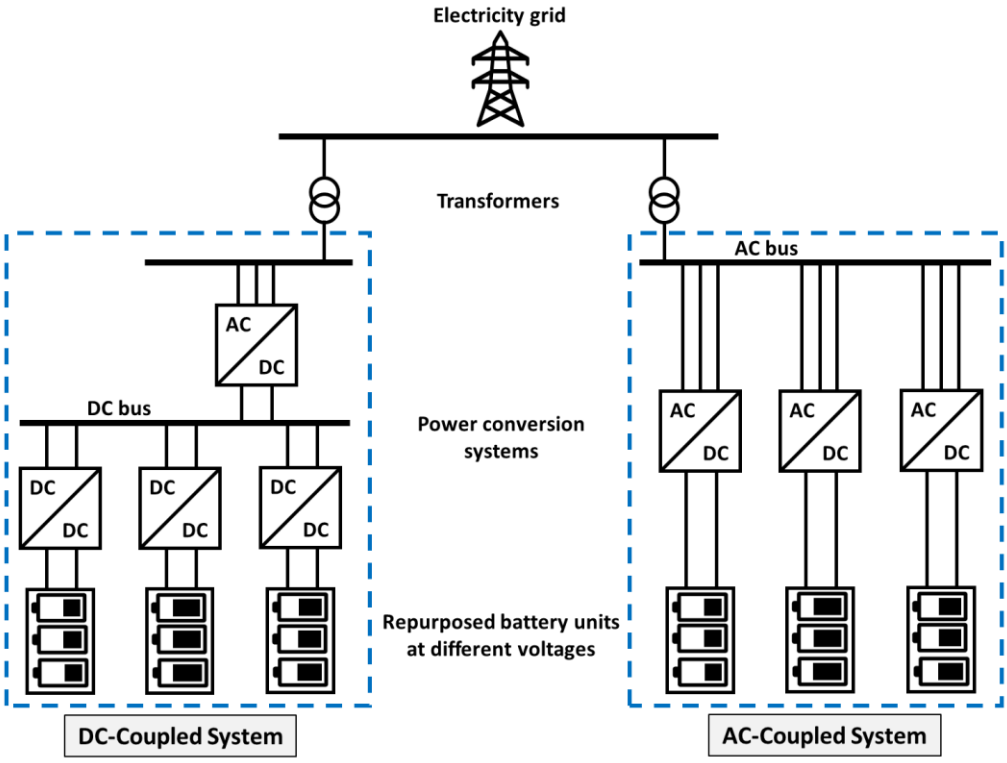

Figure 3.13 Simplified examples of two different power conversion architectures for second-life battery systems. Partially based on figures from [132].

The example of a DC-coupled system in Figure 3.13 includes a DC/DC converter for each unique battery unit, which connects the different units to a common DC bus. The common DC voltage is then converted to AC through a centralized DC/AC converter, which finally connects to the electricity grid through a transformer. In contrast, the example of an AC-coupled system includes a DC/AC converter for each unique battery unit, connecting all units to a common AC bus that connects to the transformer. Other variants of these architectures exist as well, each with advantages and disadvantages in terms of cost, modularity, flexibility, complexity, physical space, and efficiency [132]. For example, DC/DC converters tend to have wider voltage ranges than DC/AC converters (beneficial for accommodating different battery units), but DC-coupled systems require more hardware which adds cost and space requirements [100]. Note that a new stationary battery system could also employ both architectures shown in Figure 3.13, but each individual converter would be of identical voltage and power rating, which would not necessarily be the case for a second-life battery system.

4 Review of Second-life Battery Performance in Ancillary Services

This section provides a literature review on the performance of second-life batteries in the various ancillary services described in Section 2.2. Relevant performance assessment methods for stationary energy storage systems are first described, followed by samples of the most relevant results from experimental and numerical studies focused on short-term and long-term performance in ancillary services. While studies focused on second-life batteries are the primary target for this review, most such studies are limited to frequency regulation performance. Other ancillary services are commented on based on the known characteristics of these applications and of second-life batteries.

4.1 Performance test methods

Between 2012 and 2016, the USA Sandia National Laboratories (SNL) and Pacific Northwest National Laboratory (PNNL) developed a set of test protocols for uniformly measuring and expressing the performance of energy storage systems [133]. The protocols include duty cycles for a wide range of electricity grid energy storage services, including peak shaving and various ancillary services. focuses on grid service applications including frequency regulation, peak shaving, microgrids, solar photovoltaic smoothing and power quality. This appears to be the most complete set of ancillary service test protocols in the literature, covering frequency regulation, different stages of frequency response, and voltage support. The Energy Storage Integration Council (ESIC) Energy Storage Test Manual [134] provides a more recent (last updated 2021) and more detailed guide for energy storage testing procedures, but most procedures related to ancillary services are drawn from the PNNL/SNL test protocols. The subsections below will review the ancillary service test protocols prescribed by PNNL/SNL.

4.1.1 Reference performance tests

The SNL/PNNL test protocol prescribes a set of reference performance tests to evaluate general performance metrics for a given energy storage device regardless of the intended application. The prescribed tests are designed to quantify energy storage capacity, round-trip energy efficiency, response time, ramp rate, internal resistance, and self-discharge rate. These metrics provides measured benchmarks against which to evaluate performance degradation over time and use.

4.1.2 Frequency regulation duty cycle

For frequency regulation, SNL prescribes the 24 h duty cycle plotted in Figure 4.1, which is described in detail by Rosewater and Ferreira in [135]. The power signal is normalized so that it can be easily scaled to different power levels for a given energy storage system under test. Note that the convention is for positive power to represent power delivery into the electricity grid (i.e. battery discharge) and for negative power to represent power absorption from the electricity grid (i.e. battery charge). To quantitatively evaluate performance using this duty cycle, SNL recommends calculations for round-trip energy efficiency (following a return to the initial battery SOC after a given duty cycle is completed), signal tracking accuracy, and SOC excursion.

This duty cycle was proposed for standardized testing of energy storage systems in frequency regulation service. The duty cycle is constructed from segments of real frequency regulation signal data published by PJM Interconnect in 2011/2012. This predates PJM's introduction of the

Regulation D signal described in Section 2.2.1, which tends to be more aggressive. The SNL duty cycle therefore underrepresents the performance demands of modernized frequency regulation signals. However, the SNL duty cycle still allows for comparison of different energy storage systems in a common test regime, including second-life batteries and new stationary batteries.

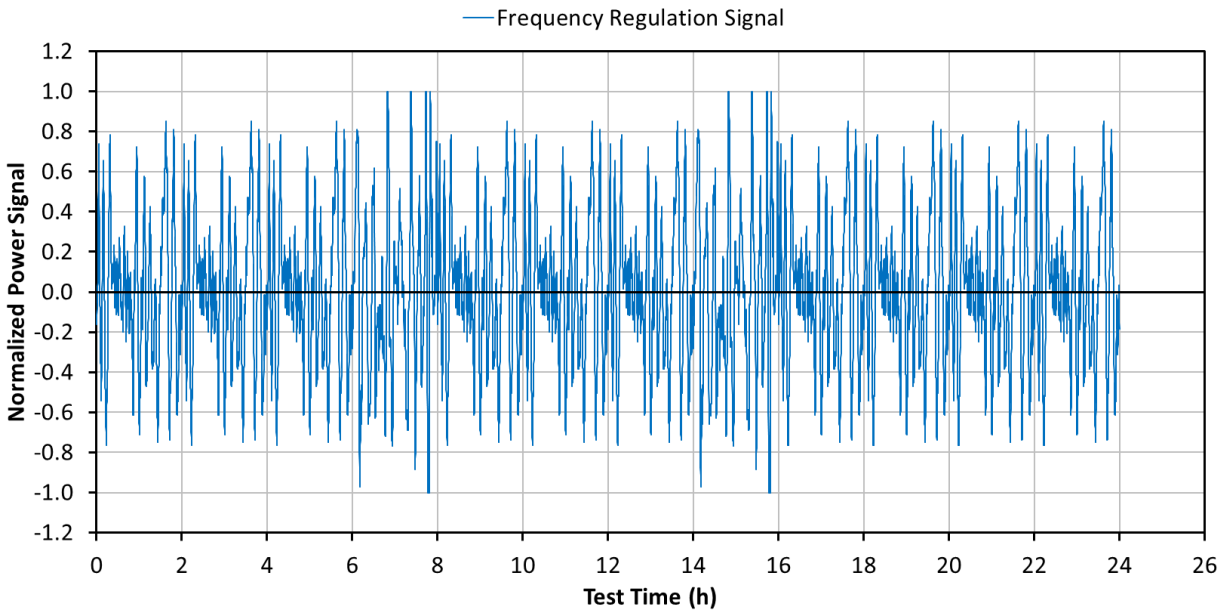

Figure 4.1 Frequency regulation duty cycle prescribed by SNL [133]. Positive power indicates battery discharge.

4.1.3 Frequency response duty cycles

For frequency response, PNNL prescribes three types of duty cycles. Figure 4.2 illustrates the prescribed duty cycle for evaluating performance in primary frequency response service. This duty cycle consists of 30 s pulses repeated every 30 minutes over a 24 h period. This emulates fast frequency response operations immediately following a contingency event on the grid (see Figure 2.6). The duty cycle can be applied to discharge or charge. The signal, as shown is unidirectional, meaning only charging or discharging. Therefore it would be expected that if the duty cycle were continued the battery would fully discharge or charge. It seems appropriate to test this duty cycle with continued pulses on the basis of both the application (due to repeated events on a grid associated with reconnecting customers) and the desire to determine response of the battery (can it repeatedly respond in time).

Figure 4.3 illustrates the prescribed duty cycle for evaluating performance in secondary frequency response service. This duty cycle consists of 20-minute pulses repeated every hour until a low SOC limit is reached (nominally after 3 pulses when the rated 1 h energy capacity is exhausted). This emulates the secondary response that restores grid frequency following a contingency event (see Figure 2.6). This duty cycle can also be applied to discharge or charge, and similar to the preceding signal cannot be done in perpetuity due to it lopsidedness. It also seems appropriate to test this duty cycle with continued pulsed on the basis of both the application (due to repeated failures of generators on grid, or need for continued support as major generation is restarted) and the desire to

determine response of the battery (can it maintain for many minutes without overheating of reducing in power).

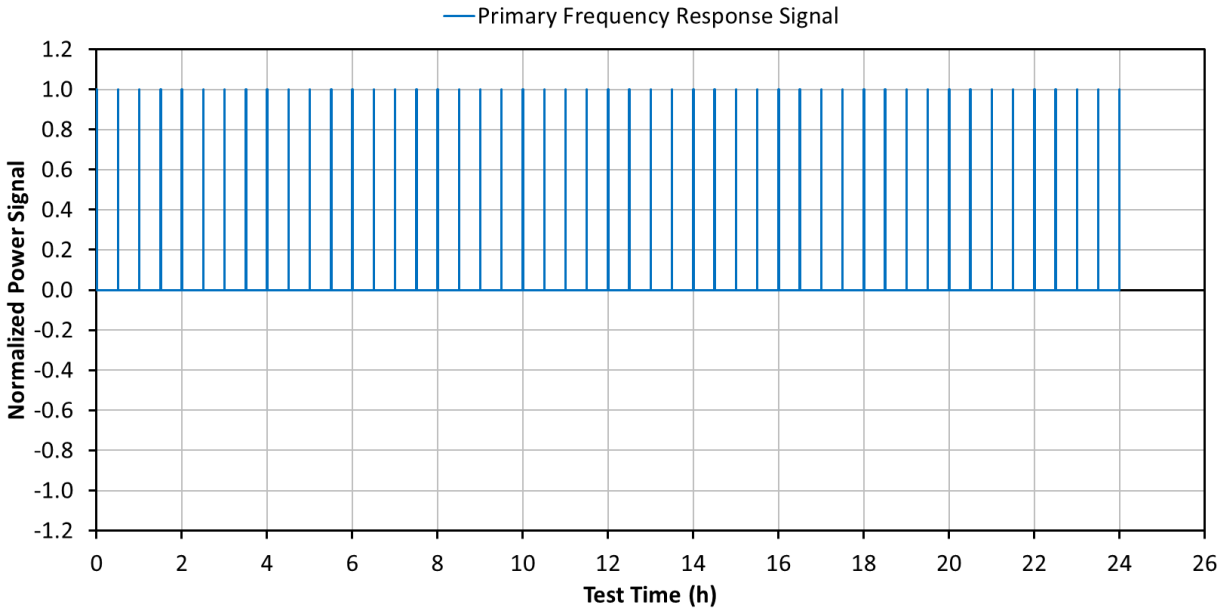

Figure 4.2 Primary frequency response duty cycle prescribed by PNNL [133]. Positive power indicates battery discharge.

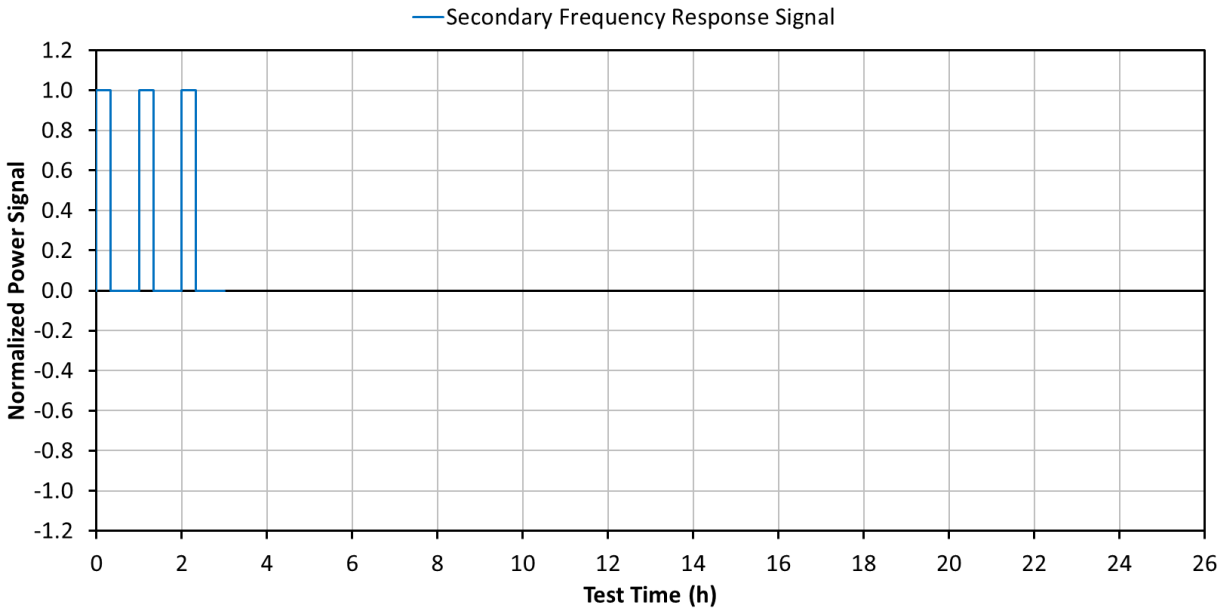

Figure 4.3 Secondary frequency response duty cycle prescribed by PNNL [133]. Positive power indicates battery discharge.

PNNL does not prescribe a tertiary frequency response signal to emulate spinning or non-spinning reserves. However, the progression from Figure 4.2 to Figure 4.3 could be easily extrapolated to create duty cycles for evaluating performance in these longer-duration frequency response services.

For example, a spinning reserve duty cycle could feature a single 1 hour discharge or charge, while a non-spinning reserve duty cycle could feature a single 4 hour discharge or charge.

PNNL also prescribes four separate 'dynamic frequency response' duty cycles to represent typical operations in each season of the year. Figure 4.4 shows the prescribed duty cycle for autumn. The practical representation of this duty cycle is not made clear in [133], and the cited reference document is no longer retrievable online. The duty cycle may be intended to emulate the primary response to the pure frequency signal during normal grid operations (not accounting for ACE as frequency regulation does). A similar duty cycle was developed in [136] based on real-time local frequency measurements.

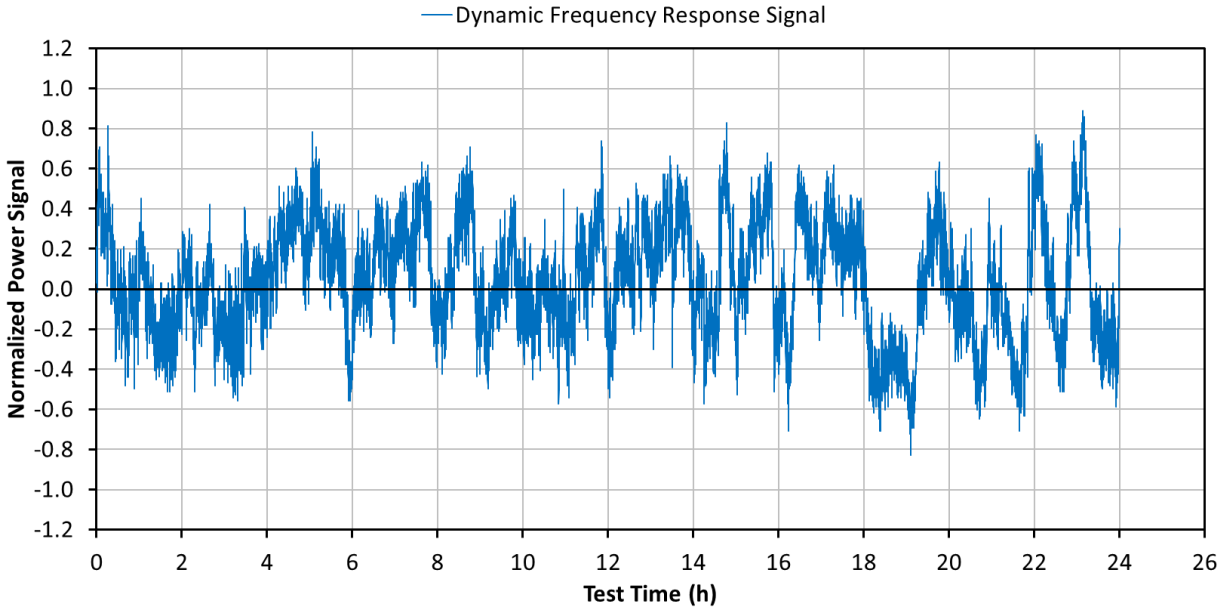

Figure 4.4 One of four seasonal dynamic frequency response duty cycles prescribed by PNNL [133]. Positive power indicates battery discharge.

To quantitatively evaluate performance using the frequency response duty cycles, PNNL recommends calculations for round-trip energy efficiency (following a return to the initial battery SOC after a given duty cycle is completed) and signal tracking accuracy.

PNNL also prescribes that energy storage systems used in frequency response applications be evaluated for peak discharge power and peak charge power at intervals of 1 minute and 20 minutes. According to the prescribed test protocol, peak power is determined by positioning the battery at an initial SOC and applying a complete discharge or charge to a set SOC limit. This process is repeated at various multiples of the rated power, ranging from 1.25 to 10. The applied power multiplier is then plotted against the resulting discharge or charge duration to interpolate the peak 1-minute power (relevant for primary frequency response) and the peak 20-minute power (relevant for secondary frequency response). A similar test method was carried out in [137], but with power multipliers ranging 0.25 to 2.0 (resulting dataset shown in Figure 4.5). The higher power multipliers prescribed by PNNL are more appropriate for evaluating frequency response services.

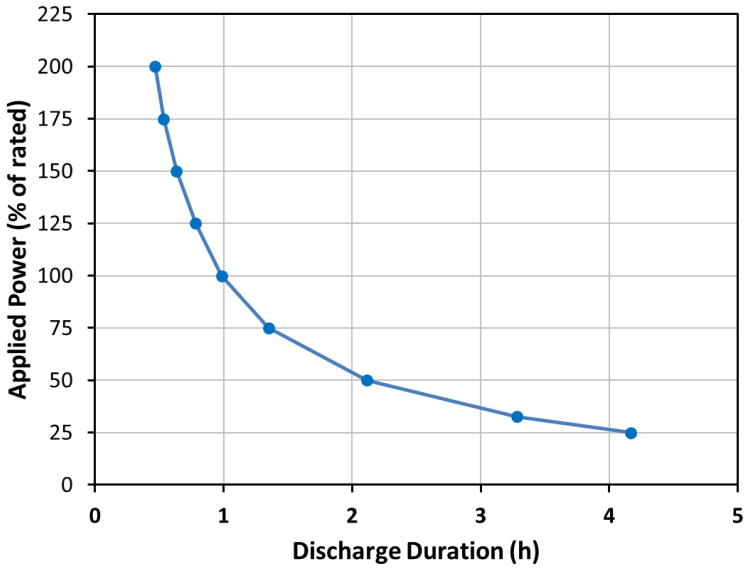

Figure 4.5 Example of peak power test results. Based on data and figure from [137].

4.1.4 Voltage support duty cycle

PNNL offers five different voltage support duty cycles, one of which is illustrated in Figure 4.6. Unlike the frequency regulation and frequency response duty cycles shown previously, the voltage support duty cycles prescribe reactive power (from an inverter in the case of a battery energy storage system). Since there is no real power, round-trip energy efficiency is not an applicable metric for this duty cycle. Instead, PNNL recommends calculations for signal tracking accuracy and SOC excursions.

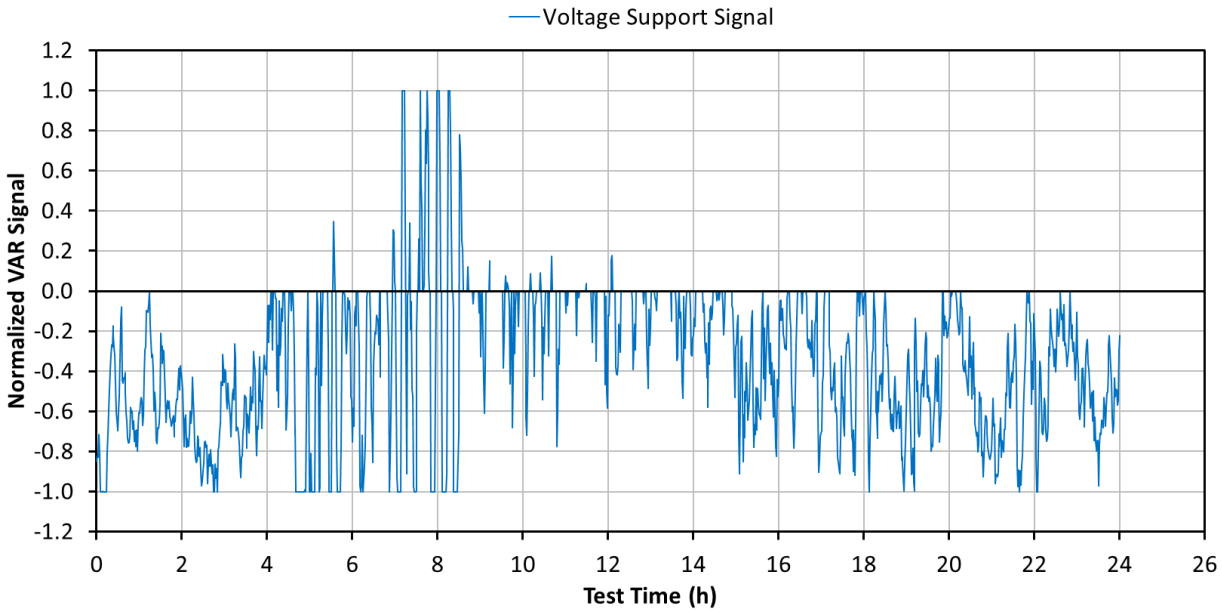

Figure 4.6 Voltage support duty cycle prescribed by PNNL [133]. Positive power indicates reactive power injected into the grid.

4.1.5 Stacked duty cycle

PNNL also prescribes a duty cycle that stacks multiple electricity grid energy services, as shown in Figure 4.7. This duty cycle combines the original SNL frequency regulation duty cycle from Figure 4.1 with a duty cycle representing energy storage services for an islanded microgrid with wind and solar generation. The same evaluation metrics for frequency regulation are recommended.

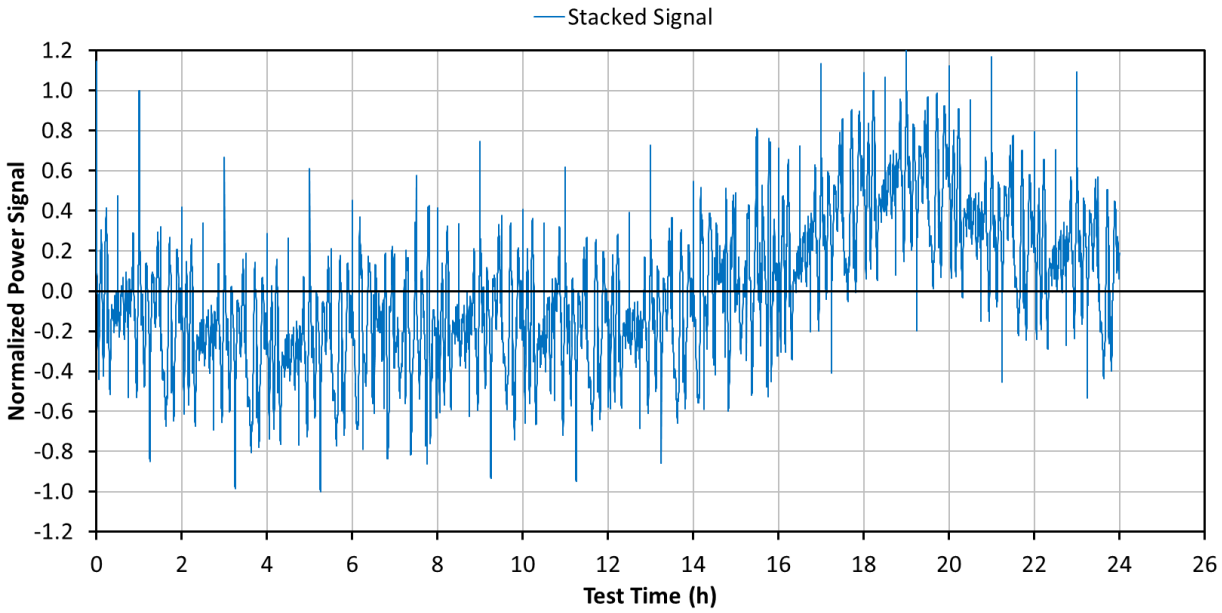

Figure 4.7 Stacked service (microgrid with renewable energy + frequency regulation) duty cycle prescribed by PNNL [133]. Positive power indicates battery discharge.

Ellis et al. [138] designed a stacked signal test for determining degradation. It superimposes a shallow cycle frequency regulation signal riding on top of a deep cycle energy arbitrage signal, as shown in Figure 4.8 The intent of this signal is to conduct both an energy and power based signal, at varying degrees of intensity to determine their impact on degradation of the battery. Examples of this are shown in Figure 4.10, with an energy dominant (33% frequency regulation) and a power dominant, meaning ancillary services dominant signal (66% frequency regulation).

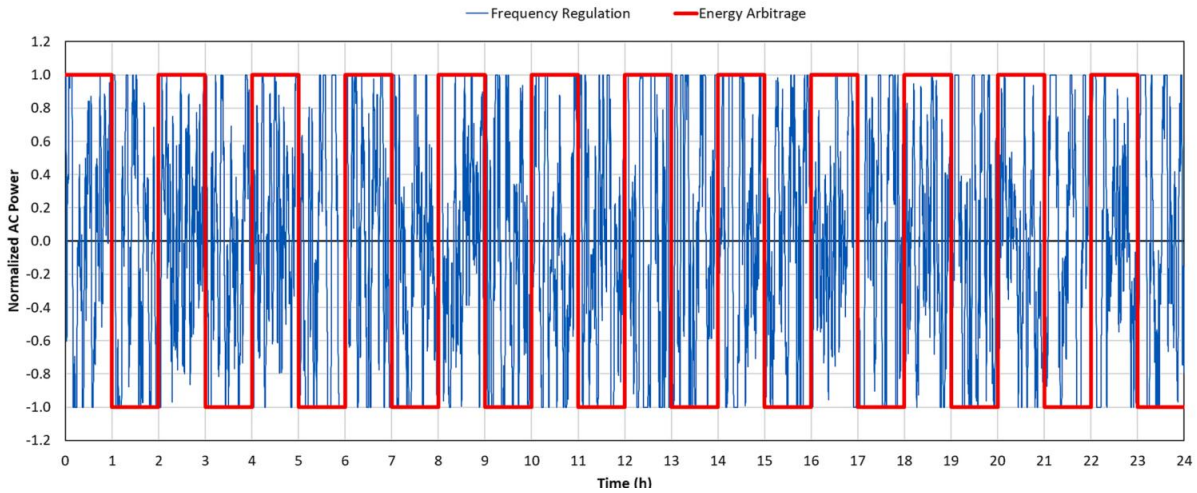

Figure 4.8 Frequency regulation and energy arbitrage duty cycles to be combined in stacked service duty cycles as prescribed in [138]. Positive power indicates battery discharge.

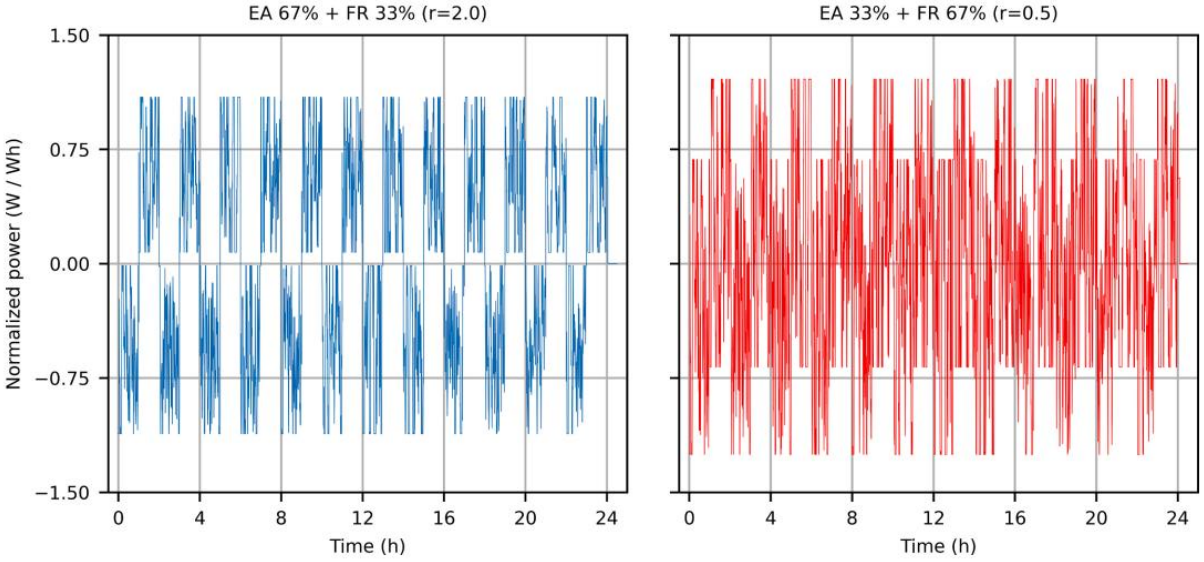

Figure 4.9 Two different stacked service duty cycles designed to be more energy-intensive (left) or power-intensive (right) as prescribed in [138]. Positive power indicates battery discharge.

4.2 Electrical and thermal performance characteristics

Short-term performance of battery energy storage systems in electricity grid applications can be broadly grouped into electrical and thermal categories. The subsections below will consider electrical and thermal performance of second-life batteries in ancillary services. Long-term degradation performance characteristics in ancillary services will be reviewed in Section 4.3.

4.2.1 Frequency regulation performance

The vast majority of second-life battery ancillary service performance studies are concerned with frequency regulation. This is likely because frequency regulation already has an established market and is especially suitable for second-life batteries as a high-value, energy neutral service. While some

studies adopt frequency regulation signal data directly from ISOs (e.g. PJM Interconnect), some have adopted the SNL frequency regulation test protocol to acquire standardized results. One study applied the SNL test protocol to six EV batteries (mostly at module levels), scaling the normalized duty cycle by a range of power multipliers. Round-trip energy efficiency was calculated according to SNL's recommendations, producing the results shown in the left chart of Figure 4.10 [139]. Signal tracking was found to be near-perfect for all batteries. Though SNL does not prescribe thermal performance evaluations, the authors compared the maximum battery temperature of the cycle to a reference temperature (20 °C air for air-cooled batteries and 30 °C liquid for liquid-cooled batteries) to produce the maximum battery temperature rise results shown in the right chart of Figure 4.10.

The results in Figure 4.10 show that frequency regulation performance can vary considerably across different EV battery designs, in terms of both electrical and thermal performance. The NCA battery from a Tesla Model S exhibited the lowest energy efficiencies, but remained relatively efficient at > 92 %. Despite the increased waste heat generation associated with lower energy efficiency, the Model S battery still maintained low temperatures thanks to active-liquid cooling. The two passive-cooled batteries reached nearly 30 °C above the 20 °C ambient air temperature while all active-air and active-liquid reached no more than 6 °C above their respective reference temperatures. These observations demonstrate how second-life battery system designers need to understand the performance characteristics of a given EV battery type in order to accurately anticipate the capabilities of second-life battery systems in ancillary services.

A separate study which tested LFP and NCA cells using the SNL frequency regulation duty cycle also found that NCA exhibited lower energy efficiencies than LFP [140], but temperature results were not reported. Another study applied the SNL duty cycle to an unnamed 7 kWh plug-in hybrid EV battery pack and measured a maximum temperature change of about 5 °C, energy efficiency was not reported. The same study calculated that the battery only tracked the frequency regulation signal 96 % of the time, which seems low for a battery. However, it is important to note that the study used a 1000 A power cycler to carry out a frequency regulation duty cycle with a maximum current of only about ±20 A. The low current would likely give rise to errors in control and measurement, thus lowering the measured signal tracking accuracy.

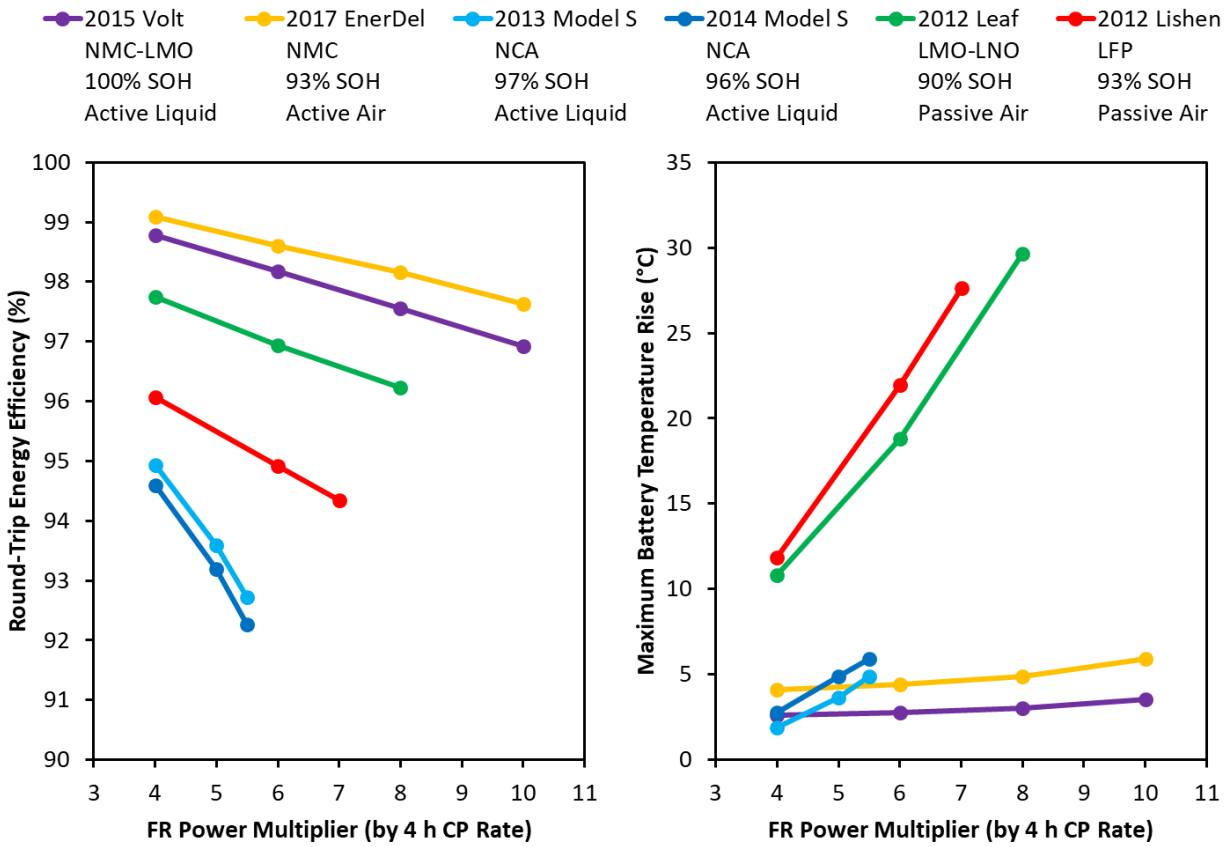

Figure 4.10 Comparison of electrical and thermal performance of different used EV batteries under the SNL frequency regulation test protocol [139].

Despite the use of a standard test protocol, the three aforementioned studies were still inconsistent in the reporting of performance metrics. Greater consistency for ancillary service performance studies would facilitate comparison of different EV battery types for the purposes of modeling, designing, and operating second-life battery systems. Thermal performance reporting is especially lacking in the literature. This will be considered further in Chapter 5.

4.2.2 Fast frequency response and contingency reserve performance

No studies were found that explicitly evaluated the performance of second-life batteries in fast frequency response or contingency reserve services. However, since fast frequency response depends primarily on the response time of the inverter, second-life batteries should be capable of providing this service. One drawback compared to new batteries would be the increased internal resistance of used EV batteries, which could limit the power envelope for fast frequency response. Thermal performance should not be of great concern for fast frequency response since the battery will typically only be called upon for a few seconds at a time.

Unlike fast frequency response, spinning and non-spinning reserves require sufficient energy capacity to be available throughout a contingency event, which means that the reduced capacity of second-life batteries is of consequence for these services. Batteries with lower SOH may be less

reliable for longer-duration non-spinning reserves unless low power commitments are offered. The extended power flow of contingency reserves also means that thermal performance will come into play. For instance, if a second-life battery attempts to fully discharge its energy in less than an hour for spinning reserve service without adequate thermal management, the battery could reach a temperature limit and trip offline during a contingency event instead of correcting the contingency. Thermal management may be of greater importance for second-life batteries compared to new batteries, especially if internal resistance growth goes undetected and results in unexpectedly high heat generation rates.

4.2.3 Voltage support performance

No studies were found that explicitly evaluated the performance of second-life batteries in electricity grid voltage support services. However, studies have concluded that battery systems in general can provide voltage support without significant impact on SOC or SOH [141]. This is because voltage support relies on reactive power to/from the inverter, which does zero work and therefore requires no real power from the battery [142]. Second-life batteries should therefore be equally capable of providing voltage support services compared to new batteries. Electrical performance would be dictated by the ability of the inverter to follow the reactive power signal (see example in Figure 4.6), while battery temperature rise would be insignificant given the absence of real power flow.

4.3 Degradation performance characteristics

The energy storage capability of a lithium-ion battery gradually declines over the course of its life due to a variety of internal degradation mechanisms. When the battery is first constructed, it is considered to be at BOL, and when it eventually degrades to the point at which it can no longer serve its designed purpose, it is considered to have reached EOL. The 'life' of the battery from BOL to EOL depends on its operational pathway , but due to relatively slow calendar aging, the life is typically denoted as cycle life of the battery, which gives the approximate number of cycles required to reach EOL under a given set of operating conditions. Cycle life is therefore an important metric for assessing the economics of second-life battery energy storage, since it determines how long the battery system will be able to meet system requirements before needing replacement.

4.3.1 Degradation of lithium-ion batteries

Lithium-ion batteries degrade over time and use through a variety of complex degradation mechanisms, which can generally can be grouped into two main categories: capacity fade and power fade [143]. Capacity fade is an irreversible decrease in the coulombic capacity of the cell, which can occur through the consumption of Li^+ in side-reactions (termed 'loss of lithium inventory' or LLI) or through the isolation or blockage of intercalation sites in the electrodes (termed 'loss of active material' or LAM) [144]. Power fade is the result of an irreversible increase in the cell internal resistance and the corresponding overpotentials, which reduces energy utilization through voltage depression, discharge truncation, and charge truncation (see Section 2.3.2).

Different electrode active materials vary in their susceptibility to different degradation mechanisms. Table 4.1 summarizes the main degradation mechanisms and their prevalence for the main positive and negative active materials used in EV applications, with 'X' representing significant degradation rates. While the vast majority of lithium-ion batteries employ graphite at the negative electrode, the

choice of positive electrode material will clearly have a significant impact on the mechanism and rate of degradation in the cell. Detailed explanations of the various degradation mechanisms are outside the scope of this report, but it is important to understand that battery SOH is a highly simplified quantification given the many complex pathways that battery degradation can take.

Table 4.1 Summary of the main degradation mechanisms for various lithium-ion battery electrode materials. Significant degradation rates are represented by 'X'.

Mechanism	LMO	LFP	NMC [a]	NCA [b]	Graphite
Lithium plating					X
SEI growth				X	X
Electrolyte decomposition	X		X	X	X
Particle cracking	X	X	X	X	X
Oxygen loss			X	X	
Transition metal dissolution	X	X	X	X	
Cation mixing [c]			X	X	

[a] NMC considered to have 33 % ≤ Ni ≤ 60 %.
[b] NCA considered to have 80 % ≤ Ni ≤ 85 %.
[c] Cation mixing occurs during material synthesis rather than battery operation, but it is included here for a more complete comparison of the main issues affecting different electrode materials.

Degradation will occur even if a battery is idle for long periods, since parasitic reactions such as electrolyte decomposition, SEI growth, and transition metal dissolution can proceed inside a lithium-ion cell without an external current [145]. This is referred to as 'calendar degradation' as opposed to 'cycling degradation'. The parasitic reaction rates tend to follow the square root of time, but increase with cell voltage and temperature [143]. One study evaluated calendar degradation in NCA, NMC, and LFP cells over a 10-month period, and measured significantly greater capacity fade and power fade in cells stored at 40 to 50 °C and 80 to 100 % SOC compared to cells stored at 25 °C and < 50 % SOC [146]. Therefore, it is generally recommended that lithium-ion batteries be stored at or below 50 % SOC in temperate or cooled environments. With such preventative measures, calendar degradation is typically < 1 % per year, while cycling degradation could be 1- 3 % per year depending on a variety of factors. Second-life batteries may be 8 to 10 years old or more at EOVL, and will therefore have undergone both cycling degradation and calendar degradation.

The rates at which the various degradation mechanisms occur in lithium-ion batteries is strongly influenced by physical design parameters and operational conditions. For instance, lithium plating is more likely to occur when charging takes place at high currents, low temperatures, and high SOC [8], while higher temperatures and voltages will generally accelerate the lithium-consuming parasitic reactions between electrode and electrolyte [9]. Though higher upper voltage limits can increase the energy utilization of layered positive electrode materials, this also promotes electrolyte decomposition and gas evolution at the positive electrode [12]. Stress-induced electrode cracking is exacerbated at extreme levels of intercalation (mitigated by tighter voltage limits) as well as high currents [10], and transition metal dissolution increases at higher temperatures and currents [11].

Since some degradation mechanisms (e.g. lithium plating) are exacerbated at lower temperatures while other degradation mechanisms (e.g. SEI growth, transition metal dissolution) are exacerbated at higher temperatures, an intermediate temperature range is generally preferred for prolonging the life of lithium-ion batteries. Lower temperatures also tend to increase battery impedance, which is detrimental to battery energy and power performance. Higher temperatures also increase the safety risks associated with lithium-ion batteries. A recommended temperature range of 25 to 40 °C [101] is commonly cited in the literature for balancing battery performance and cycle life, though other recommended ranges are reported as well, such as 20 to 45 °C [102], 15 to 40 °C [112], or 15 to 35 °C [147].

Similarly, since some degradation mechanisms (e.g. lithium plating, electrolyte decomposition, oxygen loss) are exacerbated at high SOC levels while others degradation mechanisms (e.g. particle cracking) are exacerbated at both high and low SOC levels, it is also common for battery operators to apply strategic limits on SOC or cell voltage as a means of prolonging the life of lithium-ion batteries. For example, one study reported that NCA cells degrade at a lower rate when cycled between 3.4 V and 4.0 V compared to identical cells cycled between 3.0 V and 4.3 V [10]. Though tightening the voltage limits will of course reduce the usable capacity of the battery on a given day, the battery will last longer in a commercial application before needing replacement.

Given the complex path-dependence of lithium-ion battery degradation, it is difficult to accurately quantify the extent of degradation at a given point in battery life. A 2021 review [148] reported the two most common definitions of SOH used in the literature, which are given in Equations 4.1 and 4.2.

$$\mathrm{SOH}_Q = \frac{Q_{\mathrm{dis}}}{Q_{\mathrm{dis}}^{\mathrm{BOL}}} \times 100\ \% \tag{4.1}$$

$$\mathrm{SOH}_R = \frac{R_{\mathrm{EOL}} - R}{R_{\mathrm{EOL}} - R_{\mathrm{BOL}}} \times 100\ \% \tag{4.2}$$

The capacity-based SOH_Q definition compares the present value of coulombic capacity Q_{dis} to the BOL value, which would be the more appropriate metric in applications where the importance of energy capacity outweighs the importance of power capability (e.g. EVs). A simple discharge test can determine the present value of Q_{dis} for a given battery. The resistance-based SOH_R definition compares the present value of internal resistance R to the BOL and EOL values, which would be the more appropriate metric for applications where power capability is most important (e.g. electricity grid ancillary services). The definition of R in Equation 4.2 may refer to one or more components of battery internal resistance, which may be assessed by various methods such as current pulse tests [146] or EIS [143]. Regardless of how SOH is defined, it provides a metric for estimating the position of a given battery in its cycle life between BOL and EOL. As explained in Section 3.2.3, advanced modelling techniques can also be used to estimate the RUL of a battery before it reaches EOL [149].

As an alternative to SOH_Q and SOH_R, an energy-based SOH_E definition was proposed in [150] as shown in Equation 4.3. Since the discharge energy depends on both the total coulombic capacity and the effect of internal resistance on battery voltage, this definition combines the effects of capacity fade and power fade into a single value to give a practical assessment of the ability of a battery to deliver useful energy throughout its life compared to BOL. It is important to assess this metric at rates

representative of the ancillary service being conducted, so that the relative impacts of the coulombic capacity and internal resistance are properly accounted for.

$$\mathrm{SOH}_E = \frac{E_{\mathrm{dis}}}{E_{\mathrm{dis}}^{\mathrm{BOL}}} \times 100\ \% \tag{4.3}$$

4.3.2 Degradation of second-life batteries in ancillary services

Used EV batteries are generally expected to operate for an additional ten years or more in second-life service [151], though this depends on the design and usage history of a given EV battery as well as its intended second-life application. For example, one model-based study predicted that second-life could last anywhere between 6 years and 30 years depending on the second-life operational duty cycle [152].

Batteries in frequency regulation service typically hover near mid-SOC with a relatively low depth-of-discharge, which allows the battery to avoid the SOC extremes that tend to promote degradation. The experimental cell degradation data from Elliot et al. [153] and Ellis et al. [138] shown in Figure 4.11 demonstrates how frequency regulation service is associated with lower degradation rates than energy arbitrage (respectively abbreviated as “FR” and “EA” in the chart legend), which is an electricity grid energy management services with a relatively high depth of discharge. Stacked services more heavily weighted towards frequency regulation also exhibit lower degradation rates. These is shown to be true for two types of EV battery cells featuring NMC and LFP positive active materials.

As a given EV battery degrades, internal resistance growth will tend to reduce the energy efficiency. However, energy efficiency tends to degrade at a slower rate than energy capacity, as evidenced by Figure 4.12 in comparison to Figure 4.11. In fact, the energy efficiency trends of the LFP cell seems to remain fairly consistent throughout the cycling periods. Figure 4.12 also shows how the lower depth-of-discharge associated with frequency regulation achieves higher energy efficiency than energy arbitrage.

Due to lack of published data, degradation characteristics of second-life batteries in fast frequency response, contingency reserves, and voltage support services cannot be directly reviewed. However, the known characteristics of these ancillary services and battery degradation mechanisms can be used to draw some insights. For fast frequency response, the relatively low depth-of-discharge associated with very brief, intermittent operational windows should result in a low yearly energy throughput. Spinning reserves and non-spinning reserves require progressively greater depths of discharge than fast frequency response, but these deep cycles are also called upon progressively less frequently than the primary response. Contingency reserves should therefore also have a relatively low yearly energy throughput compared to electricity grid energy management services such as arbitrage.

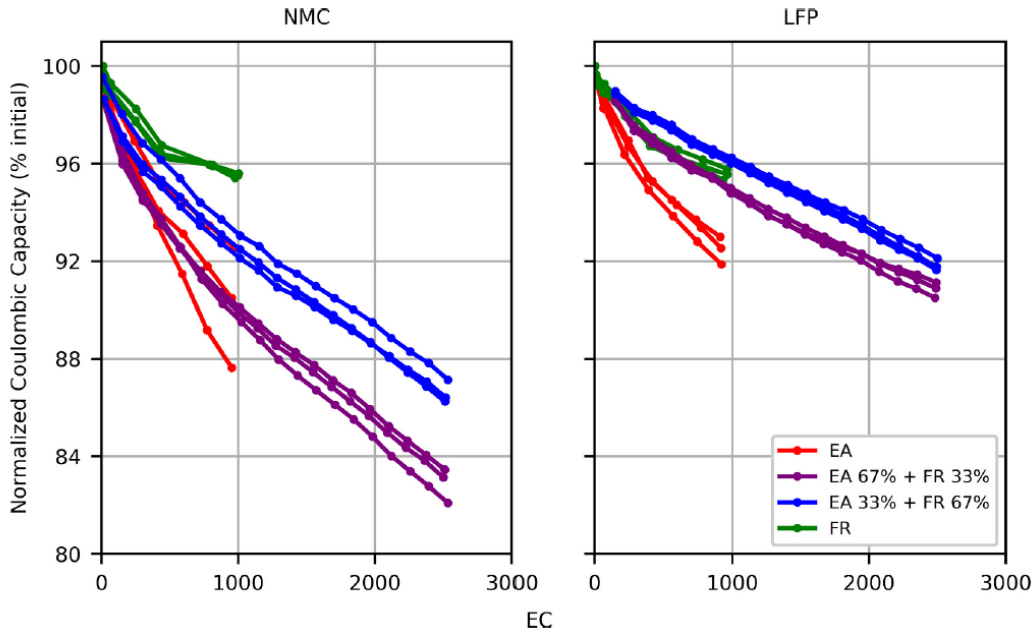

Figure 4.11 Discharge capacity fade measured over extended cycling ("EC" refers to equivalent cycles) for two EV cell types in four stacked combinations of frequency regulation and energy arbitrage (respectively abbreviated as "FR" and "EA" in chart legend) services [138], [153].

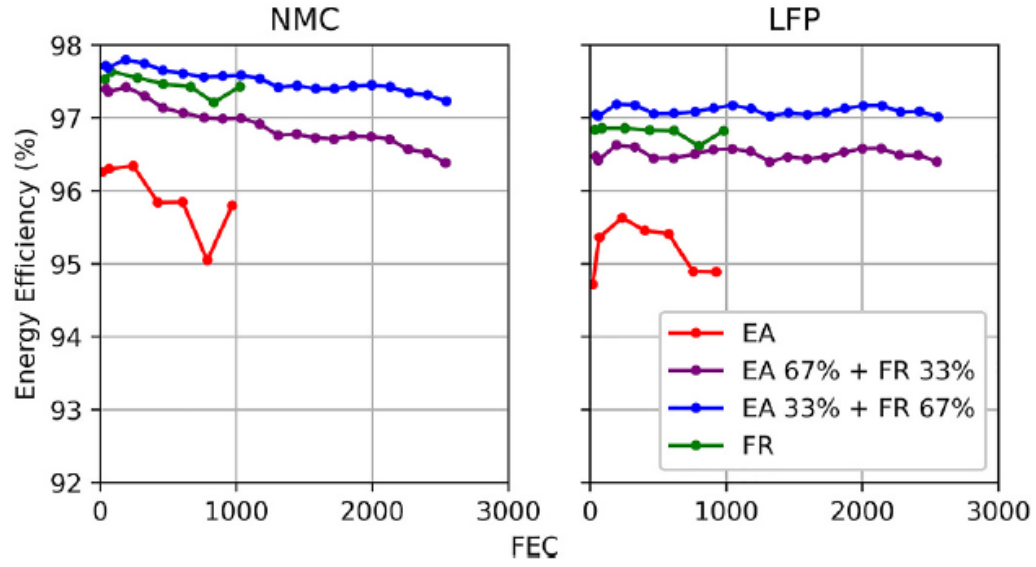

Figure 4.12 Energy efficiency measured over extended cycling ("FEC" refers to full equivalent cycles) for two EV cell types in four stacked combinations of frequency regulation and energy arbitrage services [138], [153].

5 Technical Assessment of Second-life Batteries in Ancillary Services

This section provides technical insights on how second-life batteries can generally be expected to perform in ancillary services, including suitability and challenges. Specific performance metrics are also recommended to facilitate repurposing EV batteries into ancillary services. This section is based on experience, engineering judgement, internal testing, etc.

5.1 Technical suitability

Several key factors determine the suitability of a given energy storage technology for ancillary services. The subsections below will consider these factors in the context of second-life batteries.

5.1.1 Response time

As described in Section 2.2.2, battery response time is essentially instantaneous, making the energy storage system response time limited by the inverter rather than the battery. This is why some ISOs have separated the more aggressive dynamics of frequency regulation signals into a specialized signal (such as PJM's *Regulation D*) that can benefit from the fast response of batteries. Degradation of EV batteries will not impact the response time, so the response time of second-life batteries should be comparable to that of new batteries.

5.1.2 Energy capacity and energy efficiency

Second-life batteries will of course retain lower capacity than comparable new batteries. As explained in Section 2.1.1, the future second-life battery supply chain will likely see a large majority of EV batteries reaching EOVL above 75 % SOH. This suggests that most future second-life batteries can be expected to offer at least 75 % of the capacity of new batteries, which is still a significant amount of capacity. As discussed in Section 4.3, EV batteries generally become less suitable for second-life applications once their SOH falls below approximately 60 %, but this depends on battery design and usage.

It is also important to note that the energy density of EV battery modules will typically exceed that of batteries designed for stationary applications. Figure 5.1 shows how the energy density of relatively recent EV battery designs (e.g. 2018-2019) has improved dramatically over older designs (e.g. 2012-2015). The relative system energy density of second-life batteries compared to new batteries will likely depend on the packability of a given EV battery pack or module design. For instance, the uneven shape of the Chevrolet Bolt pack (see Figure 3.2) may limit the achievable energy density of a multi-pack repurposed energy storage system compared to new batteries designed for stationary packability.

Figure 5.1 also shows that EV batteries are becoming less energy efficient as an unavoidable trade-off to increasing energy density, particularly at higher power rates. However, new stationary batteries are most typically LFP batteries, which tend to have the lowest energy efficiency among lithium-ion variants. This means that second-life batteries will not necessarily be disadvantaged compared to new batteries in terms of energy efficiency. Again, this will likely depend on the design and usage of a given EV battery.

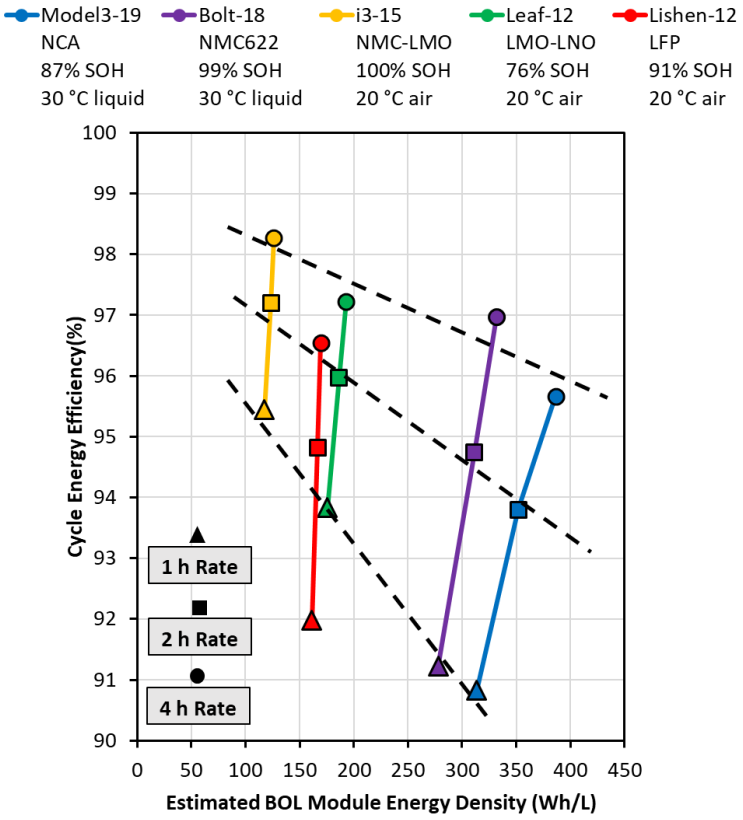

Figure 5.1 Comparison of energy efficiency and BOL module energy density showing impacts of cell internal resistance on electrical performance [1]. Dashed lines show trends among 4 h, 2 h, and 1 h datapoints for non-LFP batteries.

5.1.3 Power rate and heat generation

Both the electrical and thermal performance of batteries are impacted by the power rate. As greater power rates, increased overpotentials reduce the amount of energy that can be accessed between set voltage limits, and also increase the rate at which waste heat is generated. These concepts are illustrated in Figure 5.2, where the left and right chart shows respectively show the voltage vs SOC curve at low power and high power. The area under the discharge curve is proportional to the discharge energy, while the area between the charge and discharge curves is proportional to the waste heat generated. The 'energy utilization ratio' compares the amount of usable energy that can be discharged at a given power rate compared to a low-power discharge after a full charge. Experimental results for the energy utilization ratio are plotted for five different EV battery packs in the left chart Figure 5.3, showing that the effect of power rate can vary significantly for different EV battery designs. Note that the x-axis scales the applied power by the discharge energy of each battery to facilitate comparisons. Though Figure 5.3 refers to deep-discharge cycling, the results can extend to some ancillary services. For example, frequency regulation service may trigger a voltage limit at higher power. Spinning or non-spinning reserve services may amount to a deep discharge in response to a significant contingency event.

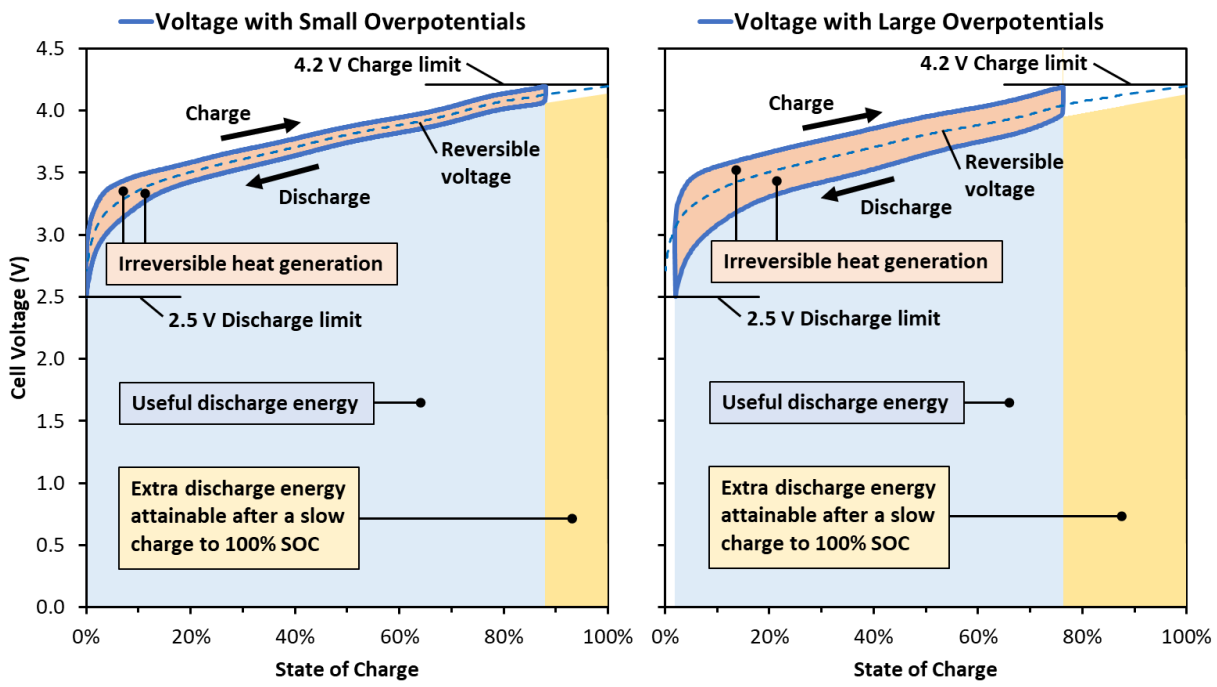

Figure 5.2 Effect of overpotentials on usable energy capacity and waste heat generation [1].

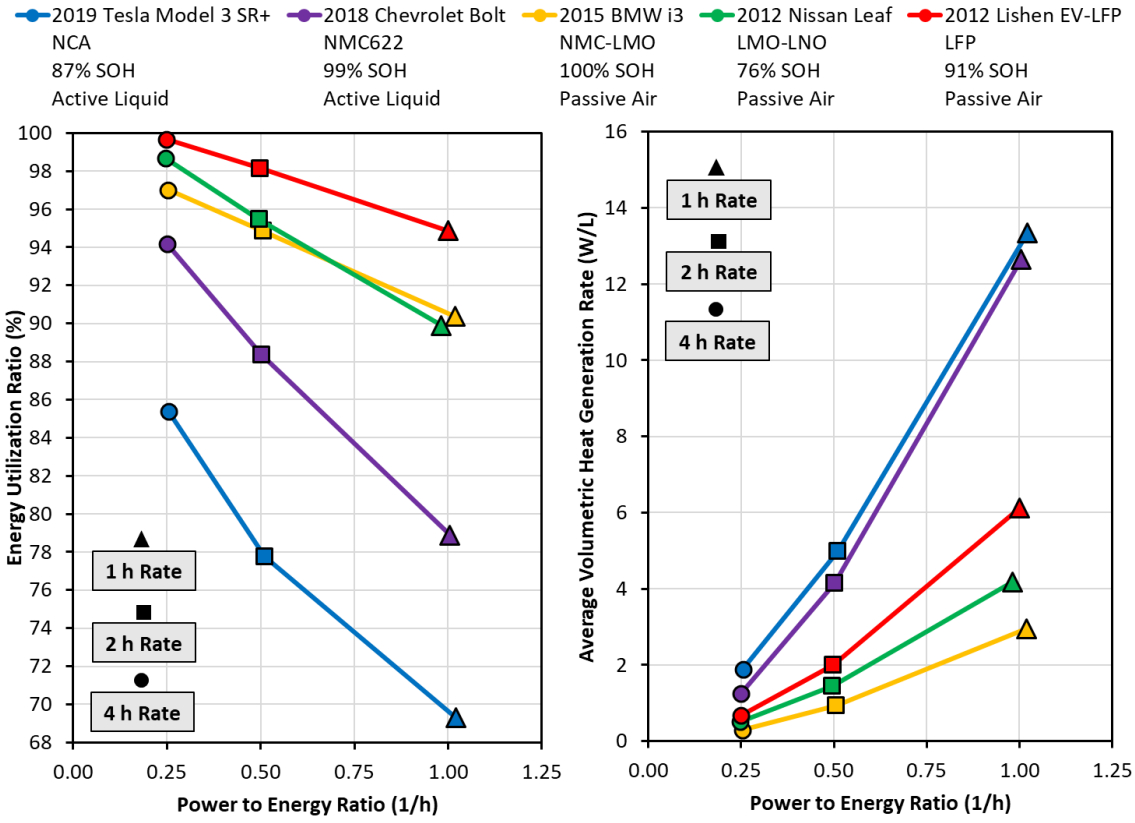

Figure 5.3 Energy utilization ratios (left) and average volumetric heat generation rates (right) during deep cycle testing at three power rates [1].

The right chart of Figure 5.3 shows the average volumetric heat generation rate of each battery during deep discharge cycling at the same three power rates. This shows that different EV battery designs can also exhibit very different heat generate rates. Generally, the higher energy density and lower energy efficiency of newer EV battery designs both contribute to increased volumetric heat generation rates, which produces a greater thermal management load. Fortunately, EV batteries with high heat generation rates are equipped with an active TMS to reject heat during EV service. These TMS capabilities can often be adapted for second-life service to help mitigate operational temperature rise.

Compared to new batteries, second-life batteries will tend to have higher internal resistance, which worsens the detrimental effects of high power rates on both energy capacity and thermal management load. This means that the necessary operational limits placed on battery voltage, SOC, and temperature may limit the power capability of some second-life batteries compared to new batteries. It is therefore important to measure the internal resistance of acquired second-life batteries and monitor resistance growth throughout second-life service. Operational limits may need to be adjusted over time based on evolving power limitations, more so than new batteries. As a simple illustrative example, if the goal is to avoid increased heat generation rates in aged batteries, then an operational limit could be applied based on Equations 5.1 and 5.2, where $\dot{q}_{\max}$ is the heat generation rate that occurs when a maximum rated current $I_{\max}$ is applied to a battery with internal resistance R. This shows that $I_{\max}$ must decrease compared to its BOL value in order to maintain a constant $\dot{q}_{\max}$ throughout battery life as R increases compared to its BOL value. If R were to double due to degradation, then $I_{\max}$ would have to be reduced to 71 % of its BOL value. In practice, a moderate increase in $\dot{q}_{\max}$ may be acceptable depending on the heat rejection capabilities of the TMS for the battery in question.

$$\dot{q}_{\max} = {I_{\max}}^2 R \tag{5.1}$$

$$I_{\max} = I_{\max,\mathrm{BOL}} \sqrt{\frac{R_{\mathrm{BOL}}}{R}} \tag{5.2}$$

From a technical standpoint, second-life batteries with high internal resistance can still provide high power rates if the system is oversized such that the total system power is distributed among a greater number of second-life batteries. The added cost of oversizing allows the operator to limit the power envelope, depth of discharge, and temperature rise of individual batteries without limiting the overall system capability. It then becomes an economic question as to whether the cost of an oversized second-life battery system can compete with a new battery system.

Note that the power limitations of second-life batteries will generally be less significant than their energy limitations. For instance, a 2021 study [154] compared first-life and second-life Nissan Leaf battery modules in terms of both energy and power capabilities, and found that the second-life modules gave about 65 % of the rated energy capacity at a 1C rate in a 25 °C environment, but still gave 90 % energy efficiency and similar power density compared to first-life modules. However, the performance of the second-life modules declined significantly when cycled at 5 °C, resulting in just 82 % energy efficiency.

5.1.4 Cycle life

Second-life batteries will certainly be disadvantaged in terms of cycle life compared to new batteries, especially considering that new LFP stationary batteries can achieve a cycle life of up to 20 years, depending on usage. However, second-life batteries can still provide a viable cycle life for electricity grid applications (5 to 10 years, depending on usage), and Section 0 demonstrated that ancillary services tend to be less detrimental to battery cycle life than other electricity grid energy storage services. Since degradation rates are most pronounced at extreme SOCs, cycle life can be further extended by oversizing the battery system such that individual batteries can be constrained to mid-range SOC. This again becomes an economic question as to whether the extended cycle life of the second-life battery system outweighs the upfront cost of oversizing.

Figure 5.4 shows experimental degradation data obtained from a diverse set of EV battery modules, including Tesla Model 3 LR, Chevrolet Bolt, BMW i3, Hyundai Genesis GV60, and Kia Niro. All modules began testing above 90 % SOH, but Figure 5.4 re-references them to 100 % at the beginning of the experiment. The cell voltage limits applied to each modules are shown in the parentheses of the chart legend The slope of each curve represents the respective degradation rate of each module, showing that the Model 3 modules have the fastest degradation rates (NCA chemistry is known to have relatively poor degradation characteristics as shown in Table 3.1) while the Bolt and Niro modules have the slowest degradation rates. With the exception of Model 3, all modules degrade by approximately Δ10% per 1000 cycles, or less. These degradation rates would be even lower for ancillary services. This shows that EV batteries can offer suitable cycle life for ancillary services, though all EV battery designs cannot be assumed to exhibit the same degradation rates. Note that this data is taken with deep discharge cycling and has had the thermal condition system de-activated. As such, we expect shallow cycling of ancillary services, along with any additional thermal management, to reduce these degradation rates. Additionally, because these degradation curves start with used EV batteries, they give a good indication that there is no catastrophic degradation point within the first few thousand cycles. And because it is expected that there will be only 1000-2000 cycles achieved in first life, this bodes well for repurposing.

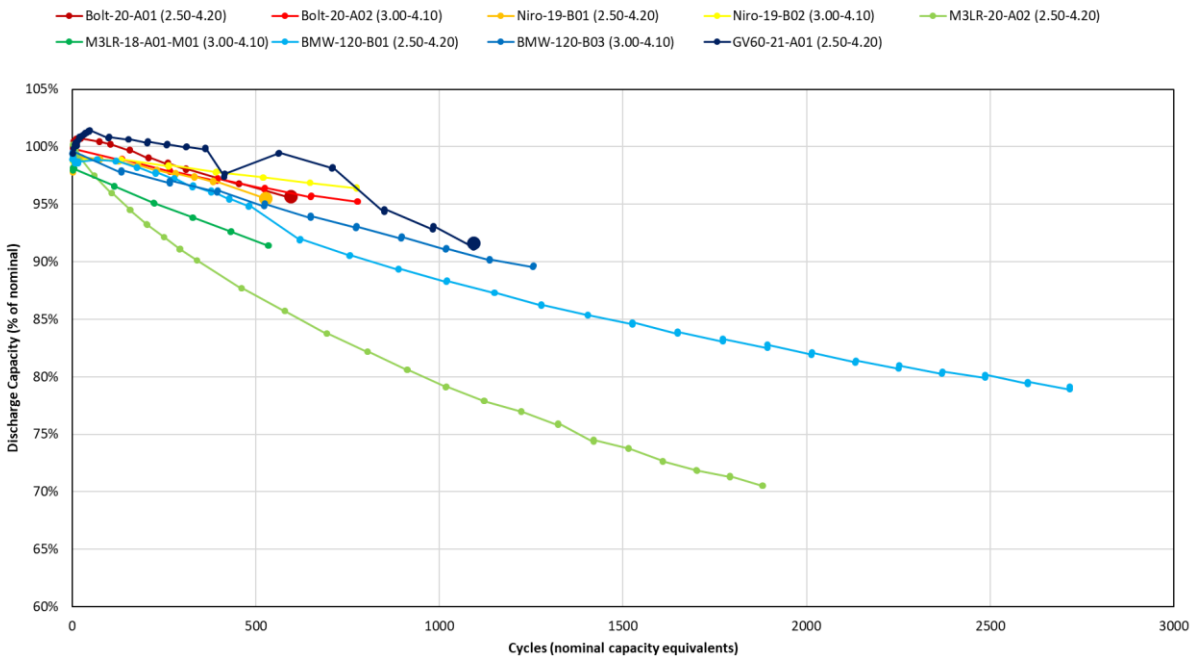

Figure 5.4 Experimental capacity degradation trends among a diverse set of EV battery modules.

Figure 5.5 shows similar testing, but is based on fresh EV cells. These cells are not clamped, have no thermal management system, and were tested individually. The benefit of this figure is that it shows the capability of EV cells throughout a longer cycling duration. Similar to the module analysis, this is deep discharge cycling, so the degradation rates of ancillary services are expected to be lower. Note again, that the various chemistries exhibit different patterns, but all proceed in a generally linear fashion. We do not see the appearance of any catastrophic capacity reduction within many thousands of cycles. Additionally, it can be seen that some cells achieve between 3000-6000 cycles, and the linear degradation has essentially continued throughout. We note that these cells in particular are over 10 years old and thus include some calendar aging. This suggests that if the second-life of ancillary service has no minimum SOH requirement, and isn't concerned with occupying space, that used EV batteries may last a very long time in second-life ancillary services.

Figure 5.6 shows the corresponding cell energy efficiency data. At beginning of life, all exhibit DC energy efficiencies within a range of 90 to 95 %. Again, they are grouped by chemistry type. Note that the energy efficiency does degrade with cycle life (e.g. Δ1 % per 1000 cycles), although the trend is nowhere near as substantial as that for discharge capacity (e.g. Δ10 % per 1000 cycles). There is no evidence of a step change in energy efficiency throughout cycling.

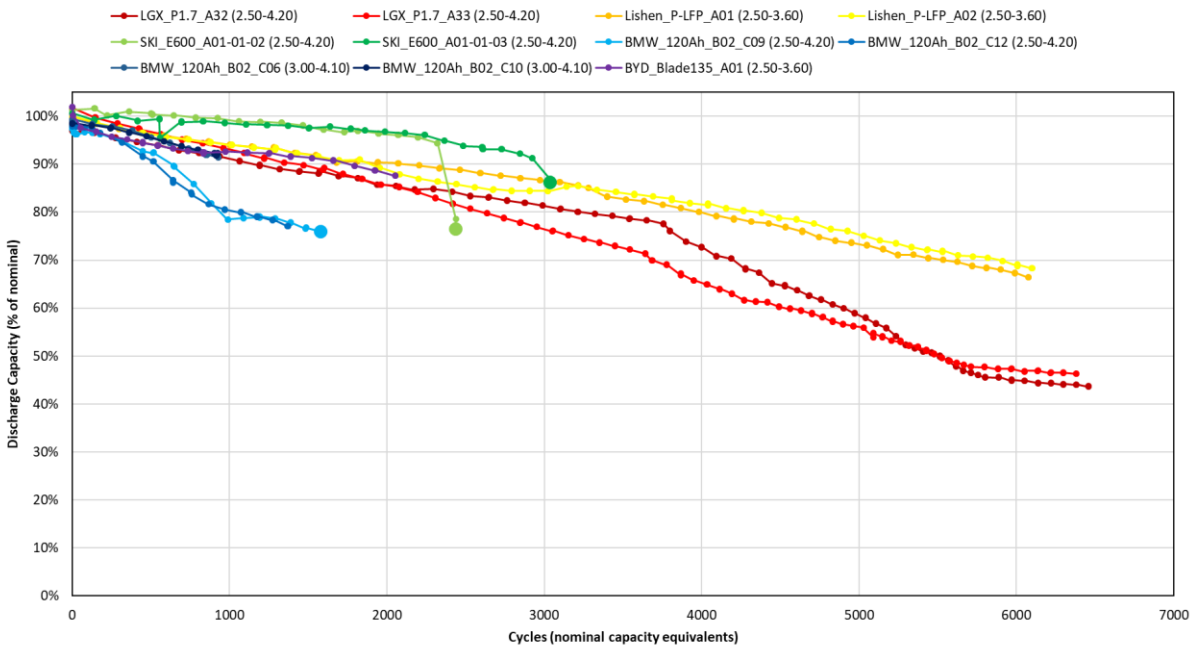

Figure 5.5 Experimental capacity degradation trends among a diverse set of EV cells, that were new (fresh) at the start of the experiment.

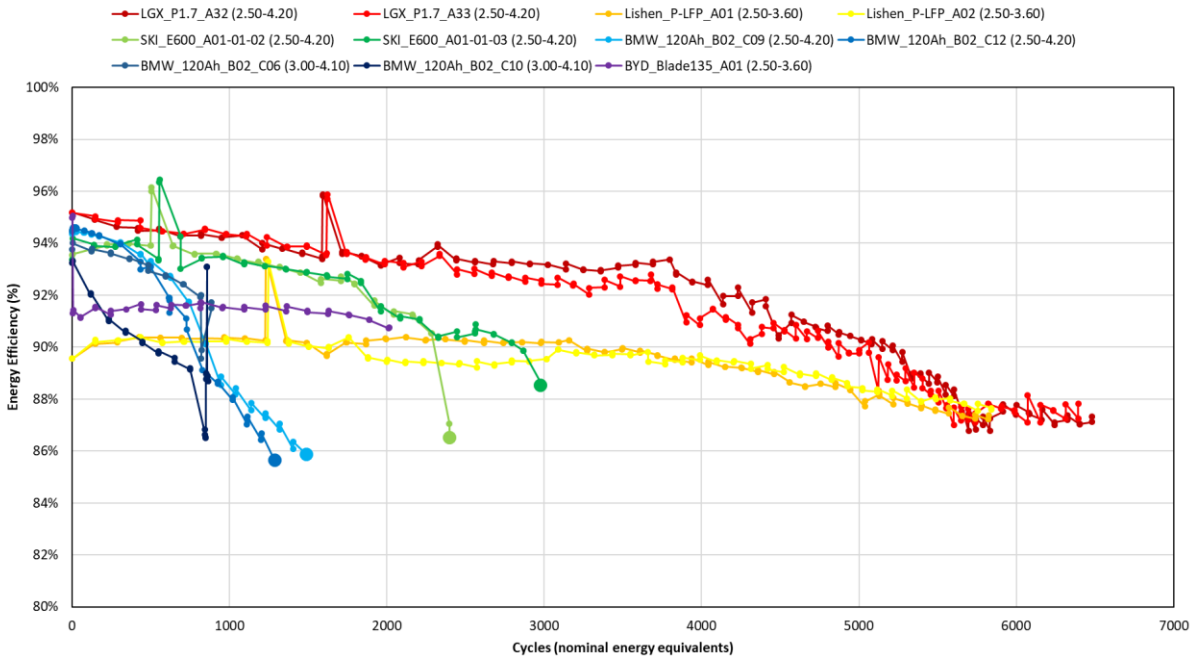

Figure 5.6 Experimental energy efficiency degradation trends among a diverse set of EV cells, that were new (fresh) at the start of the experiment.

5.2 Technical challenges

Over the last ten years, our laboratory has repurposed dozens of used EV battery packs into second-life applications. These come from a wide range of vehicles, represent vastly different designs/architecture, and have broadly varying state of health. The following assessment of technical challenges is based upon that experience.

5.2.1 Pack design and processing

Section 3.2 explained how battery repurposing involves many time-consuming steps, including battery removal, inspection, screening, modification, and testing, which are difficult to automate due to the diversity among EV battery designs. The technical challenges associated with these steps will now be described in greater detail based on our first-hand experience in a research environment.

Nearly all existing EV battery packs use a module-to-pack design. This means that discrete modules are placed onto a structural supporting base, interconnected, covered, and then bolted into the underbelly of the EV, along with electrical/thermal connections. Processing a used EV battery therefore requires a reversal of these assembly steps. Battery removal first involves raising the vehicle on a lift, detaching the electrical and thermal connections, rolling a lift table underneath, removing the supporting fasteners, and lowering the battery. The battery should ideally be fully discharged before removal to minimize safety risk, but there will be cases where this is not possible (e.g. battery being removed from a disabled vehicle). Upon receipt, visual investigation of the pack occurs. Often there are dents, scratches, etc., which can come from the first life use or the removal from the vehicle. It is important to document these so that it can be verified that they did not penetrate to the module/cell level. If available, removal of the manual safety disconnect or mid-pack fuse will halve the internal voltage to reduce safety risk for technicians.

Internal investigation is typically warranted, to visually determine if there is any physical damage, but moreover to allow for module removal if the battery is to be rearranged into a different format for second-life. Removal of the cover is simple in some circumstances, such as a rubber seal compressed by fasteners. And in other circumstances is very difficult due to the use of adhesives, requiring the application of heat, force, and cutting tools.

Once opened, the battery presents a significant safety concern, as DC voltages (nominally 400 V or 800 V when charged) are readily accessible. Extra care is required with 800 V packs, since a mid-pack disconnect feature still leaves a dangerous 400 V across half the battery width. In the instance that either a cell group has failed, or that the battery modules will be removed, the electrical connections will need to be removed/rearranged. If battery modules are removed, we have found two issues. First, they can be difficult to handle due to their shape and attachment points. For example, the Tesla Model 3 modules are long, 100 V, lack mounting points down one side, and have an exposed connections area on the bottom, making them very difficult to set down on a table or workbench. Second, many modules rely on the supporting base for their structural integrity. Because cells within modules tend to expand throughout life, the removal of the module from this support structure may allow it to extend in length and bow. This can be difficult to overcome in second-life, as recompression may require substantial force. While EV dealerships may have access to specialized tools and lift tables for a specific EV, we expect that third party handlers will use generalized tools and lift tables for the second-life market.

As described in Section 3.1.1, some emerging EV battery designs are using cell-to-pack, module-to-chassis and cell-to-chassis technologies, the latter two of which avoid a standalone pack housing altogether. While these technologies stand to offer significant enhancements to EV performance, they also stand to introduce a new hurdle for battery repurposing. Specifically, module-to-chassis and cell-to-chassis designs will complicate or even prevent access to the battery after it is installed in the vehicle, making these battery designs undesirable from the perspective of second-life applications.

5.2.2 Battery management and health monitoring

The BMS can present its own technical challenge when repurposing an EV battery pack. Even if the pack is not physically modified in any way, the original BMS is configured for EV service and may not be optimized for second-life service. It will not always be possible to reprogram or even access the original BMS installed by the manufacturer, as some manufacturers employ proprietary BMS communication protocols [155]. For example, different cell balancing settings may be appropriate for repurposed EV batteries at lower SOH levels [122]. Retrofitting an aftermarket BMS may be necessary in such cases, which would offset some of the advantages of pack-level repurposing. As an alternative, it has been proposed that original manufacturers could sell a BMS gateway tool to second-life battery developers, which would enable sufficient access to the original BMS while preserving necessary security levels for the manufacturer [156].

A BMS gateway would also help to address the challenge of health monitoring for second-life batteries. As described in Section 3.2.3, a wide variety of established and developing methods can be used to evaluate battery SOH, and the lack of standardized methods is a challenge for batteries in general. The added challenge for second-life batteries is that the usage history of a given EV battery may be unknown or inaccessible when the battery is acquired by a second-life battery company. Making this information available through the original BMS would make it much easier for second-life battery companies to evaluate both the SOH and RUL of acquired EV batteries and thereby produce more predictable and reliable second-life battery systems. Battery passports (discussed further in Section 6.2.2) could be an alternative means of making the necessary information available to users without compromising proprietary BMS technology.

Apart from software, the physical BMS connections can also present a challenge. The original EV battery is not designed and manufactured with repurposing in mind, and the most economical BMS design for the EV manufacturer may not be economical for the repurposing company. A good example of this is the Tesla Model 3 battery pack. As pictured in Figure 5.7, the BMS board on each battery module is wire bonded to a ribbon cable that runs along the module length making connections with each cell group. The lack of conventional wire connectors made it challenging to replace the original BMS with an aftermarket BMS. The retrofitted BMS connections are difficult to reliably attach to the many series-connected cell groups, making the process time-intensive and somewhat unreliable. While this was a functional solution for research purposes, it would not be a viable solution for a second-life battery company.

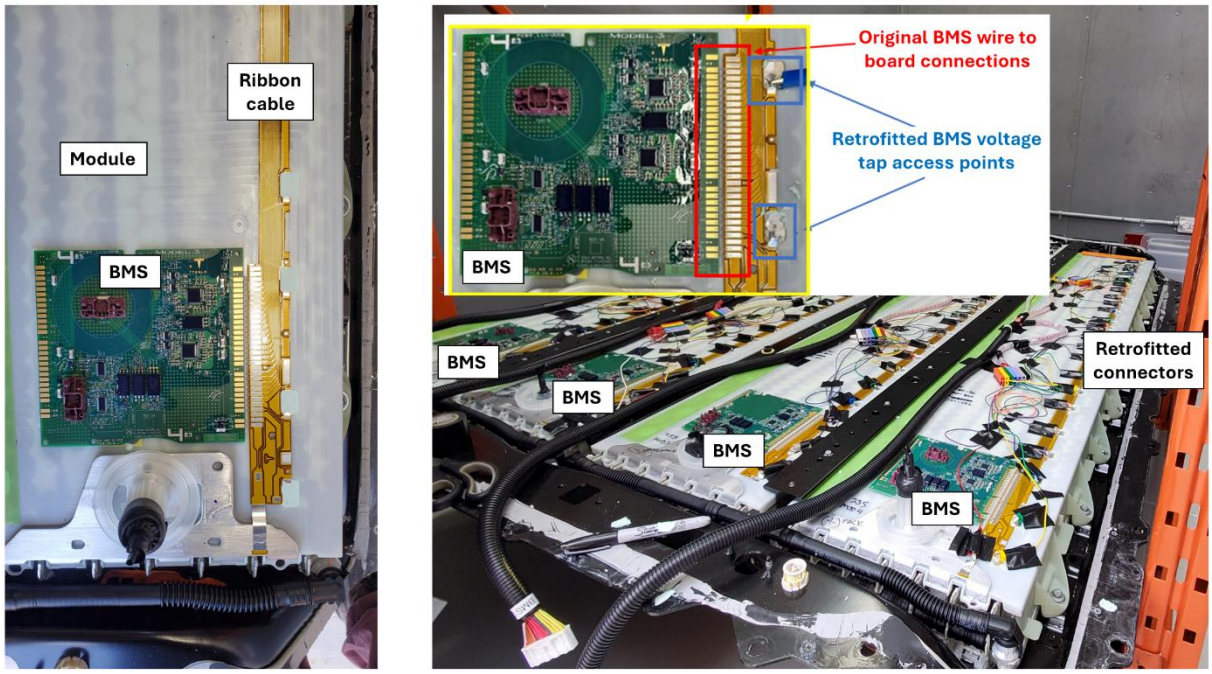

Figure 5.7 Example of a time-intensive BMS retrofit for a Tesla Model 3 LR battery pack.

5.2.3 Thermal management and safety

Thermal management is another technical challenge for both module-level and pack-level repurposing. For example, if an EV battery pack is designed with an active-liquid TMS, the second-life battery developer must decide if they will construct a liquid circulation system to utilize the liquid-cooling capabilities of the pack/modules in second-life service at the expense of increased system complexity and cost. One potential issue is the possibility of liquid leaks from retrofitted liquid circulation systems, which introduces a risk of electrical short circuits. Alternatively, if the developer opts to disable the original liquid-cooling capability and operate the battery with passive cooling, there is an added risk of the battery overheating. This dilemma introduces an additional safety risk compared to new batteries. A further risk arises from the fact that second-life batteries are already somewhat degraded and may have unknown usage histories. Second-life battery project developers may therefore opt to integrate additional safety measures into the energy storage system for risk mitigation, such as fire suppression systems [129].

If a second-life project developer does elect to disable the liquid-cooling capability of an EV battery, careful attention should be paid to the temperature monitoring system. The original temperature sensors may be strategically placed at locations that experience the highest temperatures when the battery is liquid-cooled, and these same locations may not correspond to the highest temperatures when the battery is passive-cooled. This is indeed the case for the Tesla Model 3 battery. An illustrative depiction of this is given in Figure 5.8, which shows the original thermistors located at the warm ends of the liquid-cooled modules (i.e. beneath the BMS boards pictured in Figure 5.7). To capture the most important temperatures in passive-cooled mode, the temperature monitoring system would have to be modified, or else supplemented with a spatial temperature extrapolation model such as the one proposed in [157]. Otherwise, the passive-cooled battery pack could become much hotter than measurements indicate to the operator, increasing the risk of thermal runaway.

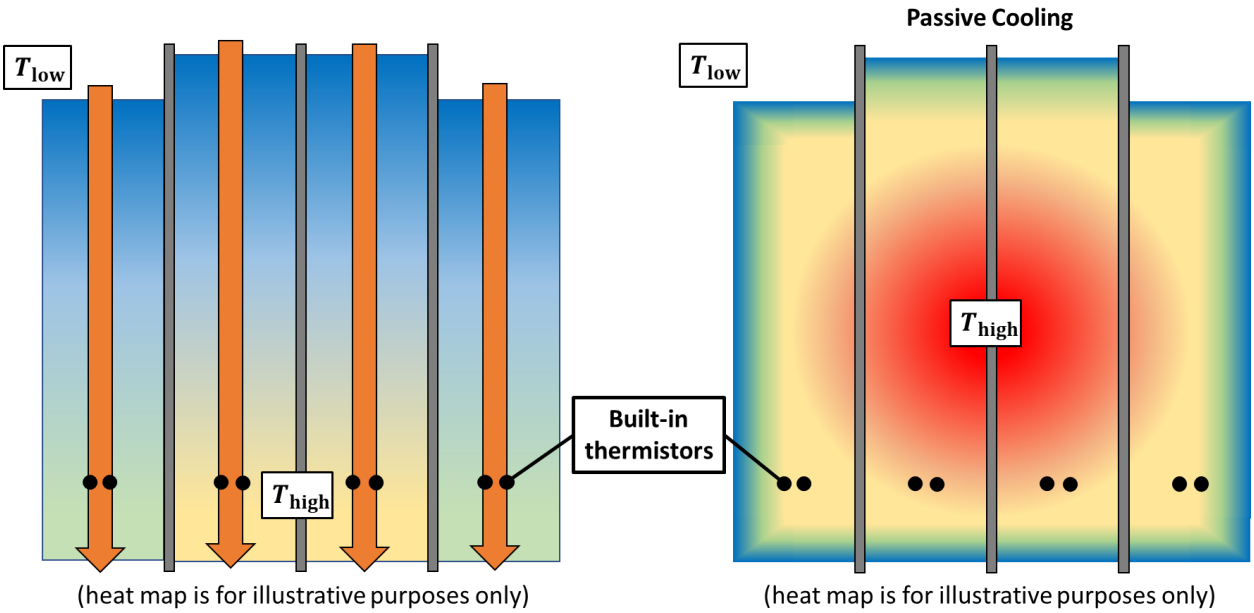

Figure 5.8 Illustration of temperature sensor placement in the Tesla Model 3 LR battery pack.

5.2.4 Operational control

As with any stationary battery system, second-life energy storage systems require appropriate hardware and software to enable remote monitoring, data logging, and control of the system [131]. An energy management system is used to automatically control the power flow in a way that optimizes battery operation for the given stationary energy storage application, sometimes using artificial intelligence methods [35]. For second-life batteries, the wide variety of EV battery designs presents a challenge for operational control of second-life battery systems, as the optimal control strategy for one EV battery design may not be transferrable to systems using other EV battery designs [123].

New stationary batteries are often LFP batteries due to their long cycle life [158], but second-life battery control systems may also have to account for pronounced degradation in the system as a whole as well as SOH differences among individual modules and cells. For example, batteries at lower SOH may need to be constrained within narrower SOC windows in order to prolong cycle life [159], or be constrained within narrower power envelopes to account for increased internal resistance compared to new batteries [35]. Such limitations will influence the economic viability of second-life batteries in more demanding stationary energy storage applications, at least in comparison to new stationary batteries. As explained in Section 5.1, one way to overcome these limitations is to oversize the second-life battery system (i.e. add more repurposed batteries) so that individual batteries can undergo relatively light cycling over an extended life without limiting the energy and power capabilities of the system as a whole [155]. Depending on how frequently and aggressively second-life batteries are cycled before and after repurposing, they can generally be expected to last up to 10 years or longer in second-life service [151], [152].

While it is presently common practice to deploy a single EV battery type in a given second-life battery system, value stacking could make it economically advantageous to combine multiple EV battery

designs in a single second-life battery system, since some battery designs may be better suited for high-energy applications like peak shaving and energy arbitrage, while other battery designs may be better suited for high-power ancillary services. Figure 5.9 shows a pilot-scale example of a 'mixed battery array' which takes this approach to pack-level repurposing. This type of system [100] could not be certified under the current edition of UL 1974, and is therefore not currently an attractive option for a company looking to sell packaged second-life battery systems to customers. However, a mixed battery array could be feasible for a company looking to construct, own, and operate a second-life battery system and sell stacked energy storage services to the electricity system operator. The energy management system would be especially critical for a mixed battery array, since the control strategy would have to account for the unique performance characteristics of each battery design in the array [123]. The control strategy would therefore need to be informed by comparable performance metrics assigned to each battery design.

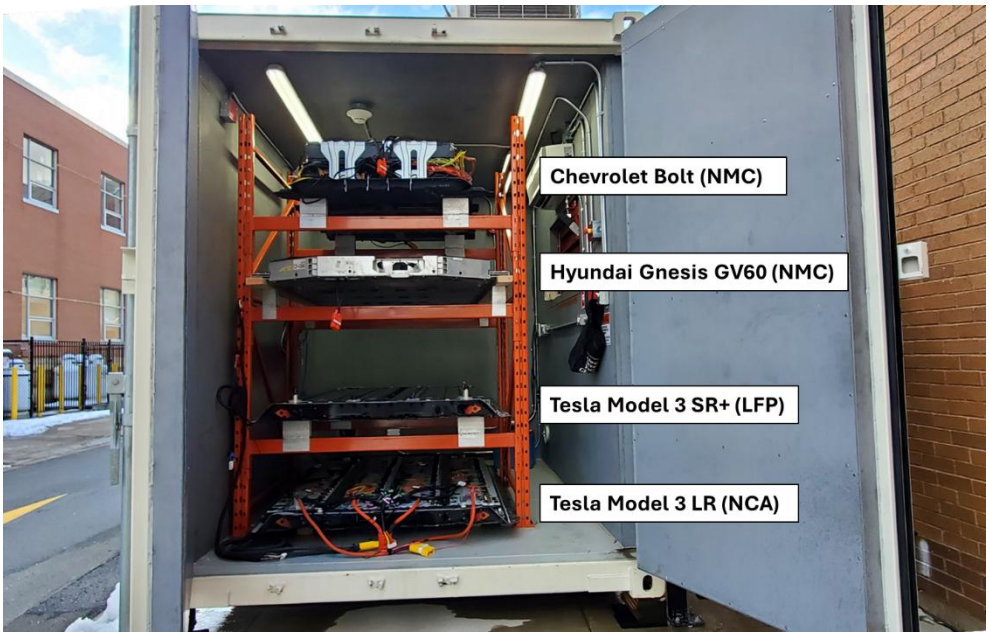

Figure 5.9 Pilot-scale example of a 'mixed battery array' second-life battery system at Dalhousie University.

6 Conclusions and Recommendations

This report has provided a detailed review of second-life battery technology and evaluated the technical feasibility of using repurposed EV batteries to provide electricity grid ancillary services as an alternative to new batteries. A number of technical challenges still remain for the second-life battery industry, such as repurposing diverse fleets of unique battery packs designed for EV service, accessing BMS data, reliably assessing the remaining operational value in used EV batteries, and accounting for decreased energy and power capability in partially aged batteries. However, these technical challenges can be overcome with continued innovation and investment. For example, minimizing the cost of repurposed batteries would allow for oversized second-life battery systems that can better compete with the performance characteristics of new batteries.

Though second-life batteries are already being deployed in electricity grid applications, the literature is still lacking in experimental studies that demonstrate second-life battery performance in ancillary services. Frequency regulation appears to be the only well-established case, and while the known characteristics of second-life batteries seem suitable for most other ancillary services as well, dedicated experimental studies should be conducted to confirm this suitability. Standard test protocols already exist for this exact purpose, but are not widely adopted for second-life batteries.

The remainder of this final section offers recommendations that will facilitate research and development of second-life batteries in ancillary services. Suitable technical criteria for the testing and characterization of these systems are presented. Potential opportunities for standardization are also identified.

6.1 Recommended technical criteria

Based on a combination of the reviewed literature and our practical experience, we detail in the following subsections our recommendations for the evaluation of second-life battery performance in ancillary services. Electrical, thermal, and degradation performance considerations are provided.

6.1.1 Electrical performance

Many of the electrical performance test methods and metrics recommended in the SNL/PNNL test protocols (Section 4.1) are suitable for evaluating second-life batteries in ancillary services. A standard set of reference performance tests should be adopted by Canada to establish baseline performance characteristics for a given battery and assess performance degradation throughout second-life. As per SNL/PNNL, these should include the following:

- A deep cycle test to measure baseline energy capacity and energy efficiency.
- A pulse test to measure discharge response time, ramp rate, and internal resistance.
- A pulse test to measure charge response time, ramp rate, and internal resistance.
- A self-discharge test to measure the self-discharge rate.

While reactive power pulse tests are also recommended by the SNL/PNNL test protocol, these tests may be unnecessary for lithium-ion batteries since a reactive power test would effectively be testing the inverter rather than the battery.

The frequency regulation, frequency response, and voltage support duty cycles prescribed by SNL/PNNL are appropriate for evaluating second-life batteries. However, more aggressive frequency regulation duty cycle standards may need to be developed to better reflect modern frequency regulation signals such as PJM's *Regulation D* signal. Since some second-life batteries may perform ancillary services simultaneously with other electricity grid energy storage services, stacked duty cycles such as those described in Section 4.1.5 may also be appropriate.

Round-trip energy efficiency is an appropriate performance metric for ancillary services, with the exception of voltage support which relies on reactive power only. Note that energy efficiency may be of little practical consequence for ancillary services that are called upon relatively infrequently (e.g. non-spinning reserves). As per the SNL/PNNL test protocol, the round-trip energy efficiency of a given duty cycle is calculated by dividing the total discharge energy E_{dis} over the total charge energy E_{chg}, where the energy totals include the energy required to return the battery to its initial SOC after the duty cycle is completed, as well as any necessary auxiliary loads E_{aux} (e.g. liquid pump + chiller). This definition is given in Equation 6.1.

$$\eta = \frac{E_{\text{dis}}}{E_{\text{chg}} + E_{\text{aux}}} \times 100\ \% \tag{6.1}$$

Signal tracking accuracy is an appropriate performance metric for ancillary services. As per the SNL/PNNL test protocol, the signal tracking error Err is calculated by summing the squared error or absolute error between the prescribed power signal P_{signal} and measured battery power P_{meas} at each time interval. This is defined in Equation 6.2. The SNL/PNNL test protocol also recommends calculating the percentage of total time intervals for which the measured battery power is within 2 % of the prescribed power signal. While it is likely that any battery will be able to perform near-perfect signal tracking, this metric still provides an opportunity to identify unforeseen technical issues in the energy storage system.

$$Err = \sum (P_{\text{signal}} - P_{\text{meas}})^2 \tag{6.2}$$

SOC excursions are also appropriate performance metrics for ancillary services. As per the SNL/PNNL test protocol, SOC excursions are determined simply by recording the minimum and maximum battery SOC reached during testing and comparing these values to preferred SOC limits.

Peak charge and discharge power are appropriate performance metrics for frequency response in particular. As per the SNL/PNNL test protocol, peak power is determined by applying a series of complete discharge or charge tests at multiples of the rated power ranging from 1.25 to 10 so that the peak 1-minute power and peak 20-minute power can be interpolated (see Figure 4.5 for a comparable example from the literature).

Apart from these SNL/PNNL performance metrics, we also recommend additional electrical performance metrics based on our practical experience. For one, the energy utilization ratio ζ (see Figure 5.2 and Figure 5.3) can be helpful for quantifying the amount of energy that a battery can discharge or charge between set voltage limits at a given power rate. A suggested definition for ζ is

given in Equation 6.3, which scales the measured discharge energy E_{dis} at a given discharge rate by the full discharge capacity $E_{\text{dis}}^{\text{full}}$ attainable from a slow discharge starting at 100 % SOC.

$$\zeta = \frac{E_{\text{dis}}}{E_{\text{dis}}^{\text{full}}} \times 100\ \% \tag{6.3}$$

Energy throughput should always be tracked throughout the operational life of a second-life battery, since this can be used to calculate the number of equivalent full cycles the battery has undergone, which in turns helps to quantify battery SOH and RUL.

A standard means of comparing the energy capacity and power capability of different EV batteries is also advisable. Potential methods include volumetric or gravimetric energy density and power density. Suggested definitions for volumetric energy density $\bar{E}_v$ (in Wh/L) and gravimetric energy density $\bar{E}_m$ (in Wh/kg) are respectively given in Equations 6.4 and 6.5 to scale the discharge energy capacity E_{dis} by battery volume v and mass m. While volume and weight may be of little consequence in many ancillary service applications, these parameters can prove helpful when dealing with diverse EV batteries of significantly different sizes. Volumetric energy density can also provide qualitative insights into battery internal resistance and energy efficiency using correlations like the one shown in Figure 5.1.

$$\bar{E}_v = \frac{E_{\text{dis}}}{v} \tag{6.4}$$

$$\bar{E}_m = \frac{E_{\text{dis}}}{m} \tag{6.5}$$

6.1.2 Thermal performance

Section 4.2 revealed that thermal performance evaluations represent a significant gap in the literature as well as the SNL/PNNL test protocols. Based on our practical experience we recommend four thermal performance metric categories to integrate with ancillary service test methods and operations. Active TMS designs will tend to produce superior results for all four metrics compared to passive TMS designs.

As illustrated in Figure 4.10, the maximum battery temperature rise $\Delta T_{\text{high}}^{\text{max}}$ is an important metric for evaluating thermal safety during second-life battery operation. While it is ultimately the battery temperature and not the temperature rise that triggers thermal runaway, evaluating temperature rise above a reference temperature T_∞ (i.e. the setpoint of the TMS) facilitates the comparison of second-life batteries employing different TMS setpoints (e.g. 20 °C air vs 30 °C liquid). This definition is stated in Equation 6.6, where $T_{\text{high}}^{\text{max}}$ is the instantaneous maximum temperature measured over a given period at a point representing the highest temperatures on a given battery.

$$\Delta T_{\text{high}}^{\text{max}} = T_{\text{high}}^{\text{max}} - T_\infty \tag{6.6}$$

Similarly, the average battery temperature rise $\Delta T_{\text{high}}^{\text{avg}}$ is an important metric for evaluating thermal durability during second-life battery operation. As described in 4.3.1, the average battery temperature should be maintained within a range of approximately 25 to 40 °C to avoid accelerated degradation and/or reduced performance. The definition in Equation 6.7 is similar to Equation 6.6 except that $T_{\text{high}}^{\text{avg}}$ represents an average is taken over a given period rather than an instantaneous maximum.

$$\Delta T_{\text{high}}^{\text{avg}} = T_{\text{high}}^{\text{avg}} - T_{\infty} \tag{6.7}$$

The temperature differential $\Delta T_{\text{diff}}^{\text{avg}}$ between the warmest $T_{\text{high}}^{\text{avg}}$ and coolest $T_{\text{low}}^{\text{avg}}$ cells in the battery is an important metric for evaluating thermal consistency during second-life battery operation. As described in Section 3.1.4, battery temperature gradients should be maintained below 5 °C to prevent cell SOH levels from diverging within the battery over time.

$$\Delta T_{\text{diff}}^{\text{avg}} = T_{\text{high}}^{\text{avg}} - T_{\text{low}}^{\text{avg}} \tag{6.8}$$

The thermal recovery rate is an important metric for evaluating thermal availability during second-life battery operation. While thermal control strategies vary, a battery may be forced into standby mode if it reaches an upper temperature limit during operation. The rate at which the TMS can cool the battery in standby mode will determine how long the battery will remain unable to fulfill its ancillary service commitments. This standby cooldown rate can be expressed as an average temperature rate of change, a time constant based on Newton's law of cooling, or simply the time duration t_{cool} required for the battery to cool to a set temperature threshold T_{cool}. One formulation for a cooling time constant τ is given in Equation 6.9, though this neglects temperature gradients within the battery.

$$\tau = \frac{t_{\text{cool}}}{\ln\left[\frac{T_{\text{high}}^{\text{max}} - T_{\infty}}{T_{\text{cool}} - T_{\infty}}\right]} \tag{6.9}$$

Figure 6.1 illustrates how three of these thermal performance categories can vary across different second-life batteries. The black datapoints represent $\Delta T_{\text{high}}^{\text{max}}$ and $\Delta T_{\text{high}}^{\text{avg}}$ measured during deep-cycle testing at three different power rates. The columns represent the total cycle durations for these power rates, where orange and yellow represent standby cooling periods required for the battery to reach a lower temperature threshold before the next charge or discharge begins. These three metrics highlight the significant thermal performance differences between liquid-cooled and passive-cooled (i.e. liquid cooling disabled) versions of Tesla Model 3 and Chevrolet Bolt battery packs.

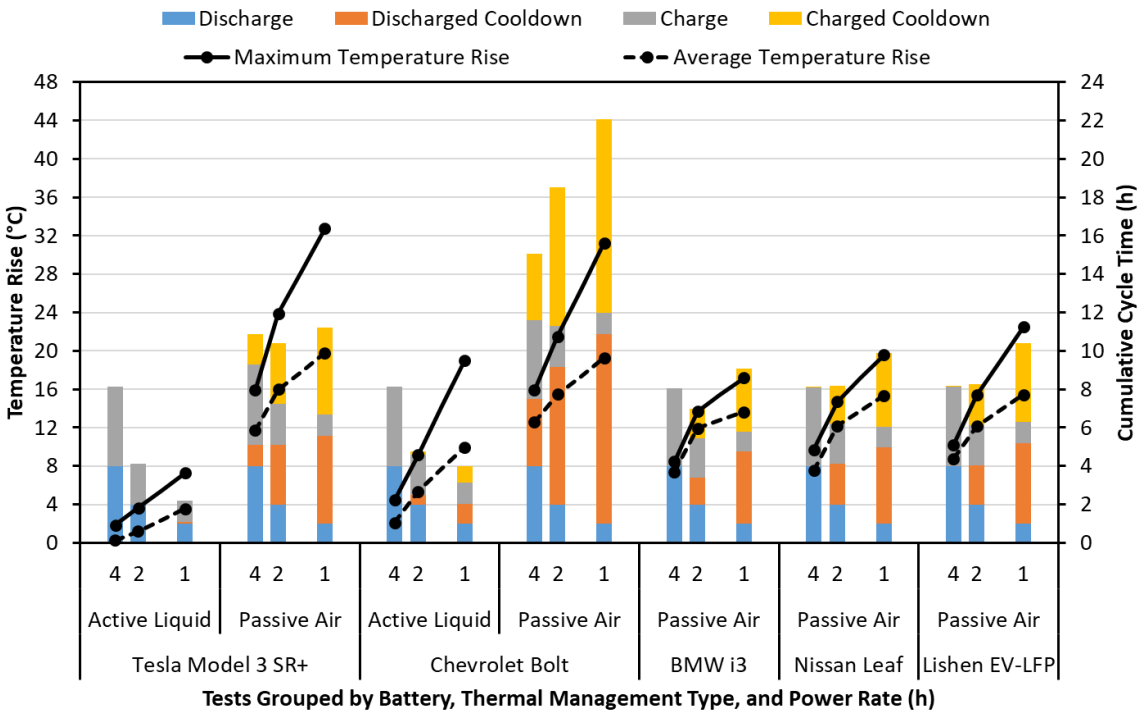

Figure 6.1 Example of maximum temperature rise, average temperature rise, and cooldown periods for a set of EV battery packs subjected to deep cycle tests at different power rates [1].

In addition to the four thermal performance categories, heat generation metrics (estimated using electrical measurements) are useful for assessing thermal management loads independently from battery temperature measurements. The average volumetric heat generation rate $\dot{\bar{q}}_v$ shown in the right chart of Figure 5.3 is calculated as the difference between the charge energy E_{chg} and discharge energy E_{dis} divided by the sum of the charge time t_{chg} and discharge time t_{dis} for a constant power cycle between set voltage limits, all scaled by the battery volume v, as shown in Equation 6.10. An equivalent definition can be stated in terms of v, the applied constant power magnitude P, and the cycle energy efficiency η. This is averaged over a full battery cycle, unlike the instantaneous heat generation rate represented by I^2R. Alternative heat generation metrics could be developed for ancillary service duty cycles.

$$\dot{\bar{q}}_v = \frac{1}{v}\left(\frac{E_{\text{chg}} - E_{\text{dis}}}{t_{\text{dis}} + t_{\text{chg}}}\right) = \frac{P}{v}\left(\frac{1-\eta}{1+\eta}\right) \tag{6.10}$$

6.1.3 Degradation performance

It is already common practice to monitor battery capacity and/or internal resistance to evaluate SOH over battery life. However, each of the recommended performance metrics in Sections 6.1.1 and 6.1.2 could degrade with extended battery use and should therefore be periodically re-evaluated where

feasible. The rate of change in capacity fade can provide an additional metric for quantifying the degradation rate.

For second-life batteries in particular, RUL is an important but challenging degradation performance metric. Where battery usage history is available, data-driven techniques should be applied to produce RUL estimations that can help to inform the EOVL battery pathways, insure second-life battery system warranties, and monitor operational second-life battery health.

Estimation methods for SOH and RUL are being researched extensively, so academic and industry developments should be monitored for future breakthroughs that facilitate battery repurposing.

6.2 Opportunities for standardization

Given the significant diversity and complexity associated with EV battery designs and repurposing processes, standard practices would help ensure that second-life batteries can be repurposed for ancillary services with optimal reliability, consistency, cost, and safety. Specific opportunities for standardization are described in the subsections below.

6.2.1 Battery design

It is commonly pointed out in the literature that the repurposing (and recycling) of EV batteries is inhibited by the diversity among EV battery pack designs as well as the fact that many EV battery packs are not designed for ease of disassembly [22]. The prospect of module-to-chassis and cell-to-chassis battery designs stands to further inhibit ease of disassembly. However, most researchers acknowledge that direct regulation of EV battery pack design and manufacturing would likely stifle innovation in the industry. Instead, some researchers recommend international collaboration between governments, manufacturers, and researchers with the goal of tracking and encouraging circular design practices in EV battery manufacturing [160], [161].

Certain battery design parameters can help to reduce battery internal resistance, which is beneficial for the high-power operational demands of most ancillary services. However, it would be unreasonable to expect EV battery manufacturers to adopt battery design practices for the benefit of second-life ancillary service performance. For one, EV battery manufacturers must prioritize battery energy density in order to offer attractive EV driving range capabilities to their customers, and cell designs with higher energy density inherently tend to have higher internal resistance. Furthermore, any given EV battery could be repurposed in a low-power or high-power application once it enters the second-life supply chain, so designing EV batteries for ancillary service performance would not necessarily be helpful for the second-life battery industry as a whole.

While it is unlikely that EV battery designs will evolve in ways that specifically benefit second-life ancillary service performance, there are clear opportunities for governments to collaborate with the EV battery manufacturing industry to ensure that EV battery designs are not needlessly inhibitive to repurposing in the general sense. Future module-to-chassis and cell-to-chassis battery designs should take battery circularity into account and avoid making EV batteries inaccessible for repurposing.

6.2.2 Battery identification

Section 3.2.2 explained that safe and effective battery repurposing requires access to as much information as possible regarding the design specifications, performance characteristics, health, and usage history of batteries acquired after EOVL. Standardization of battery identification protocols would help to ensure that this information is accessible throughout the battery life cycle. The concept of a 'battery passport' was proposed in a 2019 report by the Global Battery Alliance [161], which is a public-private collaboration platform established in 2017 to help foster a sustainable global battery value chain. The idea is to maintain a digital, cloud-based record of all pertinent information related to a given battery throughout its life, accessible by a scannable code attached to the battery. The Global Battery Alliance has since conducted two battery passport pilot programs in 2023 and 2024 to demonstrate feasibility and gain industry feedback for future developments [161]. Following the lead of the Global Battery Alliance, the 2023 EU Battery Regulation requires that all manufactured EV batteries feature a battery passport beginning on February 18, 2027, and that repurposing companies and other battery users must be granted access to the SOH and RUL data stored in the original BMS [40]. Similar regulations have not yet been developed in North America, but policy researchers have recommended that the EU Battery Regulation be used as a model [160]. CSA Group is now advising battery companies to prepare to meet new requirements that will come into effect under the EU Battery Regulation [162].

To facilitate the repurposing of EV batteries into ancillary services, battery passports could be mandated to include battery performance metrics that apply to ancillary services. These metrics could include those described in Section 6.1.

6.2.3 Battery assessment

Despite recent progress in developing standard test procedures for second-life batteries, researchers have highlighted the need for further advancement in this area [163]. For example, standard battery test procedures often require many hours to complete, which is economically inhibitive for mass production of second-life batteries [122]. Rapid test procedures for second-life batteries are being researched extensively, but have not yet been adopted into certification standards. As explained in Section 3.2.3, rapid and reliable SOH and RUL estimation methods are especially important for improving the economics of second-life batteries.

Ancillary services generally require high-power discharge and/or charge over relatively short cycles. Standard SOH assessment techniques may therefore need to be differentiated for ancillary services compared to electricity grid energy management services. In the case of ancillary services, it is especially important that battery SOH assessment account for power capability, which is influenced by battery internal resistance growth more so than energy capacity retention. Other standard performance evaluation methods and metrics specific to ancillary services would also facilitate comparison and selection among the many EV battery designs available for second-life service.

The performance metrics described in Section 6.1 could serve as a starting point for standardized ancillary service performance metrics. Researchers should collaborate with industry and government to reach consensus on what standardizations are most conducive to widespread adoption and most helpful to facilitating the repurposing of EV batteries for ancillary services.

References

[1] C. White, “Electrical and Thermal Performance Evaluations for Repurposed Electric Vehicle Batteries in Second Life Electricity Grid Energy Storage,” PhD, Mechanical Engineering, Dalhousie University, Halifax, Canada, 2025. [Online]. Available: https://dalspace.library.dal.ca/items/882d1499-c09a-457b-a6f6-3eed0fa8ab2b

[2] Accelerating to Zero Coalition, “Zero Emission Vehicles Declaration.” Accessed: Mar. 01, 2025. [Online]. Available: https://acceleratingtozero.org/the-declaration/

[3] IEA, “World Energy Outlook 2024,” IEA, Paris, 2024. [Online]. Available: https://www.iea.org/reports/world-energy-outlook-2024

[4] IEA, “Global EV Outlook 2024,” IEA, Paris, 2024. [Online]. Available: https://www.iea.org/reports/global-ev-outlook-2024

[5] BloombergNEF, “Headwinds in Largest Energy Storage Markets Won’t Deter Growth,” BloombergNEF. Accessed: Mar. 02, 2025. [Online]. Available: https://about.bnef.com/blog/headwinds-in-largest-energy-storage-markets-wont-deter-growth/

[6] Y. Zhao *et al.*, “A Review on Battery Market Trends, Second-Life Reuse, and Recycling,” *Sustain. Chem.*, vol. 2, no. 1, pp. 167–205, Mar. 2021, doi: 10.3390/suschem2010011.

[7] L. C. Casals, M. Etxandi-Santolaya, P. A. Bibiloni-Mulet, C. Corchero, and L. Trilla, “Electric Vehicle Battery Health Expected at End of Life in the Upcoming Years Based on UK Data,” *Batteries*, vol. 8, no. 10, p. 164, Oct. 2022, doi: 10.3390/batteries8100164.

[8] D. Anseán *et al.*, “Operando lithium plating quantification and early detection of a commercial LiFePO4 cell cycled under dynamic driving schedule,” *J. Power Sources*, vol. 356, pp. 36–46, Jul. 2017, doi: 10.1016/j.jpowsour.2017.04.072.

[9] A. J. Smith, J. C. Burns, and J. R. Dahn, “A High Precision Study of the Coulombic Efficiency of Li-Ion Batteries,” *Electrochem. Solid-State Lett.*, vol. 13, no. 12, p. A177, 2010, doi: 10.1149/1.3487637.

[10] J. Li, J. Harlow, N. Stakheiko, N. Zhang, J. Paulsen, and J. Dahn, “Dependence of Cell Failure on Cut-Off Voltage Ranges and Observation of Kinetic Hindrance in $LiNi_{0.8}Co_{0.15}Al_{0.05}O_2$,” *J. Electrochem. Soc.*, vol. 165, no. 11, pp. A2682–A2695, 2018, doi: 10.1149/2.0491811jes.

[11] S. Nowak and M. Winter, “The Role of Cations on the Performance of Lithium Ion Batteries: A Quantitative Analytical Approach,” *Acc. Chem. Res.*, vol. 51, no. 2, pp. 265–272, Feb. 2018, doi: 10.1021/acs.accounts.7b00523.

[12] D. J. Xiong *et al.*, “Measuring Oxygen Release from Delithiated LiNix Mny Co1-x-yO2 and Its Effects on the Performance of High Voltage Li-Ion Cells,” *J. Electrochem. Soc.*, vol. 164, no. 13, pp. A3025–A3037, 2017, doi: 10.1149/2.0291713jes.

[13] Circular Energy Storage, “The lithium-ion battery life cycle report,” Dec. 2020.

[14] A. Devie and M. Dubarry, “Durability and Reliability of Electric Vehicle Batteries under Electric Utility Grid Operations. Part 1: Cell-to-Cell Variations and Preliminary Testing,” *Batteries*, vol. 2, no. 3, p. 28, Sep. 2016, doi: 10.3390/batteries2030028.

[15] G. Harper *et al.*, “Recycling lithium-ion batteries from electric vehicles,” *Nature*, vol. 575, no. 7781, pp. 75–86, Nov. 2019, doi: 10.1038/s41586-019-1682-5.

[16] A. Zanoletti, E. Carena, C. Ferrara, and E. Bontempi, "A Review of Lithium-Ion Battery Recycling: Technologies, Sustainability, and Open Issues," *Batteries*, vol. 10, no. 1, p. 38, Jan. 2024, doi: 10.3390/batteries10010038.

[17] P. Li *et al.*, "Progress, challenges, and prospects of spent lithium-ion batteries recycling: A review," *J. Energy Chem.*, vol. 89, pp. 144–171, Feb. 2024, doi: 10.1016/j.jechem.2023.10.012.

[18] Y. E. Milian, N. Jamett, C. Cruz, S. Herrera-León, and J. Chacana-Olivares, "A comprehensive review of emerging technologies for recycling spent lithium-ion batteries," *Sci. Total Environ.*, vol. 910, p. 168543, Feb. 2024, doi: 10.1016/j.scitotenv.2023.168543.

[19] A. A. Pesaran, "Lithium-Ion Battery Technologies for Electric Vehicles: Progress and challenges," *IEEE Electrification Mag.*, vol. 11, no. 2, pp. 35–43, Jun. 2023, doi: 10.1109/MELE.2023.3264919.

[20] L. Olsson, S. Fallahi, M. Schnurr, D. Diener, and P. Van Loon, "Circular Business Models for Extended EV Battery Life," *Batteries*, vol. 4, no. 4, p. 57, Nov. 2018, doi: 10.3390/batteries4040057.

[21] L. Ahmadi, A. Yip, M. Fowler, S. B. Young, and R. A. Fraser, "Environmental feasibility of re-use of electric vehicle batteries," *Sustain. Energy Technol. Assess.*, vol. 6, pp. 64–74, Jun. 2014, doi: 10.1016/j.seta.2014.01.006.

[22] P. Eleftheriadis *et al.*, "Second Life Batteries: Current Regulatory Framework, Evaluation Methods, and Economic Assessment: Reuse, refurbish, or recycle," *IEEE Ind. Appl. Mag.*, vol. 30, no. 1, pp. 46–58, Jan. 2024, doi: 10.1109/MIAS.2023.3325091.

[23] D. De Simone and L. Piegari, "Integration of Stationary Batteries for Fast Charge EV Charging Stations," *Energies*, vol. 12, no. 24, p. 4638, Dec. 2019, doi: 10.3390/en12244638.

[24] RMI, "The Economics of Battery Energy Storage," Rocky Mountain Institute, Oct. 2015. Accessed: Mar. 01, 2025. [Online]. Available: https://rmi.org/wp-content/uploads/2017/03/RMI-TheEconomicsOfBatteryEnergyStorage-FullReport-FINAL.pdf

[25] S. U. Agamah and L. Ekonomou, "Peak demand shaving and load-levelling using a combination of bin packing and subset sum algorithms for electrical energy storage system scheduling," *IET Sci. Meas. Technol.*, vol. 10, no. 5, pp. 477–484, Aug. 2016, doi: 10.1049/iet-smt.2015.0218.

[26] T. Bowen, I. Chernyakhovskiy, and P. Denholm, "Grid-Scale Battery Storage: Frequently Asked Questions," National Renewable Energy Laboratory, 2019. Accessed: Mar. 01, 2025. [Online]. Available: https://www.nrel.gov/docs/fy19osti/74426.pdf

[27] H. Wang and B. Zhang, "Energy Storage Arbitrage in Real-Time Markets via Reinforcement Learning," in *2018 IEEE Power & Energy Society General Meeting (PESGM)*, Portland, OR: IEEE, Aug. 2018, pp. 1–5. doi: 10.1109/PESGM.2018.8586321.

[28] M. Uddin, M. F. Romlie, M. F. Abdullah, S. Abd Halim, A. H. Abu Bakar, and T. Chia Kwang, "A review on peak load shaving strategies," *Renew. Sustain. Energy Rev.*, vol. 82, pp. 3323–3332, Feb. 2018, doi: 10.1016/j.rser.2017.10.056.

[29] E. Reihani, M. Motalleb, R. Ghorbani, and L. Saad Saoud, "Load peak shaving and power smoothing of a distribution grid with high renewable energy penetration," *Renew. Energy*, vol. 86, pp. 1372–1379, Feb. 2016, doi: 10.1016/j.renene.2015.09.050.

[30] S. Tewari and N. Mohan, "Value of NAS Energy Storage Toward Integrating Wind: Results From the Wind to Battery Project," *IEEE Trans. Power Syst.*, vol. 28, no. 1, pp. 532–541, Feb. 2013, doi: 10.1109/TPWRS.2012.2205278.

[31] M. F. AL-Sunni, T. Bin-Mohaya, K. Alshehri, H. Saleh, and A.-W. Saif, "On Smoothing the Duck Curve: A Control Perspective," in *2022 19th International Multi-Conference on Systems, Signals & Devices (SSD)*, Sétif, Algeria: IEEE, May 2022, pp. 1518–1522. doi: 10.1109/SSD54932.2022.9955984.

[32] M. Rezaeimozafar, R. F. D. Monaghan, E. Barrett, and M. Duffy, "A review of behind-the-meter energy storage systems in smart grids," *Renew. Sustain. Energy Rev.*, vol. 164, p. 112573, Aug. 2022, doi: 10.1016/j.rser.2022.112573.

[33] V. S *et al.*, "State of Health (SoH) estimation methods for second life lithium-ion battery—Review and challenges," *Appl. Energy*, vol. 369, p. 123542, Sep. 2024, doi: 10.1016/j.apenergy.2024.123542.

[34] H. Rallo, G. Benveniste, I. Gestoso, and B. Amante, "Economic analysis of the disassembling activities to the reuse of electric vehicles Li-ion batteries," *Resour. Conserv. Recycl.*, vol. 159, p. 104785, Aug. 2020, doi: 10.1016/j.resconrec.2020.104785.

[35] X. Hu *et al.*, "A Review of Second-Life Lithium-Ion Batteries for Stationary Energy Storage Applications," *Proc. IEEE*, vol. 110, no. 6, pp. 735–753, Jun. 2022, doi: 10.1109/JPROC.2022.3175614.

[36] Nissan Motor Co., "Europe's largest energy storage system now live at the Johan Cruijff Arena," Nissan News. Accessed: Mar. 02, 2025. [Online]. Available: https://global.nissannews.com/ja-JP/releases/europes-largest-energy-storage-system-now-live-at-the-johan-cruijff-arena

[37] S. Hanley, "Old Nissan LEAF Batteries Being Used For Grid-Scale Storage In California," CleanTechnica. Accessed: Mar. 02, 2025. [Online]. Available: https://cleantechnica.com/2021/10/25/old-nissan-leaf-batteries-being-used-for-grid-scale-storage-in-california/

[38] C. Murray, "25MW BESS in Germany using second use battery cells completed by JT Energy Systems," Energy-Storage.News. Accessed: Mar. 02, 2025. [Online]. Available: https://www.energy-storage.news/25mw-bess-in-germany-using-second-use-battery-cells-completed-by-jt-energy-systems/

[39] Connected Energy, "Two Second Life Battery Energy Storage Systems Installed At AMRC." Accessed: Mar. 02, 2025. [Online]. Available: https://connected-energy.co.uk/news/two-second-life-battery-energy-storage-systems-installed-at-amrc-northwest/

[40] European Parliament, "Regulation (EU) 2023/1542 of the European Parliament and of the Council of 12 July 2023 concerning batteries and waste batteries, amending Directive 2008/98/EC and Regulation (EU) 2019/1020 and repealing Directive 2006/66/EC," 2023. Accessed: Mar. 01, 2025. [Online]. Available: https://eur-lex.europa.eu/eli/reg/2023/1542/oj

[41] Smartville, "DOE Awards Smartville $10M for Long Duration, Second-Life Energy Storage Projects, Providing Energy Reliability to HBCUs Among Others," Smartville. Accessed: Mar. 02, 2025. [Online]. Available: https://smartville.io/doe-awarded-ten-million/

[42] Moment Energy, "Moment Energy Secures $20.3M for EV Battery Repurposing Facility in US." Accessed: Mar. 02, 2025. [Online]. Available: https://www.momentenergy.com/news-

articles/moment-energy-awarded-us-20-3-million-by-us-dept-of-energy-to-establish-first-certified-ev-battery-repurposing-facility-in-the-us

[43] "Energy Storage Integration Council (ESIC) Energy Storage Implementation Guide," Electric Power Research Institute, Palo Alto, CA, Technical Update 3002030029, Nov. 2024. [Online]. Available: https://www.epri.com/research/products/3002030029

[44] B. P. Heard, B. W. Brook, T. M. L. Wigley, and C. J. A. Bradshaw, "Burden of proof: A comprehensive review of the feasibility of 100% renewable-electricity systems," *Renew. Sustain. Energy Rev.*, vol. 76, pp. 1122–1133, Sep. 2017, doi: 10.1016/j.rser.2017.03.114.

[45] D. B. Harrington, "Turbine Generators," in *Encyclopedia of Physical Science and Technology*, Elsevier, 2003, pp. 193–215. doi: 10.1016/B0-12-227410-5/00794-8.

[46] P. W. Carlin, A. S. Laxson, and E. B. Muljadi, "The History and State of the Art of Variable-Speed Wind Turbine Technology," 2001. Accessed: Mar. 01, 2025. [Online]. Available: https://www.nrel.gov/docs/fy01osti/28607.pdf

[47] B. Lian, D. Yu, C. Wang, S. Le Blond, and R. W. Dunn, "Investigation of energy storage and open cycle gas turbine for load frequency regulation," in *2014 49th International Universities Power Engineering Conference (UPEC)*, Cluj-Napoca, Romania: IEEE, Sep. 2014, pp. 1–6. doi: 10.1109/UPEC.2014.6934664.

[48] P. Denholm, T. Mai, R. Kenyon, B. Kroposki, and M. O'Malley, "Inertia and the Power Grid: A Guide Without the Spin," National Renewable Energy Laboratory, NREL/TP-6A20-73856, 1659820, MainId:6231, May 2020. doi: 10.2172/1659820.

[49] E. Hirst and B. Kirby, "Separating and measuring the regulation and load-following ancillary services," *Util. Policy*, vol. 8, no. 2, pp. 75–81, Jun. 1999, doi: 10.1016/S0957-1787(99)00011-9.

[50] NERC Resources Subcommittee, "Balancing And Frequency Control," North American Electric Reliability Corporation, 2021. Accessed: Mar. 01, 2025. [Online]. Available: https://www.nerc.com/comm/RSTC_Reliability_Guidelines/Reference_Document_NERC_Balancing_and_Frequency_Control.pdf

[51] B. J. Kirby, "Frequency Regulation Basics and Trends," Oak Ridge National Laboratory, 2004. Accessed: Mar. 01, 2025. [Online]. Available: https://info.ornl.gov/sites/publications/Files/Pub57475.pdf

[52] X. Li, D. Hui, and X. Lai, "Battery Energy Storage Station (BESS)-Based Smoothing Control of Photovoltaic (PV) and Wind Power Generation Fluctuations," *IEEE Trans. Sustain. Energy*, vol. 4, no. 2, pp. 464–473, Apr. 2013, doi: 10.1109/TSTE.2013.2247428.

[53] FERC, "Frequency Regulation Compensation in the Organized Wholesale Power Markets," FERC Order No. 755, Oct. 2011. Accessed: Mar. 01, 2025. [Online]. Available: https://www.ferc.gov/sites/default/files/2020-06/OrderNo.755.pdf

[54] Z. Zhao, C. Wang, and M. H. Nazari, "Revenue Analysis of Stationary and Transportable Battery Storage for Power Systems with High Penetration of Renewable Sources: A Market Participant Perspective," Oct. 15, 2021, *arXiv*: arXiv:2001.01771. doi: 10.48550/arXiv.2001.01771.

[55] P. Denholm, Y. Sun, and T. Mai, "An Introduction to Grid Services: Concepts, Technical Requirements, and Provision from Wind," *Renew. Energy*, 2019, Accessed: Mar. 01, 2025. [Online]. Available: https://www.nrel.gov/docs/fy19osti/73590.pdf

[56] R. Eriksson, N. Modig, and K. Elkington, "Synthetic inertia versus fast frequency response: a definition," *IET Renew. Power Gener.*, vol. 12, no. 5, pp. 507–514, Apr. 2018, doi: 10.1049/iet-rpg.2017.0370.

[57] L. Meng *et al.*, "Fast Frequency Response From Energy Storage Systems—A Review of Grid Standards, Projects and Technical Issues," *IEEE Trans. Smart Grid*, vol. 11, no. 2, pp. 1566–1581, Mar. 2020, doi: 10.1109/TSG.2019.2940173.

[58] D. M. Greenwood, K. Y. Lim, C. Patsios, P. F. Lyons, Y. S. Lim, and P. C. Taylor, "Frequency response services designed for energy storage," *Appl. Energy*, vol. 203, pp. 115–127, Oct. 2017, doi: 10.1016/j.apenergy.2017.06.046.

[59] X. Luo, J. Wang, M. Dooner, and J. Clarke, "Overview of current development in electrical energy storage technologies and the application potential in power system operation," *Appl. Energy*, vol. 137, pp. 511–536, Jan. 2015, doi: 10.1016/j.apenergy.2014.09.081.

[60] O. Palizban and K. Kauhaniemi, "Energy storage systems in modern grids—Matrix of technologies and applications," *J. Energy Storage*, vol. 6, pp. 248–259, May 2016, doi: 10.1016/j.est.2016.02.001.

[61] FERC, "Electric Storage Participation in Markets Operated by Regional Transmission Organizations and Independent System Operators," FERC Order No. 841, Feb. 2018. Accessed: Mar. 01, 2025. [Online]. Available: https://ferc.gov/sites/default/files/2020-06/Order-841.pdf

[62] F. Pampel, S. Pischinger, and M. Teuber, "A systematic comparison of the packing density of battery cell-to-pack concepts at different degrees of implementation," *Results Eng.*, vol. 13, p. 100310, Mar. 2022, doi: 10.1016/j.rineng.2021.100310.

[63] G. Silva, T. Assis Dutra, J. Nunes-Pereira, and A. P. Silva, "Coupled and decoupled structural batteries: A comparative analysis," *J. Power Sources*, vol. 604, p. 234392, Jun. 2024, doi: 10.1016/j.jpowsour.2024.234392.

[64] P. Donaldson, "Cell-to-pack batteries," E-Mobility Engineering. Accessed: Mar. 01, 2025. [Online]. Available: https://www.emobility-engineering.com/cell-to-pack-batteries/

[65] U. Plewnia and R. Tan, "How is 'cell-to-pack' revolutionizing EV battery pack designs?," EV Engineering & Infrastructure. Accessed: Mar. 01, 2025. [Online]. Available: https://www.evengineeringonline.com/how-is-cell-to-pack-revolutionizing-ev-battery-pack-designs/

[66] A. Johannisson, "Outlook of EV battery pack design trends," BSc, KTH Royal Institute of Technology, Stockholm, Sweden, 2023. Accessed: Mar. 01, 2025. [Online]. Available: https://kth.diva-portal.org/smash/get/diva2:1786790/FULLTEXT01.pdf

[67] C. Yang, N. Sunderlin, W. Wang, C. Churchill, and M. Keyser, "Compressible battery foams to prevent cascading thermal runaway in Li-ion pouch batteries," *J. Power Sources*, vol. 541, p. 231666, Sep. 2022, doi: 10.1016/j.jpowsour.2022.231666.

[68] T. Waldmann *et al.*, "A Direct Comparison of Pilot-Scale Li-Ion Cells in the Formats PHEV1, Pouch, and 21700," *J. Electrochem. Soc.*, vol. 168, no. 9, p. 090519, Sep. 2021, doi: 10.1149/1945-7111/ac208c.

[69] S. A. Arote, *Lithium-ion and Lithium–Sulfur Batteries: Fundamentals to performance*. IOP Publishing, 2022. doi: 10.1088/978-0-7503-4881-2.

[70] H.-K. Kim, J. H. Choi, and K.-J. Lee, "A Numerical Study of the Effects of Cell Formats on the Cycle Life of Lithium Ion Batteries," *J. Electrochem. Soc.*, vol. 166, no. 10, pp. A1769–A1778, 2019, doi: 10.1149/2.0261910jes.

[71] H. Walvekar, H. Beltran, S. Sripad, and M. Pecht, "Implications of the Electric Vehicle Manufacturers' Decision to Mass Adopt Lithium-Iron Phosphate Batteries," *IEEE Access*, vol. 10, pp. 63834–63843, 2022, doi: 10.1109/ACCESS.2022.3182726.

[72] N. Nitta, F. Wu, J. T. Lee, and G. Yushin, "Li-ion battery materials: present and future," *Mater. Today*, vol. 18, no. 5, pp. 252–264, Jun. 2015, doi: 10.1016/j.mattod.2014.10.040.

[73] M. Armand *et al.*, "Lithium-ion batteries – Current state of the art and anticipated developments," *J. Power Sources*, vol. 479, p. 228708, Dec. 2020, doi: 10.1016/j.jpowsour.2020.228708.

[74] H. Beltran, S. Harrison, A. Egea-Àlvarez, and L. Xu, "Techno-Economic Assessment of Energy Storage Technologies for Inertia Response and Frequency Support from Wind Farms," *Energies*, vol. 13, no. 13, p. 3421, Jul. 2020, doi: 10.3390/en13133421.

[75] A. Manthiram, B. Song, and W. Li, "A perspective on nickel-rich layered oxide cathodes for lithium-ion batteries," *Energy Storage Mater.*, vol. 6, pp. 125–139, Jan. 2017, doi: 10.1016/j.ensm.2016.10.007.

[76] A. J. Smith, S. R. Smith, T. Byrne, J. C. Burns, and J. R. Dahn, "Synergies in Blended $LiMn_2O_4$ and $Li[Ni_{1/3}Mn_{1/3}Co_{1/3}]O_2$ Positive Electrodes," *J. Electrochem. Soc.*, vol. 159, no. 10, pp. A1696–A1701, 2012, doi: 10.1149/2.056210jes.

[77] C. Heubner, T. Liebmann, C. Lämmel, M. Schneider, and A. Michaelis, "Insights into the buffer effect observed in blended lithium insertion electrodes," *J. Power Sources*, vol. 363, pp. 311–316, Sep. 2017, doi: 10.1016/j.jpowsour.2017.07.108.

[78] S. B. Chikkannanavar, D. M. Bernardi, and L. Liu, "A review of blended cathode materials for use in Li-ion batteries," *J. Power Sources*, vol. 248, pp. 91–100, Feb. 2014, doi: 10.1016/j.jpowsour.2013.09.052.

[79] W.-J. Huang *et al.*, "Boosting rate performance of LiNi0.8Co0.15Al0.05O2 cathode by simply mixing lithium iron phosphate," *J. Alloys Compd.*, vol. 827, p. 154296, Jun. 2020, doi: 10.1016/j.jallcom.2020.154296.

[80] H. Y. Tran, C. Täubert, M. Fleischhammer, P. Axmann, L. Küppers, and M. Wohlfahrt-Mehrens, "LiMn2O4 Spinel/LiNi0.8Co0.15Al0.05O2 Blends as Cathode Materials for Lithium-Ion Batteries," *J. Electrochem. Soc.*, vol. 158, no. 5, p. A556, 2011, doi: 10.1149/1.3560582.

[81] D. Andre *et al.*, "Future generations of cathode materials: an automotive industry perspective," *J. Mater. Chem. A*, vol. 3, no. 13, pp. 6709–6732, 2015, doi: 10.1039/C5TA00361J.

[82] M. D. Radin *et al.*, "Narrowing the Gap between Theoretical and Practical Capacities in Li-Ion Layered Oxide Cathode Materials," *Adv. Energy Mater.*, vol. 7, no. 20, p. 1602888, Oct. 2017, doi: 10.1002/aenm.201602888.

[83] S.-J. Kwon, S.-E. Lee, J.-H. Lim, J. Choi, and J. Kim, "Performance and Life Degradation Characteristics Analysis of NCM LIB for BESS," *Electronics*, vol. 7, no. 12, p. 406, Dec. 2018, doi: 10.3390/electronics7120406.

[84] K. Min *et al.*, "A comparative study of structural changes in lithium nickel cobalt manganese oxide as a function of Ni content during delithiation process," *J. Power Sources*, vol. 315, pp. 111–119, May 2016, doi: 10.1016/j.jpowsour.2016.03.017.

[85] Y. Ding, D. Mu, B. Wu, R. Wang, Z. Zhao, and F. Wu, "Recent progresses on nickel-rich layered oxide positive electrode materials used in lithium-ion batteries for electric vehicles," *Appl. Energy*, vol. 195, pp. 586–599, Jun. 2017, doi: 10.1016/j.apenergy.2017.03.074.

[86] U.-H. Kim, L.-Y. Kuo, P. Kaghazchi, C. S. Yoon, and Y.-K. Sun, "Quaternary Layered Ni-Rich NCMA Cathode for Lithium-Ion Batteries," *ACS Energy Lett.*, vol. 4, no. 2, pp. 576–582, Feb. 2019, doi: 10.1021/acsenergylett.8b02499.

[87] J. Asenbauer, T. Eisenmann, M. Kuenzel, A. Kazzazi, Z. Chen, and D. Bresser, "The success story of graphite as a lithium-ion anode material – fundamentals, remaining challenges, and recent developments including silicon (oxide) composites," *Sustain. Energy Fuels*, vol. 4, no. 11, pp. 5387–5416, 2020, doi: 10.1039/D0SE00175A.

[88] C. Heubner, T. Liebmann, O. Lohrberg, S. Cangaz, S. Maletti, and A. Michaelis, "Understanding Component-Specific Contributions and Internal Dynamics in Silicon/Graphite Blended Electrodes for High-Energy Lithium-Ion Batteries," *Batter. Supercaps*, vol. 5, no. 1, p. e202100182, Jan. 2022, doi: 10.1002/batt.202100182.

[89] R. Schmuch, R. Wagner, G. Hörpel, T. Placke, and M. Winter, "Performance and cost of materials for lithium-based rechargeable automotive batteries," *Nat. Energy*, vol. 3, no. 4, pp. 267–278, Apr. 2018, doi: 10.1038/s41560-018-0107-2.

[90] Y.-S. Duh, C.-Y. Lee, Y.-L. Chen, and C.-S. Kao, "Characterization on the exothermic behaviors of cathode materials reacted with ethylene carbonate in lithium-ion battery studied by differential scanning calorimeter (DSC)," *Thermochim. Acta*, vol. 642, pp. 88–94, Oct. 2016, doi: 10.1016/j.tca.2016.09.007.

[91] S. Ma *et al.*, "Temperature effect and thermal impact in lithium-ion batteries: A review," *Prog. Nat. Sci. Mater. Int.*, vol. 28, no. 6, pp. 653–666, Dec. 2018, doi: 10.1016/j.pnsc.2018.11.002.

[92] I. Belharouak, Y.-K. Sun, J. Liu, and K. Amine, "Li(Ni1/3Co1/3Mn1/3)O2 as a suitable cathode for high power applications," *J. Power Sources*, vol. 123, no. 2, pp. 247–252, Sep. 2003, doi: 10.1016/S0378-7753(03)00529-9.

[93] X. Feng *et al.*, "Thermal runaway features of large format prismatic lithium ion battery using extended volume accelerating rate calorimetry," *J. Power Sources*, vol. 255, pp. 294–301, Jun. 2014, doi: 10.1016/j.jpowsour.2014.01.005.

[94] T. M. Bandhauer, S. Garimella, and T. F. Fuller, "A Critical Review of Thermal Issues in Lithium-Ion Batteries," *J. Electrochem. Soc.*, vol. 158, no. 3, p. R1, 2011, doi: 10.1149/1.3515880.

[95] D. Doughty and E. P. Roth, "A General Discussion of Li Ion Battery Safety," *Electrochem. Soc. Interface*, 2012.

[96] P. Weicker, *A systems approach to lithium-ion battery management*. in Artech house power engineering series. Boston: Artech house, 2014.

[97] M. R. M. Kassim, W. A. W. Jamil, and R. M. Sabri, "State-of-Charge (SOC) and State-of-Health (SOH) Estimation Methods in Battery Management Systems for Electric Vehicles," in *2021 IEEE International Conference on Computing (ICOCO)*, Kuala Lumpur, Malaysia: IEEE, Nov. 2021, pp. 91–96. doi: 10.1109/ICOCO53166.2021.9673580.

[98] S. B and P. Pradeepa, “Review on Battery Management System in EV,” in *2022 International Conference on Intelligent Controller and Computing for Smart Power (ICICCSP)*, Hyderabad, India: IEEE, Jul. 2022, pp. 1–4. doi: 10.1109/ICICCSP53532.2022.9862367.

[99] S. Mishra, S. C. Swain, and R. K. Samantaray, “A Review on Battery Management system and its Application in Electric vehicle,” in *2021 International Conference on Advances in Computing and Communications (ICACC)*, Kochi, Kakkanad, India: IEEE, Oct. 2021, pp. 1–6. doi: 10.1109/ICACC-202152719.2021.9708114.

[100] X. Ning, “Mixed Battery Array Energy Storage System,” M.A.Sc., Dalhousie University, Halifax, Canada, 2024. [Online]. Available: https://dalspace.library.dal.ca/items/a776b976-4063-46c5-aded-18697e3a8180

[101] A. A. Pesaran, “Battery thermal models for hybrid vehicle simulations,” *J. Power Sources*, vol. 110, no. 2, pp. 377–382, Aug. 2002, doi: 10.1016/S0378-7753(02)00200-8.

[102] N. Yang, X. Zhang, B. Shang, and G. Li, “Unbalanced discharging and aging due to temperature differences among the cells in a lithium-ion battery pack with parallel combination,” *J. Power Sources*, vol. 306, pp. 733–741, Feb. 2016, doi: 10.1016/j.jpowsour.2015.12.079.

[103] P. R. Tete, M. M. Gupta, and S. S. Joshi, “Developments in battery thermal management systems for electric vehicles: A technical review,” *J. Energy Storage*, vol. 35, p. 102255, Mar. 2021, doi: 10.1016/j.est.2021.102255.

[104] W. Wu, S. Wang, W. Wu, K. Chen, S. Hong, and Y. Lai, “A critical review of battery thermal performance and liquid based battery thermal management,” *Energy Convers. Manag.*, vol. 182, pp. 262–281, Feb. 2019, doi: 10.1016/j.enconman.2018.12.051.

[105] C. Roe *et al.*, “Immersion cooling for lithium-ion batteries – A review,” *J. Power Sources*, vol. 525, p. 231094, Mar. 2022, doi: 10.1016/j.jpowsour.2022.231094.

[106] M. Bernagozzi, A. Georgoulas, N. Miché, and M. Marengo, “Heat pipes in battery thermal management systems for electric vehicles: A critical review,” *Appl. Therm. Eng.*, vol. 219, p. 119495, Jan. 2023, doi: 10.1016/j.applthermaleng.2022.119495.

[107] X. Zhang, Z. Li, L. Luo, Y. Fan, and Z. Du, “A review on thermal management of lithium-ion batteries for electric vehicles,” *Energy*, vol. 238, p. 121652, Jan. 2022, doi: 10.1016/j.energy.2021.121652.

[108] V. Mali, R. Saxena, K. Kumar, A. Kalam, and B. Tripathi, “Review on battery thermal management systems for energy-efficient electric vehicles,” *Renew. Sustain. Energy Rev.*, vol. 151, p. 111611, Nov. 2021, doi: 10.1016/j.rser.2021.111611.

[109] G. Zhao, X. Wang, M. Negnevitsky, and H. Zhang, “A review of air-cooling battery thermal management systems for electric and hybrid electric vehicles,” *J. Power Sources*, vol. 501, p. 230001, Jul. 2021, doi: 10.1016/j.jpowsour.2021.230001.

[110] L. He, H. Jing, Y. Zhang, P. Li, and Z. Gu, “Review of thermal management system for battery electric vehicle,” *J. Energy Storage*, vol. 59, p. 106443, Mar. 2023, doi: 10.1016/j.est.2022.106443.

[111] B. Gohla-Neudecker, V. S. Maiyappan, S. Juraschek, and S. Mohr, “Battery 2nd life: Presenting a benchmark stationary storage system as enabler for the global energy transition,” in *2017 6th International Conference on Clean Electrical Power (ICCEP)*, Santa Margherita Ligure, Italy: IEEE, Jun. 2017, pp. 103–109. doi: 10.1109/ICCEP.2017.8004799.

[112] Q. Wang, B. Jiang, B. Li, and Y. Yan, "A critical review of thermal management models and solutions of lithium-ion batteries for the development of pure electric vehicles," *Renew. Sustain. Energy Rev.*, vol. 64, pp. 106–128, Oct. 2016, doi: 10.1016/j.rser.2016.05.033.

[113] S. Arora, "Selection of thermal management system for modular battery packs of electric vehicles: A review of existing and emerging technologies," *J. Power Sources*, vol. 400, pp. 621–640, Oct. 2018, doi: 10.1016/j.jpowsour.2018.08.020.

[114] J. R. Patel and M. K. Rathod, "Recent developments in the passive and hybrid thermal management techniques of lithium-ion batteries," *J. Power Sources*, vol. 480, p. 228820, Dec. 2020, doi: 10.1016/j.jpowsour.2020.228820.

[115] Canadian Vehicle Manufacturers' Association and Call2Recycle, "Electric Vehicle Battery Management at End-of-Vehicle Life: A Primer for Canada," 2022. Accessed: Mar. 01, 2025. [Online]. Available: https://www.cvma.ca/wp-content/uploads/2022/11/EV-Battery-Primer-%E2%80%93-CVMA-Call2Recycle-%E2%80%93-November-25-2022.pdf

[116] Cox Automotive, "Cox Automotive Charges Forward With New EV Battery Solutions Facility in Georgia," EV Battery Solutions. Accessed: Mar. 01, 2025. [Online]. Available: https://www.coxautoinc.com/ev-battery-solutions/insights/new-ev-battery-solutions-facility-in-georgia/

[117] H. Huo, Y. Xing, M. Pecht, B. J. Züger, N. Khare, and A. Vezzini, "Safety Requirements for Transportation of Lithium Batteries," *Energies*, vol. 10, no. 6, p. 793, Jun. 2017, doi: 10.3390/en10060793.

[118] Transport Canada, "Transportation of Dangerous Goods Bulletin: Transporting Batteries," Jan. 2018. Accessed: Mar. 01, 2025. [Online]. Available: https://tc.canada.ca/sites/default/files/2024-09/tdg_bulletin_transportation_of_batteries.pdf

[119] Y. Kotak *et al.*, "End of Electric Vehicle Batteries: Reuse vs. Recycle," *Energies*, vol. 14, no. 8, p. 2217, Apr. 2021, doi: 10.3390/en14082217.

[120] M. Terkes, A. Demirci, E. Gokalp, and U. Cali, "Battery Passport for Second-Life Batteries: Potential Applications and Challenges," *IEEE Access*, vol. 12, pp. 128424–128467, 2024, doi: 10.1109/ACCESS.2024.3450790.

[121] ReJoule, "Product Solution," ReJoule Energy. Accessed: Mar. 01, 2025. [Online]. Available: https://rejouleenergy.com/solution

[122] A. Kampker, H. H. Heimes, C. Offermanns, J. Vienenkötter, M. Frank, and D. Holz, "Identification of Challenges for Second-Life Battery Systems—A Literature Review," *World Electr. Veh. J.*, vol. 14, no. 4, p. 80, Mar. 2023, doi: 10.3390/wevj14040080.

[123] J. C. Kelly and O. Winjobi, "Battery Second Life: A Review of Challenges and Opportunities," presented at the 33rd Electric Vehicle Symposium (EVS33) Portland, Oregon, June 14-17, 2020, 2020.

[124] F. Salek, S. Resalati, M. Babaie, P. Henshall, D. Morrey, and L. Yao, "A Review of the Technical Challenges and Solutions in Maximising the Potential Use of Second Life Batteries from Electric Vehicles," *Batteries*, vol. 10, no. 3, p. 79, Feb. 2024, doi: 10.3390/batteries10030079.

[125] P. A. Christensen, W. Mrozik, and M. S. Wise, "A Study on the Safety of Second-life Batteries in Battery Energy Storage Systems," Office for Product Safety & Sandards, United Kingdom, Jan. 2023. Accessed: Mar. 01, 2025. [Online]. Available:

https://assets.publishing.service.gov.uk/media/63d91ff0e90e0773da7fdb92/safety-of-second-life-batteries-in-bess.pdf

[126] Underwriters Laboratories, "ANSI/CAN/UL 1974, Evaluation for Repurposing Batteries," Standard for Safety, 2018.

[127] M. Resendiz, "Moment Energy First in North America to Achieve UL 1974 Certification," Moment Energy. Accessed: Mar. 01, 2025. [Online]. Available: https://www.momentenergy.com/news-articles/moment-energy-ul-1974-certification

[128] Underwriters Laboratories, "UL Issues World's First Certification for Repurposed EV Batteries to 4R Energy," UL Solutions. Accessed: Mar. 01, 2025. [Online]. Available: https://www.ul.com/news/ul-issues-worlds-first-certification-repurposed-ev-batteries-4r-energy

[129] E. Fonseca, R. A. Franco, B. Simons, and M. D. Paiss, "Challenges in Deploying a Second-Life Battery System: Engineering, Fire Safety, UL Certifications, and NFPA Requirements," in *2024 IEEE Electrical Energy Storage Application and Technologies Conference (EESAT)*, San Diego, CA, USA: IEEE, Jan. 2024, pp. 1–5. doi: 10.1109/EESAT59125.2024.10471221.

[130] N. Mukherjee and D. Strickland, "Analysis and Comparative Study of Different Converter Modes in Modular Second-Life Hybrid Battery Energy Storage Systems," *IEEE J. Emerg. Sel. Top. Power Electron.*, vol. 4, no. 2, pp. 547–563, Jun. 2016, doi: 10.1109/JESTPE.2015.2460334.

[131] A. Hassan *et al.*, "Second-Life Batteries: A Review on Power Grid Applications, Degradation Mechanisms, and Power Electronics Interface Architectures," *Batteries*, vol. 9, no. 12, p. 571, Nov. 2023, doi: 10.3390/batteries9120571.

[132] M. Bauer, J. Wiesmeier, and J. Lygeros, "A comparison of system architectures for high-voltage electric vehicle batteries in stationary applications," *J. Energy Storage*, vol. 19, pp. 15–27, Oct. 2018, doi: 10.1016/j.est.2018.06.007.

[133] D. Conover *et al.*, "Protocol for Uniformly Measuring and Expressing the Performance of Energy Storage Systems," Prepared by Pacific Northwest National Laboratory and Sandia National Laboratories, Apr. 2016.

[134] "Energy Storage Integration Council (ESIC) Energy Storage Test Manual," Electric Power Research Institute, Palo Alto, CA, Technical Update 3002021710, Nov. 2021. [Online]. Available: https://www.epri.com/research/products/000000003002021710

[135] D. Rosewater and S. Ferreira, "Development of a frequency regulation duty-cycle for standardized energy storage performance testing," *J. Energy Storage*, vol. 7, pp. 286–294, Aug. 2016, doi: 10.1016/j.est.2016.04.004.

[136] CSE, "Final Long-Term Duty Cycle Report: Primary Frequency Response (PFR) Duty Cycle," Report prepared for NREL by Center for Sustainable Energy, Jul. 2015. Accessed: Mar. 01, 2025. [Online]. Available: https://energycenter.org/sites/default/files/docs/nav/programs/second-life/Long-Term-Test-Report_PFR_CH1-CH4_Final_08-21-2015.pdf

[137] Y. Zhang *et al.*, "Performance assessment of retired EV battery modules for echelon use," *Energy*, vol. 193, p. 116555, Feb. 2020, doi: 10.1016/j.energy.2019.116555.

[138] B. Ellis, C. White, and L. Swan, "Degradation of lithium-ion batteries that are simultaneously servicing energy arbitrage and frequency regulation markets," *J. Energy Storage*, vol. 66, p. 107409, Aug. 2023, doi: 10.1016/j.est.2023.107409.

[139] C. White, B. Thompson, and L. G. Swan, “Repurposed electric vehicle battery performance in second-life electricity grid frequency regulation service,” *J. Energy Storage*, vol. 28, p. 101278, Apr. 2020, doi: 10.1016/j.est.2020.101278.

[140] A. J. Crawford *et al.*, “Lifecycle comparison of selected Li-ion battery chemistries under grid and electric vehicle duty cycle combinations,” *J. Power Sources*, vol. 380, pp. 185–193, Mar. 2018, doi: 10.1016/j.jpowsour.2018.01.080.

[141] Y. P. Gusev and P. V. Subbotin, “Using Battery Energy Storage Systems for Load Balancing and Reactive Power Compensation in Distribution Grids,” in *2019 International Conference on Industrial Engineering, Applications and Manufacturing (ICIEAM)*, Sochi, Russia: IEEE, Mar. 2019, pp. 1–5. doi: 10.1109/ICIEAM.2019.8742909.

[142] E. Nyemah, “Use of Battery Systems for VAR Support in Con Edison’s Distribution Network/Substation,” MEng Thesis, City University of New York, New York. Accessed: Mar. 01, 2025. [Online]. Available: https://academicworks.cuny.edu/cgi/viewcontent.cgi?article=2069&context=cc_etds_theses

[143] J. Schmitt, A. Maheshwari, M. Heck, S. Lux, and M. Vetter, “Impedance change and capacity fade of lithium nickel manganese cobalt oxide-based batteries during calendar aging,” *J. Power Sources*, vol. 353, pp. 183–194, Jun. 2017, doi: 10.1016/j.jpowsour.2017.03.090.

[144] M. Dubarry, C. Truchot, and B. Y. Liaw, “Synthesize battery degradation modes via a diagnostic and prognostic model,” *J. Power Sources*, vol. 219, pp. 204–216, Dec. 2012, doi: 10.1016/j.jpowsour.2012.07.016.

[145] T. R. Ashwin, A. Barai, K. Uddin, L. Somerville, A. McGordon, and J. Marco, “Prediction of battery storage ageing and solid electrolyte interphase property estimation using an electrochemical model,” *J. Power Sources*, vol. 385, pp. 141–147, May 2018, doi: 10.1016/j.jpowsour.2018.03.010.

[146] P. Keil *et al.*, “Calendar Aging of Lithium-Ion Batteries: I. Impact of the Graphite Anode on Capacity Fade,” *J. Electrochem. Soc.*, vol. 163, no. 9, pp. A1872–A1880, 2016, doi: 10.1149/2.0411609jes.

[147] D. Chen, J. Jiang, G.-H. Kim, C. Yang, and A. Pesaran, “Comparison of different cooling methods for lithium ion battery cells,” *Appl. Therm. Eng.*, vol. 94, pp. 846–854, Feb. 2016, doi: 10.1016/j.applthermaleng.2015.10.015.

[148] S. Yang, C. Zhang, J. Jiang, W. Zhang, L. Zhang, and Y. Wang, “Review on state-of-health of lithium-ion batteries: Characterizations, estimations and applications,” *J. Clean. Prod.*, vol. 314, p. 128015, Sep. 2021, doi: 10.1016/j.jclepro.2021.128015.

[149] B. Ma *et al.*, “Remaining useful life and state of health prediction for lithium batteries based on differential thermal voltammetry and a deep-learning model,” *J. Power Sources*, vol. 548, p. 232030, Nov. 2022, doi: 10.1016/j.jpowsour.2022.232030.

[150] W. Diao, J. Jiang, C. Zhang, H. Liang, and M. Pecht, “Energy state of health estimation for battery packs based on the degradation and inconsistency,” *Energy Procedia*, vol. 142, pp. 3578–3583, Dec. 2017, doi: 10.1016/j.egypro.2017.12.248.

[151] L. Ahmadi, S. B. Young, M. Fowler, R. A. Fraser, and M. A. Achachlouei, “A cascaded life cycle: reuse of electric vehicle lithium-ion battery packs in energy storage systems,” *Int. J. Life Cycle Assess.*, vol. 22, no. 1, pp. 111–124, Jan. 2017, doi: 10.1007/s11367-015-0959-7.

[152] L. C. Casals, B. Amante García, and C. Canal, “Second life batteries lifespan: Rest of useful life and environmental analysis,” *J. Environ. Manage.*, vol. 232, pp. 354–363, Feb. 2019, doi: 10.1016/j.jenvman.2018.11.046.

[153] M. Elliott, L. G. Swan, M. Dubarry, and G. Baure, “Degradation of electric vehicle lithium-ion batteries in electricity grid services,” *J. Energy Storage*, vol. 32, p. 101873, Dec. 2020, doi: 10.1016/j.est.2020.101873.

[154] E. Braco, I. San Martin, A. Berrueta, P. Sanchis, and A. Ursua, “Experimental Assessment of First- and Second-Life Electric Vehicle Batteries: Performance, Capacity Dispersion, and Aging,” *IEEE Trans. Ind. Appl.*, vol. 57, no. 4, pp. 4107–4117, Jul. 2021, doi: 10.1109/TIA.2021.3075180.

[155] M. F. Börner *et al.*, “Challenges of second-life concepts for retired electric vehicle batteries,” *Cell Rep. Phys. Sci.*, vol. 3, no. 10, p. 101095, Oct. 2022, doi: 10.1016/j.xcrp.2022.101095.

[156] L. C. Casals and B. A. Garca, “Communications concerns for reused electric vehicle batteries in smart grids,” *IEEE Commun. Mag.*, vol. 54, no. 9, pp. 120–125, Sep. 2016, doi: 10.1109/MCOM.2016.7565258.

[157] C. White and L. G. Swan, “Spatial extrapolation of temperature measurements in second-life battery packs using simplified thermal network modelling,” *J. Energy Storage*, vol. 112, p. 115476, Mar. 2025, doi: 10.1016/j.est.2025.115476.

[158] D.-I. Stroe, V. Knap, M. Swierczynski, A.-I. Stroe, and R. Teodorescu, “Operation of a Grid-Connected Lithium-Ion Battery Energy Storage System for Primary Frequency Regulation: A Battery Lifetime Perspective,” *IEEE Trans. Ind. Appl.*, vol. 53, no. 1, pp. 430–438, Jan. 2017, doi: 10.1109/TIA.2016.2616319.

[159] J. Lacap, J. W. Park, and L. Beslow, “Development and Demonstration of Microgrid System Utilizing Second-Life Electric Vehicle Batteries,” *J. Energy Storage*, vol. 41, p. 102837, Sep. 2021, doi: 10.1016/j.est.2021.102837.

[160] Action Canada, “Positive Charge: Maximizing Canada’s Electric Vehicle Battery Repurposing and Recycling Ecoystem,” 2024. Accessed: Mar. 01, 2025. [Online]. Available: https://actioncanada.ca/publications/positive-charge-maximizing-canadas-electric-vehicle-battery-repurposing-and-recycling-ecosystem/

[161] Global Battery Alliance, “A Vision for a Sustainable Battery Value Chain in 2030: Unlocking the Full Potential to Power Sustainable Development and Climate Change Mitigation,” World Economic Forum, Sep. 2019. Accessed: Mar. 01, 2025. [Online]. Available: https://www3.weforum.org/docs/WEF_A_Vision_for_a_Sustainable_Battery_Value_Chain_in_2030_Report.pdf

[162] “What the New EU Battery Regulation Means for Manufacturers,” CSA Group. Accessed: Apr. 21, 2025. [Online]. Available: https://www.csagroup.org/article/what-the-new-eu-battery-regulation-means-for-manufacturers

[163] C. A. Rufino Júnior *et al.*, “Towards to Battery Digital Passport: Reviewing Regulations and Standards for Second-Life Batteries,” *Batteries*, vol. 10, no. 4, 2024, doi: 10.3390/batteries10040115.